Photochemistry and photophysics of guanines
by James Paul Morgan

A thesis submitted in partial fulfillment of the requirements for the degree of DOCTOR OF PHILOSOPHY in Chemistry
Montana State University

Abstract:
Guanine and several derivatives undergo photochemistry in glycol-water glasses, below -100°C. The photochemistry can be sensitized with light of ?'s > 300 nm when acetone is added. The product is not photoreversible, and the molar extinction coefficients are 19.4xl03, 3.7xl03, and 8.3x103 at 225 nm, 265 nm, and 305 nm maxima. The product fluorescence maximum is at 418 nm. The fluorescence yield is 0.35 at -112°C in the 7:3 glycol-water glass. The photochemical quantum yield is 2% exciting at GMP's absorption maximum, and increases to more than 4% when exciting at ?'s > 285 nm. Wavelength dependent effects are seen for the luminescence yields of the derivatives studied. Cu2+, Co2+, and Ni2+ show evidence for com-plexation with GMP in the absorption and severely reduce the photochemical and luminescence yields.

The product reverts to the parent compound when warmed rapidly to room temperature. If the product is warmed slowly in the -85°C to -74°C region, a conversion to a stable product with a 360 nm fluorescence maximum results. At warmer temperatures, ~-70°C, only the stable product is produced. The 360 nm fluorescent product can be photosensitized at room temperature via acetone, even in t-RNA.

A photophysical, photochemical study of GMP containing dinucleotides was made. F, 3t, and rate studies indicated that: singlet electronic transfer in CpG and dpGpT is efficient; GpA, GpU, and GpC are partially in the form of exciplexes and the exciplexes intersystem cross as the nucleotide with the lower energy singlet. Photochemical and luminescence yields in ApG and GpA are nearly that of GMP, but are much less in CpG, GpC, UpG, and GpU.

PHOTOCHEMISTRY AND PHOTOPHYSICS OF GUANINES

by

JAMES PAUL MORGAN

A thesis submitted in partial fulfillment
of the requirements for the degree

of

DOCTOR OF PHILOSOPHY

in

Chemistry

Approved:

Patrick R. Callis
Chairman, Examining Committee

E. W. Gaucher
Head, Major Department

K. Goering
Graduate Dean

MONTANA STATE UNIVERSITY
Bozeman, Montana

September, 1974

ACKNOWLEDGMENTS

A great deal of appreciation is expressed to Dr. Pat Callis for his tutelage and support during the course of this work. While his reservoir of intelligence and knowledge have been indispensible, his ability to regenerate enthusiasm at times when this investigator's interest waned was probably most effective in prompting the research efforts toward a reasonable conclusion.

All computer assisted calculations cited in the thesis are the handiwork of Rob Wilson, my lab partner during graduate study. In addition to the numerous computer programs provided by Rob, he was a collaborator in defining the optical properties of molecules which were of mutual interest. An even disposition and a selfless attitude by Rob made my tasks easier.

Many faculty members provided both encouragement and the use of various research materials, which is gratefully acknowledged.

TABLE OF CONTENTS

LIST OF TABLES

LIST OF FIGURES

ABSTRACT

Guanine and several derivatives undergo photochemistry in glycol-water glasses, below -100°C. The photochemistry can be sensitized with light of λ's > 300 nm when acetone is added. The product is not photoreversible, and the molar extinction coefficients are 19.4×10^3, 3.7×10^3, and 8.3×10^3 at 225 nm, 265 nm, and 305 nm maxima. The product fluorescence maximum is at 418 nm. The fluorescence yield is 0.35 at -112°C in the 7:3 glycol-water glass. The photochemical quantum yield is 2% exciting at GMP's absorption maximum, and increases to more than 4% when exciting at λ's > 285 nm. Wavelength dependent effects are seen for the luminescence yields of the derivatives studied. Cu^{2+}, Co^{2+}, and Ni^{2+} show evidence for complexation with GMP in the absorption and severely reduce the photochemical and luminescence yields.

The product reverts to the parent compound when warmed rapidly to room temperature. If the product is warmed slowly in the -85°C to -74°C region, a conversion to a stable product with a 360 nm fluorescence maximum results. At warmer temperatures, ~-70°C, only the stable product is produced. The 360 nm fluorescent product can be photosensitized at room temperature via acetone, even in t-RNA.

A photophysical, photochemical study of GMP containing dinucleotides was made. Φ, $^3\tau$, and rate studies indicated that: singlet electronic transfer in CpG and dpGpT is efficient; GpA, GpU, and GpC are partially in the form of exciplexes and the exciplexes intersystem cross as the nucleotide with the lower energy singlet. Photochemical and luminescence yields in ApG and GpA are nearly that of GMP, but are much less in CpG, GpC, UpG, and GpU.

INTRODUCTION

The Molecules

The chromophores responsible for photophysical and photochemical effects in GMP and GMP containing dinucleotides are the nucleic bases. What are thought to be the principle tautomeric forms are shown below, along with the numbering systems used for the bases, depending on whether they are purine or pyrimidine derivatives.

Purines

Adenine

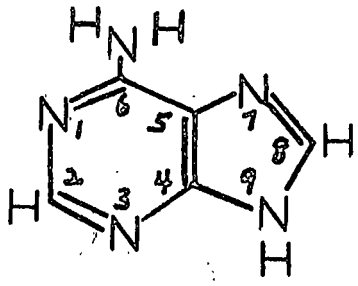

Guanine

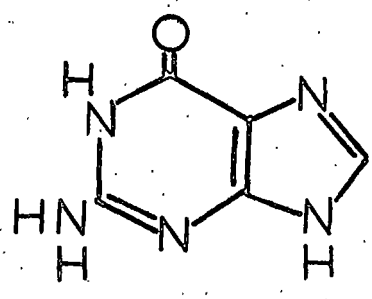

Pyrimidines

Cytosine

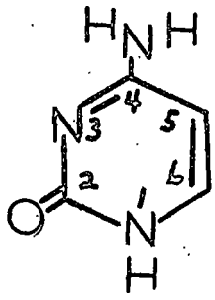

Thymine

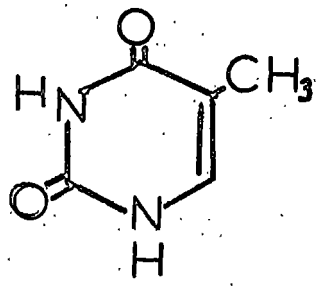

Uracil

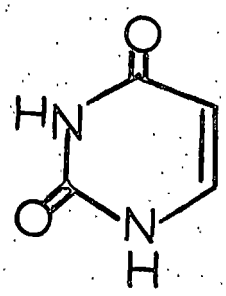

In the form of a nucleoside, there is a substitution at the 9 position in the purines, and at the 1 position in the pyrmidines. The substituting group is ribose in the case of a ribonucleoside; or it is deoxyribose in the case of a deoxyribonucleoside. The substitution is by a glycoside linkage at the 1′ position of the sugar. Adenosine, guanosine, cytidine, thymidine, and uridine are the terms applied to the ribonucleosides. Deoxyribonucleosides have the prefix deoxy added to the terms used for the ribonucleosides.

Nucleotides are the sugar-O-phosphate esters of the nucleosides, with substitution at the 2′, 3′, 5′ positions possible in ribosides, and substitution at the 3′ and 5′ positions in the deoxyribosides. Adenosine monophosphate is abbreviated AMP, and similar abbreviations apply to the other nucleotides: GMP, CMP, TMP, and UMP. Since TMP exists only as the derivative of a deoxyribonucleoside, it is understood to be such. dAMP, dGMP, and dCMP designate the deoxynucleotides of adenosine, guanosine, and cytidine. UMP does not exist in a deoxy form.

A short segment of a nucleic acid polymer may be made by the formation of two sugar-O-phosphate ester bonds with two nucleosides and one phosphate. A molecule of this

type, such as adenyl, 3′, 5′ guanylate, is abbreviated to ApG(3′, 5′). The conformation in a dinucleotide is believed to be similar to that of the Watson-Crick geometry for a nucleic acid polymer. Crystal structures have been determined for two dinucleotides, ApU (1) and GpC (2).

Principles of Photophysics

The basic elements of the principles, which are believed to govern photophysical processes, can be expressed in terms of a kinetic scheme portrayed on an energy level diagram. Such a diagram, commonly referred to as a Jablonski diagram, is shown in Figure 1.

In the diagram, the vertical transitions of increasing energy are representative of absorption events related to a change in vibrational-electronic energy states. The absorption intensity is related to two considerations: 1) the degree of interaction of the light wave with the molecule, and 2) the population differences between the initial and final states.

Experimentally, the transmitted intensity at a given energy of excitation is observed to be governed by; the concentration of the molecules in the medium, the distance of penetration of the light wave into the absorbing medium,

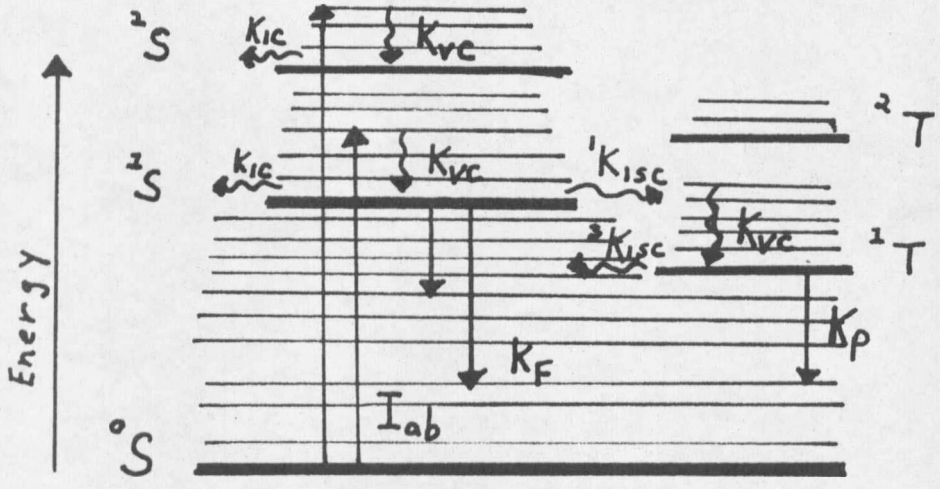

Figure 1. Jablonski diagram for widely separated chromaphores. Straight vertical lines depict radiative processes. Wavy lines represent nonradiative processes. Dark horizontal lines represent electronic state energy minima. Lighter horizontal lines represent combined vibrational-electronic states.

and a constant characteristic of the absorbing molecule. The expression relating these effects is

$$I(x) = I_0 10^{-\epsilon cx}$$

where $I(x)$ = the intensity of the light at distance x in the medium,

I_0 = the intensity of the light just as it enters the medium,

c = concentration of the absorbing molecules in moles per liter,

ϵ = a constant related to the degree of interaction of the molecule with the light wave being absorbed, and given the name molar extinction coefficient.

The intensity of the absorbed light, I_{ab}, is the difference between the intensities of, the incident light, I_0, and the light at distance x, $I(x)$, so that

$$I_{ab} = I_0 - I(x)$$

$$= I_0(1 - 10^{-\epsilon cx}).$$

I_{ab} is observed to vary as the energy of excitation is varied, when I_0, c, and x are held constant. Therefore, ϵ can only be considered a constant for a given excitation energy.

The variation of ϵ with energy of excitation in the visible and UV regions of the spectrum is approximately a series of gaussian shaped curves, with varying degrees of overlap, beginning at the minimum excitation energy for absorption, and continuing to point where ϵ becomes a constant, indicating photodissociation. Molecules in the vapor phase, and some molecules in condensed media, show additional fine structure in the electronic absorption bands, whose energy spacings are of the nature of vibrational transitions. However, many complex molecules in solution, and at room temperature, display smooth unstructured bands with band widths of from 3,000 cm^{-1} to 10,000 cm^{-1}. These individual bands are considered to be the result of transitions between the spin-paired ground energy state ^0S, and some higher spin-paired electronic state ^nS. The variation in intensity across a particular band is attributed to a variation in "overlap" between the lowest vibronic state of the ground electronic state and the vibronic states of some higher energy electronic state. The

value of ϵ at its maximum within an electronic band is found to vary by many orders of magnitude (10^0 to 10^5). This variation is thought to be the result of certain selection rules which apply to an electronic transition; for example, transitions between states of different spin are not "allowed", nor would the transition between two states with a zero value of the integral $\langle\psi_1|\sum_i q_i r_i|\psi_2\rangle$ be allowed.

The time required for an electronic transition must be near that of the oscillation period of the light wave inducing the transition, $\sim 10^{-15}$ seconds.

Once a molecule reaches a higher electronic state, it does not remain there indefinitely but relaxes to the ^{0}S state, after a time interval dependent on the individual molecule and the degree of external perturbation.

Most often, the vibronic state reached on excitation is some higher vibrational level of the ^{n}S. As, with only a few known exceptions, the observed relaxation processes of the spin-paired ^{n}S states take place only from the lowest vibrational level of ^{1}S, the dissipation of energy in excess of ^{1}S must be more rapid than a process such as the re-emission of the light. Rentzepis, by an elegant technique using laser excitation, was able to observe a

vibration relaxation time of 20 picoseconds (10^{-12} sec.) for an excited vibronic state of benzophenone (3). The rates of vibrational cascade, k_{vc}, and k_{IC} ($^{n}S \rightarrow {}^{n-1}S$) of other molecules may also be of the order of 10^{11} - 10^{13} sec^{-1}. The invariance of observable relaxation processes with excitation energy is commonly referred to as Kasha's rule.

The depopulation of lowest vibrational level ^{1}S state occurs via three pathways: 1) emission to some vibrational level of ^{0}S (fluorescence) at a rate k_f (10^6 - 10^9 sec^{-1}); 2) nonradiative isoenergetic transfer to a spin-unpaired triplet state, ^{1}T, (intersystem crossing) at a rate, $^{1}k_{ISC}$ ($10^{?}$ - 10^9 sec^{-1}); and 3) nonradiative isoenergetic transfer to a highly excited vibrational level of ^{0}S with retention of paired spin-state (internal conversion) at a rate k_{IC} ($10^{?}$ - $10^{?}$ sec^{-1}).

The idea of invariance of the fluorescing state with excitation energy has its basis in three experimental observations: 1) the highest energy fluorescence seen is very close to the lowest possible absorption energy, 2) the shape of the fluorescence band is not dependent on excitation energy, and 3) the intensity of fluorescence at any

one point in the fluorescence band is directly proportional to the ϵ values at varying excitation energies.

Additionally, from 1) above, the energy of the transition of minimum energy absorption and maximum energy fluorescence should be located at the intersection of the absorption and fluorescence bands (0-0 energy). From 2) above, since the shape of the fluorescence band for a particular species is not dependent on excitation energy, an observed variance is evidence of more than one species, thus providing a test for fluorescent impurities. From 3) above, by monitoring the fluorescence intensity at any given point in the fluorescence band, and then varying the excitation wavelength across the absorption band, what should be observed is a fluorescence intensity variation exactly parallel to the varying $\epsilon(\lambda_{ex})$, i.e., the absorption band shape should be reproduced.

While the basic features of absorption and fluorescence of molecules can be understood by an extension of Einstein's treatment of transitions in atoms (see Birks (4)), nonradiative deactivation processes such as internal conversion and intersystem crossing are the objects of intensive theoretical consideration. Nonradiative internal conversion from ^1S is often minor, and is thought to be so

because of the relatively large energy separation (1-8 eV) between ^0S and ^1S. However, in some cases (such as for the molecules being examined for this work), it is the dominant deactivation pathway even though the ^0S - ^1S energy separation is quite large (>7 eV for the nucleic acids). Intersystem crossing is formally forbidden by the selection rules, but is thought to be partially allowed by a quantum mechanical spin-orbit coupling of the ^1S and ^1T states.

The spin-unpaired triplet state, ^1T, once populated by nonradiative intersystem crossing (the radiative ISC is even more "forbidden") undergoes relaxation processes similar to those of the ^1S state, except due to the forbidden nature of decay to the ground ^0S state, the radiative process (phosphorescence) has a rate, k_p, (10^{-2} - 10 sec^{-1}) that is much less than k_F, so that is observed only when the nonradiative deactivation rate, $^3k_{ISC}$, is reduced substantially. Experimentally, this is achieved by immersing the molecules in a low temperature matrix. As indicated in the diagram, phosphorescence ensues at a lower energy than does fluorescence.

Two additional experimental parameters, related to the competition between radiative and nonradiative deactivation of the lowest lying excited states, are used to gain

information about excited state pathways. These are the relaxation times, and the efficiencies or quantum yields, of luminescence.

The relaxation time τ, or lifetime as it is normally called, is defined as the time that is required for an observed luminescence intensity to fall to 1/e of a given value on termination of the excitation beam.

$$I_{t=t} = I_{t=0}e^{-t/\tau}, \quad I_{t=\tau} = \frac{I_{t=0}}{e}$$

$^1\tau$ = lowest singlet state lifetime

$^3\tau$ = lowest triplet state lifetime

$^1\tau_0$, $^3\tau_0$ = natural radiative lifetimes (only radiative deactivation is possible)

$$\tau = \frac{1}{\sum_i k_i}, \text{ where } k_i = \text{any deactivation rate constant}$$

The quantum yield Φ is defined as the fraction of molecules undergoing a certain photophysical or photochemical process out of the total number of molecules excited.

$$\Phi_x = \frac{\text{Number of molecules undergoing process x}}{\text{Total number of molecules excited}}$$

In the steady state approximation, which usually applies in the absence of photochemistry, any sampling period

after the establishment of the steady state will give the same result for Φ_x.

The quantum yield can also be expressed in terms of rate constants

$$\Phi_x \quad \frac{k_x}{k_x + \sum_i k_i},$$

where k_x is the rate constant for the process whose quantum yield is being measured, and k_i is the rate constant for any other process proceeding from the same excited state.

The previous discussion alluded to the situation where the molecules were dissolved in an inert, transparent medium at low concentration ($<10^{-5}$ M), so that the interaction between solute chromophores was negligible. As the concentration is increased and the solute molecules are brought closer together, they interact more strongly, and a variety of effects may be evidenced as a result. Varying solvent conditions may also produce photophysical effects. Some of the more commonly observed effects are listed below.

1. Inner filter effect - A decrease in luminescence intensity due to reabsorption within the solution.

2. Nonlinear absorption dependence on concentration - Ground state dimer formation.

3. Excimer fluorescence - An unstructured fluorescence band 5,000 cm^{-1} to the red (lower energy) of the monomer fluorescence due to excited state dimer formation.

4. A variation in the O-O energy due interaction of the solute chromophores, in the excited state or ground state, with solvent molecules or other solutes.

5. A shortened lifetime of some solute chromophores and a related luminescence yield increase of other solute chromophores, due to nonradiative electronic energy transfer.

6. A variation in lifetimes and yields due to a change in the rates of internal conversion or collision deactivation.

Nucleic Acids and UV Light

Since the discovery of the nucleic acids as the genetic material, scientists have attempted to gain exacting information about these very important molecules by a variety of methods. The ideal method to apply would be one where the investigational probe would have a perturbing effect that was transitory in time and minor in degree, so that it would be possible to elicit information about the detailed functioning of the system, without serious

disruption of the system. Nonionizing electromagnetic radiation in the ultraviolet region would seem suited to these purposes as the time of the perturbation is quite small, ~10^{-8} seconds, and only a very small fraction of the molecules need be disturbed to quantitatively gauge the overall conditions.

Indeed, the absorption of UV light by the nucleic acids has served well as a detection method for the molecules, both quantitatively and qualitatively. Even such subtle effects as the degree of helical conformation in a nucleic acid polymer may be obtained by means of absorption spectroscopy, due to the variation of absorbance properties of the helical conformer as opposed to the non-helical form. As convenient as the UV absorption method is, it is not without limitations.

While only 10^{-15} seconds is required to absorb the UV light, as much as one second may be required for an excited molecule to relax back to the ground state under certain conditions. It is known that the nucleic acids undergo photoalteration to a small degree within this relaxation period, so that the perturbing effect is not entirely transitory. Additionally, the individual nucleotide components of the nucleic acids have very similar absorbance

properties, so that it is nearly (if not totally) impossible to excite any one nucleotide independently of the others in a polymer.

Luminescence measurements allow one to detect excited molecules as they relax, via a radiative mechanism, to the ground state. If the efficiencies, lifetimes, and/or energies of the radiative processes are sufficiently different for molecules which have similar absorbance properties, then these detection methods may be used in place of absorption techniques to monitor a particular chromophore. It has been found that the individual nucleotide components do have luminescence properties (considering both fluorescence and phosphorescence) which do differ enough that luminescence measurements are capable of distinguishing any one nucleotide.

What is unfortunate, as far as the technique is concerned, is that it is necessary to have the nucleotides dissolved in a low temperature glass, in order to observe the fluorescence (this is always the case for phosphorescence) by conventional techniques. This is necessary because the nucleotides exhibit a high degree of nonradiative decay (internal conversion) at room temperature, so that the efficiency for the fluorescence process is only about

10^{-4}. Even at liquid nitrogen temperature, the internal conversion processes account for up to 90% of the deactivation for the nucleotides. This is somewhat unusual in that most molecules which fluoresce, do so at room temperature, internal conversion not being an efficient deactivation pathway between the ground state and the first excited singlet level. The low quantum efficiencies of luminescence (on the order of a few percent), even at 77°K, has been the cause of a rather slow development in this area of research. Only within the last fifteen years or so has the necessary instrumentation been devised which could give good results for such low luminescence yields and which are so environmentally dependent. A group of investigators at Bell Telphone Laboratories, Murray Hill, New Jersey has been most responsible for defining the properties of the excited states of the nucleotides. The bulk of their published work appeared in the years 1966-1970. Eisinger and Lamola have published a review of the group's research results incorporated in a general review of the area (5). In Table 1 are listed some of their results for the nucleotides as given in the above mentioned review.

In 1971, Daniels and Hauswirth published luminescence and excitation spectra for the nucleic bases

dissolved in water at 300°K (6). A specialized digital signal accumulation technique was necessary at the low Φ_F's evidenced (~10^{-4}). The major features of the spectra were similar to those of the nucleotides observed at the lower temperature, alcohol-glass environment although the differences observed (changes in shape and energies of fluorescence, and a variation of Φ_F with λ_{ex}) could be pertinent for the nucleotides under similar conditions.

Table 1. Excited state properties of the nucleotide as observed when dissolved in a 1:1, V/V, ethylene glycol-water (pH 7) glass at 77°K (5). The λ^P_{max} for TMP and UMP were obtained by sensitization.

	$^1E_{O-O}$ ($10^3 cm^{-1}$)	λ^{ab}_{max} (nm)	λ^F_{max}	$^1\Phi_F$	Φ_{ISC}	λ^P_{max}	Φ_P
AMP	35.2	258	313	0.01	0.02	404	0.015
GMP	34.0	253,274	323	0.13	0.15	401	0.07
CMP	33.7	274	322	0.05	0.03	405	0.01
TMP	34.1	268	323	0.16	~ 0	432	~ 0
UMP	34.9	265	316	0.01	--	423	~ 0

If it is not enough that the nucleotides individually have luminescence properties which make them difficult to deal with experimentally, the situation becomes increasingly complex when the nucleotides are brought together in

the form of a polymer. It is generally known (see the above mentioned review) that the fluorescence intensity of the polymer is considerably reduced and red-shifted as compared to what would be expected from a summation of the individual nucleotide components. The current interpretation is that the quenching results from some unknown deactivation process which effectively quenches guanine and cytosine fluorescence when they are hydrogen bonded (7). The red-shift of the fluorescence band is attributed to excimer (excited state dimer) formation, which has an unstable ground state and has a lower energy excited singlet state than the excited state monomer forms. The phosphorescence observed in the polymer case, as in DNA, has been reported to be that of thymine alone, so that energy transfer at the triplet level is indicated (8).

Due to the complexity of the excited state pathways in nucleic acid polymers, investigators (9,10,11,12) have made optical studies on the dinucleotide components of the polymers. A variety of results and interpretations have appeared as a consequence of the studies. The most variable result was the extent of excimer formation found for any particular dinucleotide. Differing environmental conditions seem to be the cause of the disparity. Most

investigators were in agreement on the nature of the emitting triplet states for the dinucleotides. With few exceptions, the emitting triplet was found to be that of the nucleotide having the lower energy ^1T state, in agreement with thymine triplet emission in DNA. Theoretical predictions of energy transfer at the singlet level were presented in a paper by Gueron et al. (13).

In order to circumvent the apparently unlikely success of monitoring the individual components of the nucleic acids when they are in a polymer form by means of their optical properties, investigators have turned to the use of fluorescent probes to induce luminescence in the nucleic acid systems under biological conditions. The probes used have been; either some of the naturally occurring modified forms of the normal bases which fluoresce weakly at room temperature, or chemically altered forms of the bases, or even molecules which have no analog character but which may be covalently or noncovalently attached to the nucleic acid polymers. Limited successes with some of these probes have been evidenced, but in general, the probes fluoresce only weakly when in a polymer, or they are unstable, or their introduction into the system causes too large of a perturbation. In spite of the limited success to date with such

probes, the technique is very promising and should there be found a modified form for each of the normal bases, which is biologically active, as well as having distinctive optical properties when incorporated in a polymer, important information could be gained. A review on the topic of fluorescent probes for the nucleic acids has been published by Cantor and Tao (14).

Aside from the desire to use optical methods as an analytical tool in nucleic acid research, a knowledge of the excited state pathways is important in terms of understanding the photochemical effects which result on UV absorption. It has been known for some time that the action spectrum of photoinactivation of many small organisms is similar to the absorption spectrum of nucleic polymers (15). The photodamage in cells is repairable to a greater or lesser extent depending on the organism affected. The repair mechanisms, although not completely understood, are seen to be a combination of photoreactivation and dark reversal.

Model studies with isolated DNA's, synthetic nucleic polymers, and the individual bases have shown that cyclobutane-type dimers of the pyrimidines (especially thymine), photohydrates of the pyrimidines, and

pyrimidine-pyrimidine photoadducts are largely responsible for the UV inactivation of certain transforming DNA's at room temperature (e.g., haemophilus influenza transforming DNA)(16). The inactivation due to dimer formation is severely reduced at temperatures of -100°C or colder (17).

Ultraviolet light rapidly inactivates both ribonucleic and deoxyribonucleic acids. Merriam and Gordon could find no correlation of pyrimidine dimers with any biologically defined lesion in TMV-RNA. In the absence of this correlation, they proposed that the photohydrates might be responsible for all inactivation (18).

Until quite recently, the purine base components of the nucleic polymers had been considered immune to photoalteration by non-ionizing UV irradiation. It was not until recently (1969) that there was a report of the formation of an alcohol (2-propanol) adduct at the C-8 position of either adenosine or guanosine, when they were dissolved in the alcohol and irradiated (19). The efficiency of the reaction was reportedly improved when sensitized with acetone (Φ's of ~0.1% unsensitized, with no Φ value given for the sensitized case, although a product yield of 45% was listed). They also report that the reactions may be photoreversed with an efficiency of 1% in the presence

of photosensitizers such as hydroquinone (20). Success at producing these photoproducts in DNA in the presence of 2-propanol and with or without acetone was published in 1973 (21). A severe reduction in thymine dimer formation was seen simultaneously.

STATEMENT OF THE PROBLEM

The research originated from the discovery by Dr. P. R. Callis that the dinucleotides ApG (3′ → 5′) and ApA (3′ → 5′) showed evidence for photochemical alteration when irradiated in a low temperature (-110°C) glycol-water glass (22). The evidence was an irradiation-time dependent formation of a new fluorescence band, coupled with a decrease in the parent fluorescence. This was a novel finding, as no other purine nucleic acid photochemistry had been reported in the literature at that time.

The research that developed as a consequence of this initial finding had two objectives.

1. To learn as much as possible about the purine photochemistry itself, because of the biological implications present,

2. The use of the spectral evidence of photoproduct formation as an additional probe into the complex photophysical pathways of the nucleic acid polymers.

EXPERIMENTAL

Instrumentation

1. Luminescence apparatus. A block diagram of the essential components is given in Figure 2. An individual listing of the modules is as follows:

a. Universal power supply - Required to maintain the proper amperage, voltage, needed to produce a stable light flux from the light source.

Oriel-Model No. C-72-20
Oriel Optics Corporation
Stanford, Connecticut

b. Light source - A stable, high intensity source, with a near continum in the accessible UV, was needed to satisfy the requirements relevant to both photochemistry and photophysics. A high pressure Xenon lamp was most suited to these restrictions. The operating voltage was 18 volts, while drawing 7.7 amps of current.

OSRAM XBO 150 W/1
High Pressure Xenon

c. Excitation monochromator - A 500 mm focal length grating monochromator blazed at 300 nm, and having a reciprocal linear dispersion of 3.3 mμ/mm was used to select narrow bandwidth excitation from the light source. The exit and entrance slits were opened to 3.0 mm during photochemical production, and were set to 1.0 mm for

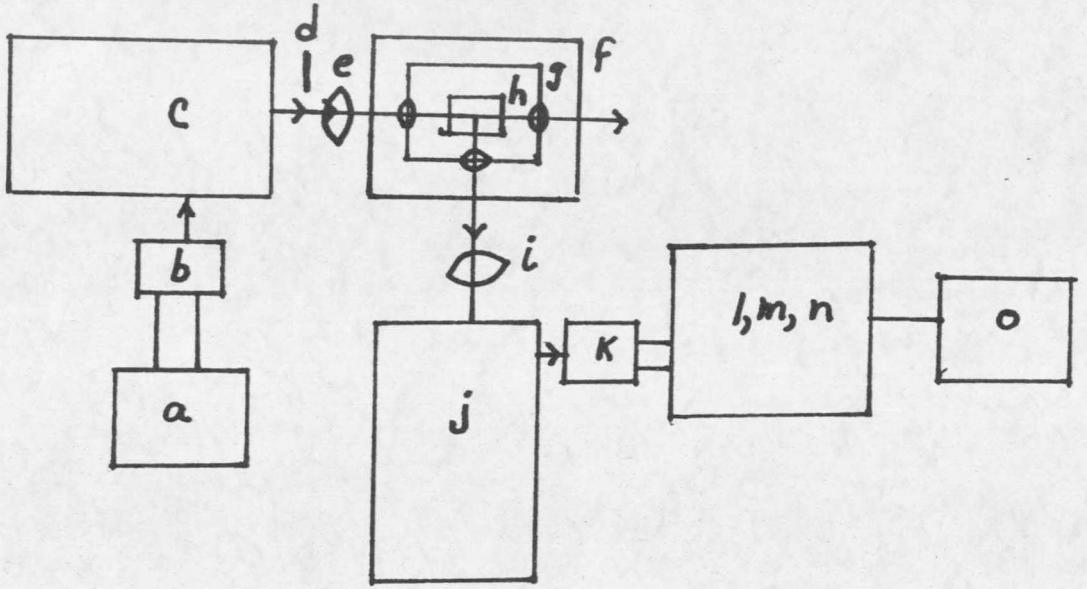

Figure 2. Block diagram (not to scale) of the luminescence apparatus.

quantum yield determinations, or for luminescence excitation spectra.

Bausch & Lomb Model 33-86-45
Rochester, New York

d. Chopper - A motor with an attached blade, having equal areas of light passage and blockage around the circumference, was used to study the light intensity dependency of the photochemistry and also provided an AC signal to the lock-in amplifier, when it was in use.

e. Condensing lens - Quartz, 11 cm focal length.

f. Cell platform - Attached to an optical rail extending from the analyzing monochromator and provided a stable platform for any cell or cell holder required.

g. Cell holder - As most work was done at reduced temperatures, it was necessary to have a holder which would also function as a dewar. A rectangular double-walled steel dewar having these dimensions: o. d. = 3.8×3.8×54 cm, i. d. = 2.3×2.3×52 cm, was used. Silica windows in three faces of the dewar allowed both absorption and luminescence measurements to be made.

Sulfrian Cryogenics
Rahway, New Jersey

h. Cell - A rectangular high purity fused silica cell. Dimensions: o. d. = 12×12×23 mm, i. d. = 6×6×20 mm.

Optical Cell Company
10792 Tucker St.
Beltsville, Maryland

i. Condensing lenses - Quartz, two 6 cm focal length lenses set 11 cm apart.

j. Analyzing monochromator - Identical to c, except that the entrance and exit slits were set at 2.0 mm for all work.

k. Photo tube - EMI 9558QB
Whittaker Corporation
Plainview, Long Island, N.Y.

l. Photometer - Laboratory Photometer-Model 11
Pacific Photomer Instruments
Berkeley, California

m. X-Y Recorder - Mosly 7030 A
Hewlet Packard
Pasadena, California

n. Lock-in amplifier - Model 122
Princeton Applied Research
Princeton, New Jersey

o. Storage oscilloscope and camera - Used to record phosphorescence decay curves.

Type 564
Tektronics, Inc.
Beaverton, Oregon

2. Absorption monitored photochemical generator

a. Absorption spectrophotometer, double beam

Cary Model 14
VARIAN

b. Steel dewar - Same as g above, except that an aluminum collar and plate were attached, so that the steel dewar with the enclosed sample cell could be placed in the sample compartment of the Cary 14.

c. Light source - Used to produce photochemistry. Operated at 50 volts, and 4 amps of current.

OSRAM HBO 200 W/2
Super Pressure Hg

d. Power supply - Gates, Model P215D
George W. Gates Co.
Long Island, N.Y.

e. Condensing lens - Quartz, 6 cm focal length. Positioned so that the area of the exciting beam was slightly larger than the entrance window area of the steel dewar.

f. 2 cm cylindrical cell - Quartz, used to hold the chemical filter solution of "Cation X (2.7-dimethyl-diaza-(3,6)-cyclopentadiene-perchlorate)". Placed between the exciting light and the condensing lens.

g. Holder - A homemade apparatus designed to keep the steel dewar and cell positioned in the beam of

the exciting light. Illustrated in Figure 3 from a side view.

3. Associated instrumental materials

a. Mineralight UV Lamp - Used to detect spots on TLC's.

Ultra-violet Products, Inc.
San Gabriel, California

b. Cell - Used for quantum counting experiments and also for chemical actinometry. Composed of silica and having rectangular dimensions of: o. d. = 12×12×48 mm, i. d. = 10×10×46 mm.

Optical Cell Co.
Beltsville, Maryland

c. Low temperature apparatus - In order to maintain the low temperatures necessary to do luminescence experiments on the nucleic acids, cooled N_2 gas was blown on the sample cell. The N_2 gas was cooled by passing the dry gas through N_2 liquid which was contained in a dewar of approximately 7 pounds capacity. The adjusted flow rate determined the degree of cooling. The temperature was monitored by means of a copper-constantan thermocouple positioned directly above the sample cell. An ice water mixture in a small dewar provided a temperature reference.

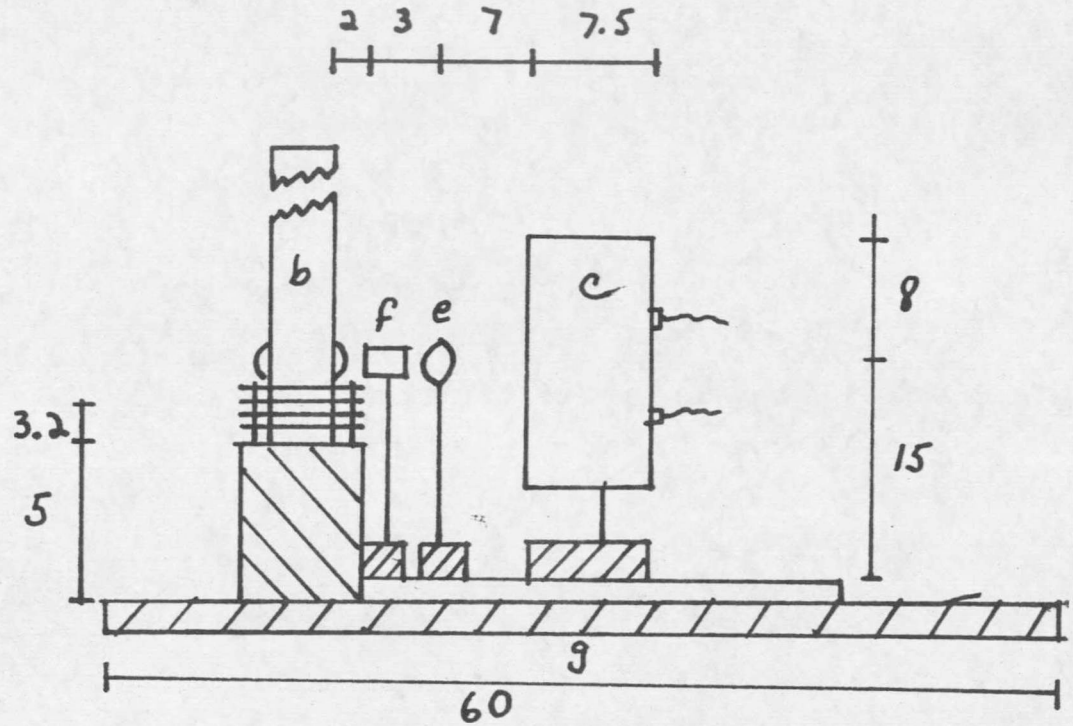

Figure 3. Absorption monitored photochemical generator, side view. Dimensions in cm.

The potential difference was read and compared to a calibration curve.

d. Absorption spectrometer, single beam - Used to measure the optical density of chemical actinometry solutions.

Beckman-Model B

e. Photochemical immersion device - Used for preparative scale photochemistry.

(1) 450-W medium pressure Hg lamp

(2) 800 ml immersion well, Pyrex

(3) power supply with Mercoid Pressure Control

Hanovia

Chemicals

1. Purity - All solid chemicals that were to be used as chromophores were the highest purity commercially available. Their optical properties, both absorbance and luminescence, were checked prior to any determination. Solvents with the exception of the glycols were distilled in a glass apparatus, and the optical properties checked prior to use. Ethylene glycol was purified by introducing activated carbon into the liquid, allowed to sit for a few days, and then passed through a sintered glass filter to

remove the carbon. All solvents tested optically free of contaminating materials as compared with distilled water subjected to the same tests, i.e., no absorbance or fluorescence in the spectral region where the pure solvents were known not to absorb or fluoresce.

2. Identity and origin

Name	Company	Lot No.
Purine	Aldrich	083017
Guanine	Cal Biochem	801853
Guanosine	Cal Biochem	300435
1 Me-Guanosine	Sigma	100C-0050
N_2, Me-Guanosine	Sigma	13C-3130
7 Me-Guanosine	Sigma	37B-5060
GMP	Sigma	87B-2350
GMP	Cal Biochem	300712
GpG	Sigma	
ApG	Sigma	46B-1030
GpA	Sigma	98B-2340
CpG	Sigma	
GpC	Sigma	
UpG	Sigma	88B-0150
GpU	Sigma	
GpT	Collaborative Research	421-40B
AMP	Cal Biochem	100275
CMP	Sigma	117B-2968
UMP	Sigma	51B-701

TMP	Cal Biochem	110012
GpG	P-L Biochem	023161
DNA	Sigma	58B-2080
Sol. RNA		
Xanthine	Nutritional Biochem	4092
Theobromine	Sigma	106B-1270
Tryptophan		
Tyrosine		
Salicylic Acid	Mallinckrodt	
Rhodamine B	J. T. Baker Chem	1-1379
DMANS	Eastman	
Quinine bisulfate	Eastman	
Cation X	Cal Biochem	620322
1-10 phenanthroline		
$Fe(NH_4)_2(SO_4)_2 \cdot 6H_2O$	Mallinckrodt	
$Fe_2(C_2O_4)_3$	Merck	
$K_2C_2O_4$	BTA	
Activated carbon	Nuchar	
Ethylene glycol	Eastman Matheson, Coleman, Bell Fluka AG, Buchs SG	
Methanol	J. T. Baker	
2-propanol	Matheson, Coleman Bell	
propylene glycol	J. T. Baker	
glycerol		
Acetone	Fisher	
$NaNO_3$		

$Mg(NO_3)_2$
$Ca(NO_3)_2$
$Zn(NO_3)_2$
$Mn(NO_3)_2$
$Cu(NO_3)_2$
$Co(NO_3)_2$
$Ni(NO_3)_2$

3. Glasses - Alcohol-water mixtures were the solvents for low temperature work. These mixtures form transparent glasses on cooling, making them an excellent medium for conducting optical measurement at reduced temperatures. The mixture most often used was of the composition; ethylene glycol:water, 7:3, Volume:volume. This solvent mixture will be referred to as G-70. The aqueous phase contained 1×10^{-2} M phosphate to maintain a pH near 7.

Calibrations and Standards

In order to quantify the results, e.g., photochemical quantum yields, and to ensure that experimental conditions remained constant for repeated experiments over an extended period of time, it was necessary to perform a series of experiments designed to calibrate the instruments; and to select a set of standards which could be used routinely to check the operational status of the instruments.

1. Temperature measurements

a. A temperature - potential difference calibration curve, previously constructed by Dr. P. R. Callis for the copper-constantan thermocouple, based on the known melting temperatures of a series of materials (plus liquid N_2), against the observed potential differences produced when the referencing material was a 0°C ice water mixture, is represented in Figure 4.

b. By carefully monitoring the flow rate of cooled N_2 gas over the sample, it was found that the observed potential difference could be maintained with ±0.05 mV of the desired reading. This corresponds to temperature variation of ±1.5°C.

c. A periodic check of the temperature monitor was made by plunging the bimetallic end of the thermocouple into liquid N_2 and observing a potential difference reading of 5.50 mV.

2. Absolute incident light intensities, I_0. The chemical actinometry method of Hatchard and Parker (23), employing potassium ferrioxalate, was used to determine the incident intensities emanating from the Xenon lamp and striking a sample cell when positioned at the cell

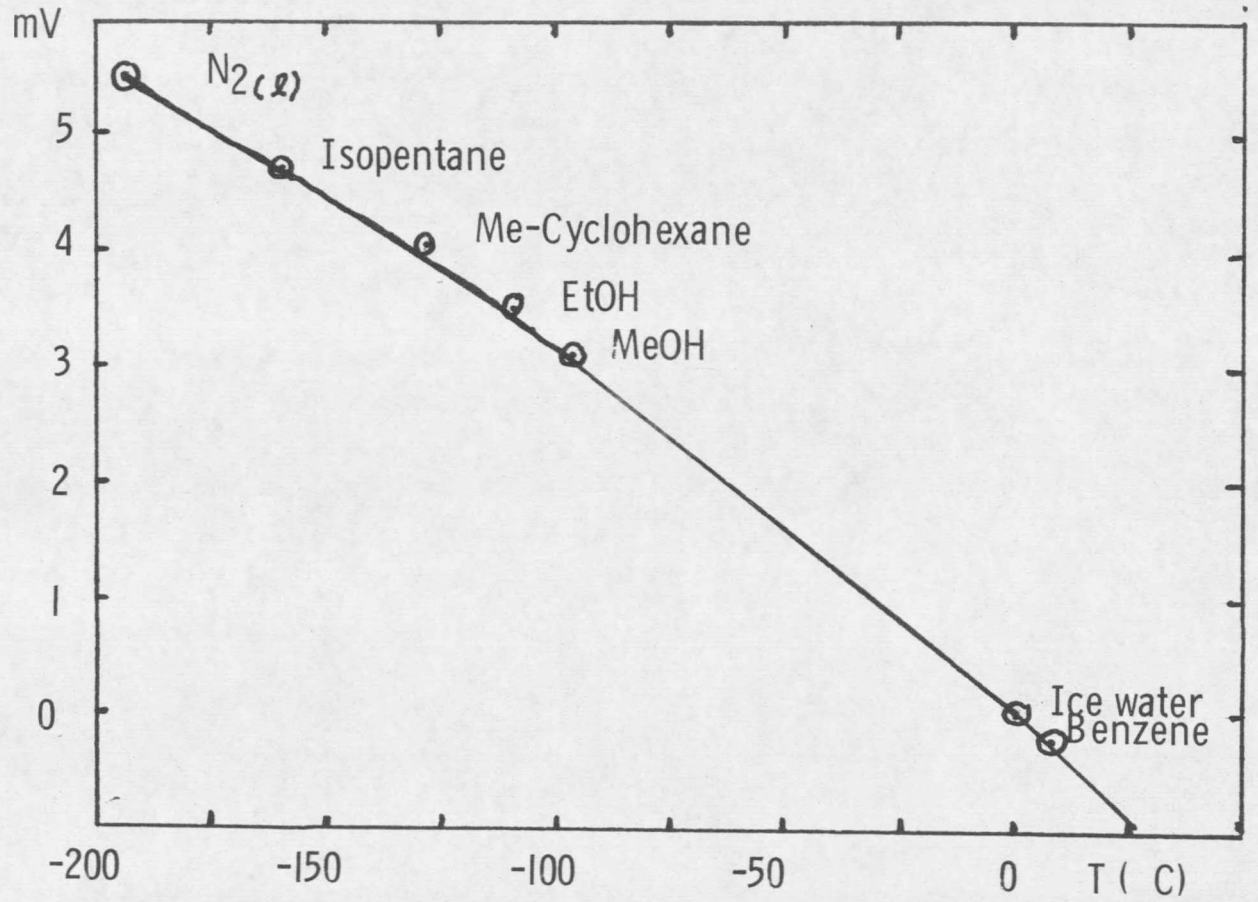

Figure 4. Calibration curve for copper-constantan thermocouple.

position of the luminescence apparatus. The method, as abbreviated from the original paper, and with the particular conditions of our experimental set-up, are described below. The method is based on the observation that the ferric ion, Fe^{+3}, is photoreduced to the ferrous ion, Fe^{+2}, with a constant quantum efficiency over an extended spectral region of excitation, when in the solution used. The amount of Fe^{+2} produced is detected by complexation with 1:10 phenanthroline, resulting in a species which absorbs strongly at 510 nm.

a. Preparation of calibration graph for ferrous iron.

(1) A series of 25 ml volumetric flasks had 0-5.0 ml of freshly prepared 0.4×10^{-3} M $FeSO_4$ in 0.1 N H_2SO_4 added.

(2) Sufficient 0.1 N H_2SO_4 to make a total of 10 ml of 0.1 N H_2SO_4, 5 ml of buffer (6:3.6,V:V,1 N NaAc:1 N H_2SO_4), and 2 ml of 0.1% of 1:10 phenanthroline monohydratic in H_2O, were added to each flask.

(3) Distilled water was added to make a total of 25 ml, the solution was mixed, allowed to stand for 40 mins., and the optical density was measured in a 1 cm

cell at 510 nm. The Beckman Model B spectrometer being the instrument used.

(4) The calibration graph formed as a result of these experiments is shown in Figure 5.

b. Preparation of 0.006 M of actinometry solution.

(1) Potassium ferrioxalate was prepared by mixing 3 volumes of 1.5 M A. R. potassium oxalate with 1 volume of 1.5 M ferric chloride. The precipitate was recrystallized from warm water and air dried.

(2) 2.947 g of the $K_3Fe(C_2O_4)_3$ 3 H_2O was diluted to 1 liter with with 0.1 N H_2SO_4 and stored in the dark. All preparation steps, as well as subsequent handling of the actinometry solution, were made with a red photographic safe-light as the only illumination source.

c. Determination of I (λ), Xenon lamp

(1) Photolize 3 ml of the acinometry solution which is contained in a 1 cm quartz cell positioned at the cell position of the luminescence apparatus. Xenon lamp as the excitation source. Excitation monochromator slit widths of 3 mm and 3 mm. Irradiation time of 60 minutes.

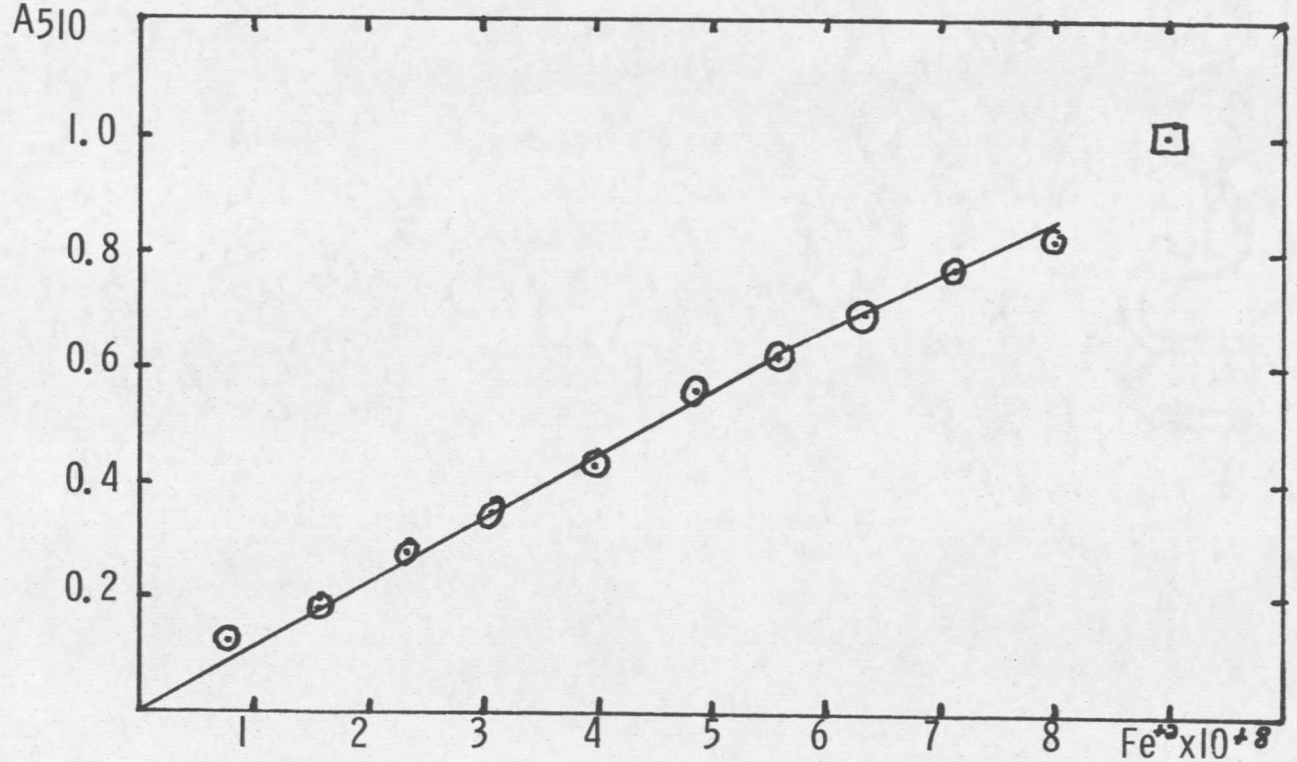

Figure 5. Ferrous ion, Fe^{+2}, calibration curve. Fe^{+2} concentration in mole/ml. ⊡ , literature value.

(2) Pipette 2 ml of the irradiated solution into a 25 ml volumetric flask. Add 2 ml of phenanthroline solution, 2 ml of buffer, water to make up to 25 ml.

(3) Mix, allow to stand for 0.5 hour, and take the optical density at 510 nm in a 1 cm cuvette.

(4) From the moles/ml of Fe^{+2} produced (as determined from the calibration graph), the Φ of 1.24, and the time of excitation, determine I_0 in units of Einsteins/min for each wavelength of excitation used.

$$I_0(\lambda_{ex}) = \text{moles } Fe^{+2} \times \Phi^{-1} \times t^{-1}$$

(5) The results for a series of determinations at different excitation wavelengths are given in Table 2.

d. Determination of I_0, Hg lamp - As the Hg lamp excitation device was located in an area which could not be darkened sufficiently to allow use of the ferrioxalate method, an alternate technique was used.

(1) Purine in methanol undergoes photochemistry, with a considerable change in extinction coefficients, Linschitz and Connolly (24). See Figure 6.

Table 2. I_0, Xenon lamp, as determined by ferrioxalate actinometry. Irradiation time 60 minutes. Monochromator slits, 3 mm and 3 mm.

λ_{ex} (nm)	$A_{510\,nm}^{(\ell=1cm)}$	$Fe^{+2}\ \frac{mole}{m\ell}\times10^{+8}$	$I^0, \frac{E}{min}\times10^{+8}$
230	0.035	0.35	0.162
240	0.050	0.50	0.232
250	0.125	1.15	0.532
260	0.135	1.25	0.578
270	0.185	1.70	0.785
280	0.320	2.92	1.35
290	0.380	3.45	1.60
300	0.410	3.75	1.69
310	0.440	4.00	1.85

(2) By monitoring the change in absorbance at 260 nm as a function of time of excitation with the Hg lamp in the device used to photolize the nucleic compounds for absorbance measurements, as compared to the absorbance change resulting when the same purine-methanol solution was irradiated with the Xenon lamp in the luminescence apparatus (excitation slits at 3 mm, λ_{ex} = 260 nm), it was determined that I_0, Hg lamp for broad band excitation (225-285 nm), is approximately 50 times that of the Xenon (half band width excitation of 10 nm at 260 nm average λ_{ex}).

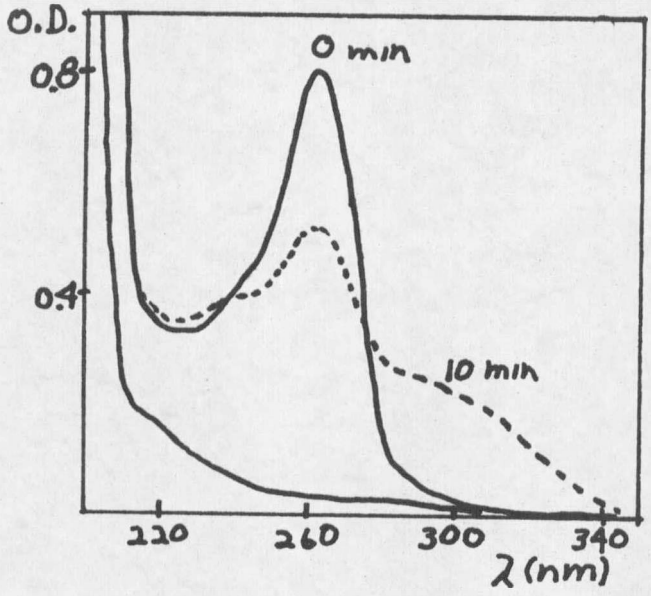

Figure 6. Spectral changes during photolysis (2537 Å) of purine in degassed methanol

(3) A 5 minute excitation of a stock solution of purine in methanol was also used as a I_0 standard for the Hg excitation apparatus before use in any photochemical result to be measured by means of absorption spectroscopy. The ΔA_{260} taken to be a measure of the I_0 of the Hg lamp at that time.

3. $I_0(\lambda)$, (relative) for Xenon lamp. While it is necessary to have a method such as chemical actinometry to determine I_0(absolute) for the measurement of photochemical quantum yields, it is also necessary to have a very precise knowledge of the relative variation of intensity of the exciting light as a function of wavelength. This was required to evaluate possible wavelength dependent phenomena which might be manifested in luminescence excitation spectra, or in photochemical action spectra. In principle, ferrioxalate actinometry could serve this purpose; but in practice, variations of up to 15% I_0 for a given λ_{ex} are observed, probably a result of having to perform analytical procedures in a darkened room. A precision of ±15% can be easily tolerated for photochemical quantum yields at a single excitation wavelength, but not where more subtle wavelength dependent effects may be involved. The

rhodamine B quantum counting technique of Melhuish (25) was found to be a simple and very effective method. A concentrated (3 g/liter) solution of rhodamine B in ethylene glycol is viewed at 90° to the exciting light, and near the frontal surface. The emission monochromator was set to 620 nm, the wavelength of the fluorescence maximum; and excitation wavelength was varied from 220-320 nm, excitation slitwidths of 1.0 mm and 1.0 mm. Due to the high dye concentration, and therefore, high optical density, any absorbed photon would be captured in a very short distance into the cell, and any variation in phototube response would be the result of a variation of the intensity of the exciting light.*

a. The results are shown in Table 3, with the relative response normalized at 280 nm. (The cell used was the 6 mm i.d. supracil cell used in low temperature work, and placed in the steel dewar, to mimic experimental conditions used for work with the nucleic acid components).

---

*Note: Since the variation observed is that for exciting light incident on the sample cell, it includes variation in the excitation monochromator efficiency with wavelength and any other wavelength dependencies of the optical components in the optical train which intercede, as well as the I_0 variation due to the Xenon lamp.

Table 3. Xenon lamp intensity measurements taken using Rodamine B in ethylene glycol.

λ_{ex}	Reading(1)	Reading(2)	Normalized	Reading(3)	Reading(4)	Normalized
220	0.4	1.1	0.025 (0.023)	.3	1.0	0.023
225	0.6	1.9	0.037 (0.039)	.5	1.6	0.037
230	1.0	3.4	0.062 (0.070)	1.0	2.8	0.064
235	1.9	5.7	0.12 (0.12)	1.6	5.0	0.11
240	2.8	8.5	0.17 (0.17)	2.5	7.7	0.17
245	3.9	12.3	0.24 (0.25)	3.5	10.8	0.25
250	5.2	16.0	0.32 (0.33)	4.6	14.0	0.32
255	6.5	19.9	0.40 (0.41)	5.9	17.8	0.41
260	8.0	24.4	0.49 (0.50)	7.3	22.0	0.50
265	9.6	29.3	0.59 (0.60)	8.7	26.5	0.61
270	11.2	34.3	0.69 (0.70)	10.7	32.3	0.74
275	13.5	40.9	0.83 (0.84)	12.7	38.2	0.87
280	16.2		1.00	14.6		1.00
285	18.6		1.15	17.4		1.19
290	21.7		1.34	20.3		1.39
295	24.6		1.52	23.4		1.60
300	27.9		1.72	26.4		1.80
305	31.3		1.93	29.5		2.02
310	34.2		2.11	32.9		2.25
315	37.6		2.32	36.5		2.50
320	39.9		2.46	40.2		2.75

(1) Measurement taken in 1 cm fluorescence cell S = 0.3.
(2) " " " " " " S = 0.1.
(3) " " " 6 mm " " S = 0.3.
(4) " " " 6 mm " " S = 0.1
Measurements taken at front edge (maximum signal) of a solution of concentrated Rodamine B with slits of 1 mm. Fluorescence viewed at 620 nm.

b. A stoppered, 1 cm path length cell was filled with the quantum counting solution and used as a fluorescence standard prior to any luminescence determination. These results are also shown in Table 3.

c. A concentrated solution of fluorescein was found to give similar results. Quine bisulphate was found to be inappropriate due to a deep minimum near 270 nm in its absorption spectrum, making quantum counting measurements in this spectral region inexact.

As a check on the quality of the $I_0(\lambda)$ results obtained by the quantum counting technique, it was decided that the uncorrected fluorescence excitation spectra of a number of compounds which have absorption maxima in this spectral region, and those for which it is known that the corrected excitation spectra are coincident with their absorption spectra, would be corrected using the $I_0(\lambda)$ results.

a. The corrected fluorescence excitation spectra, as compared with absorption spectra, are shown in Figure 7 for tryptophan, tyrosine, salicylic acid, and quinine bisulphate.

b. Equally good results were obtained with salicylic acid in G-70 at reduced temperatures, thus proving the effectiveness of the method for the nucleic acid

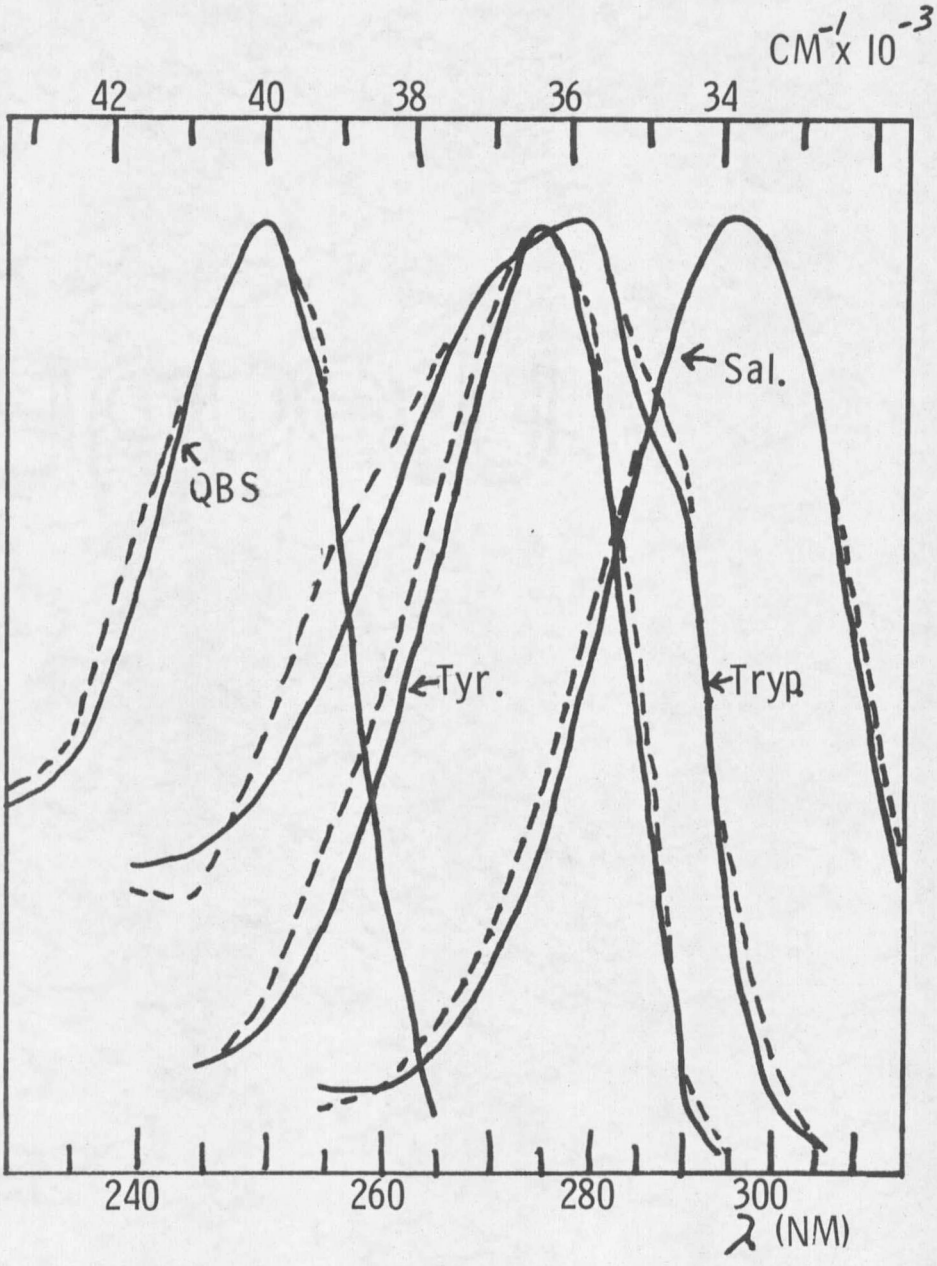

Figure 7. Absorption —— , vs. corrected fluorescence excitation spectra - - - -, for; quinine bisulphate, tyrosine, tryptophan, and salicylic acid.

components when excitation spectra are done under these conditions.

Phototube Response Curve

Luminescence quantum yields can only be obtained when the true luminescence spectra are recorded. This requires that the observed response of the detector be corrected for wavelength dependent variations of the phototube, emission monochromator, and associated components. The method of Parker (26), slightly modified, was used to obtain a total emission response correction curve. The phototube response curve is obtained from the relation $PR(\lambda_i) = R(\lambda_i)\ S/I_0(\lambda_i)$ where

$PR(\lambda_i)$ = Emission detector response at λ_i,

$R(\lambda_i)$ = The photometer reading at λ_i,

S = Sensitivity setting of the detector,

$I_0(\lambda_i)$ = The relative intensity of the exciting/emitted light at λ_i.

The key to the method is having the exciting light and the light viewed by the emission detector maintain the same relative intensities as a function of wavelength. This is accomplished by reflecting the exciting light into the emission detector by means of a metal plate coated

with magnesium oxide. The reflectivity of the MgO is constant to within a few percent over the spectral region of interest, so that the intensity distribution of the exciting light, which can be determined by the quantum counting technique, is the same viewed by the emission detector. Once the correction for $I_0(\lambda_i)$ has been made, then any variation in the emission detector response as a function of wavelength is due to a variable response of the detector components, phototube, monochromator, etc., with respect to wavelength. This variable response vs. wavelength is here termed the "phototube" response curve. This curve can then be used as a correction curve for any observed luminescence spectra.

1. $I_0(\lambda_{ex})$(relative) were extended to 600 nm by use of the rhodamine B quantum counting technique slits at 0.1 mm and 0.1 mm.

2. An aluminum plate was coated with MgO by burning magnesium ribbon under the plate.

3. The MgO coated plate was placed in the cell position of the luminescence apparatus and at an angle of near 45° to the exciting light.

4. The exciting light (λ_i) was varied from 250-600 nm and the observed response $R(\lambda_i)$, and the sensitivity setting, S, were recorded at 5 nm intervals.

5. Values for $PR(\lambda_i)$ were calculated, recorded as in Table 4, and plotted as in Figure 8.

Monochromatic Wavelength Adjustment

To ensure that the excitation and emission monochromators were recording the true wavelengths of excitation and emission, the following adjustment was made:

1. The emission monochromator was allowed to scan the spectral distribution of a low pressure Hg lamp. From the known wavelengths of the Hg resonance lines, the reading of the wavelength drum of the monochromator was adjusted to coincide at the position of the resonance peaks.

2. Light from the excitation monochromator was then reflected into the emission monochromator, both monochromators set to the same wavelength. If a maximum response was obtained, the excitation monochromator was considered calibrated. If a maximum response was not obtained, the exciting wavelength was varied until a maximum response was obtained and the wavelength reading of the excitation

Table 4. Phototube response data

λ_i(nm)	R	S	I_0(Relative)	P.R.
250	6.92	.01	0.10	.692
255	9.25	.01	0.144	.642
260	4.10	.03	0.160	.769
265	5.32	.03	0.195	.818
270	6.40	.03	0.235	.817
275	7.95	.03	0.280	.852
280	9.65	.03	0.320	.905
285	3.35	.1	0.392	.855
290	3.92	.1	0.460	.852
295	4.68	.1	0.525	.891
300	5.32	.1	0.592	.899
305	6.88	.1	0.665	1.03
310	7.10	.1	0.741	.958
315	8.90	.1	0.810	1.04
320	9.38	.1	0.870	1.08
325	3.35	.3	0.935	1.07
330	3.62	.3	0.990	1.10
335	3.90	.3	1.07	1.09
340	4.15	.3	1.128	1.10
345	4.32	.3	1.20	1.08
350	4.62	.3	1.268	1.09
355	4.82	.3	1.32	1.10
360	5.08	.3	1.365	1.12
365	5.30	.3	1.380	1.15
370	5.42	.3	1.395	1.16
375	5.35	.3	1.385	1.15
380	5.40	.3	1.440	1.13
385	5.28	.3	1.440	1.10
390	5.35	.3	1.515	1.06
395	5.45	.3	1.680	.970
400	5.48	.3	1.620	1.08
405	5.30	.3	1.590	.981
410	5.15	.3	1.635	.942
415	4.90	.3	1.605	.913
420	5.20	.3	1.71	.912
425	4.35	.3	1.520	.821
430	4.08	.3	1.575	.775

Table 4 (continued)

λ_i(nm)	R	S	I_0(Relative)	P.R.
435	4.15	.3	1.545	.803
440	3.90	.3	1.500	.780
445	3.85	.3	1.380	.837
450	6.52	.3	1.620	1.21
455	3.80	.3	1.500	.760
460	4.00	.3	1.725	.694
465	4.00	.3	2.10	.571
470	4.40	.3	2.70	.489
475	3.00	.3	2.20	.409
480	3.55	.3	1.80	.592
485	2.88	.3	1.97	.441
490	7.08	.1	1.66	.426
495	6.80	.1	1.89	.360
500	6.10	.1	1.62	.377
505	5.72	.1	1.63	.351
510	5.62	.1	1.63	.345
515	5.62	.1	1.68	.335
520	5.38	.1	1.71	.315
525	4.50	.1	1.70	.265
530	3.85	.1	1.59	.242
535	3.52	.1	1.53	.230
540	3.18	.1	1.48	.215
545	9.52	.03	1.41	.203
550	8.25	.03	1.38	.179
555	8.40	.03	1.35	.187
560	7.72	.03	1.31	.177
565	7.10	.03	1.29	.165
570	6.45	.03	1.32	.146
575	5.60	.03	1.35	.125
580	5.55	.03	1.36	.122
585	4.65	.03	1.41	.099
590	4.80	.03	1.37	.105
595	4.20	.03	1.35	.093
600	3.70	.03	1.35	.083

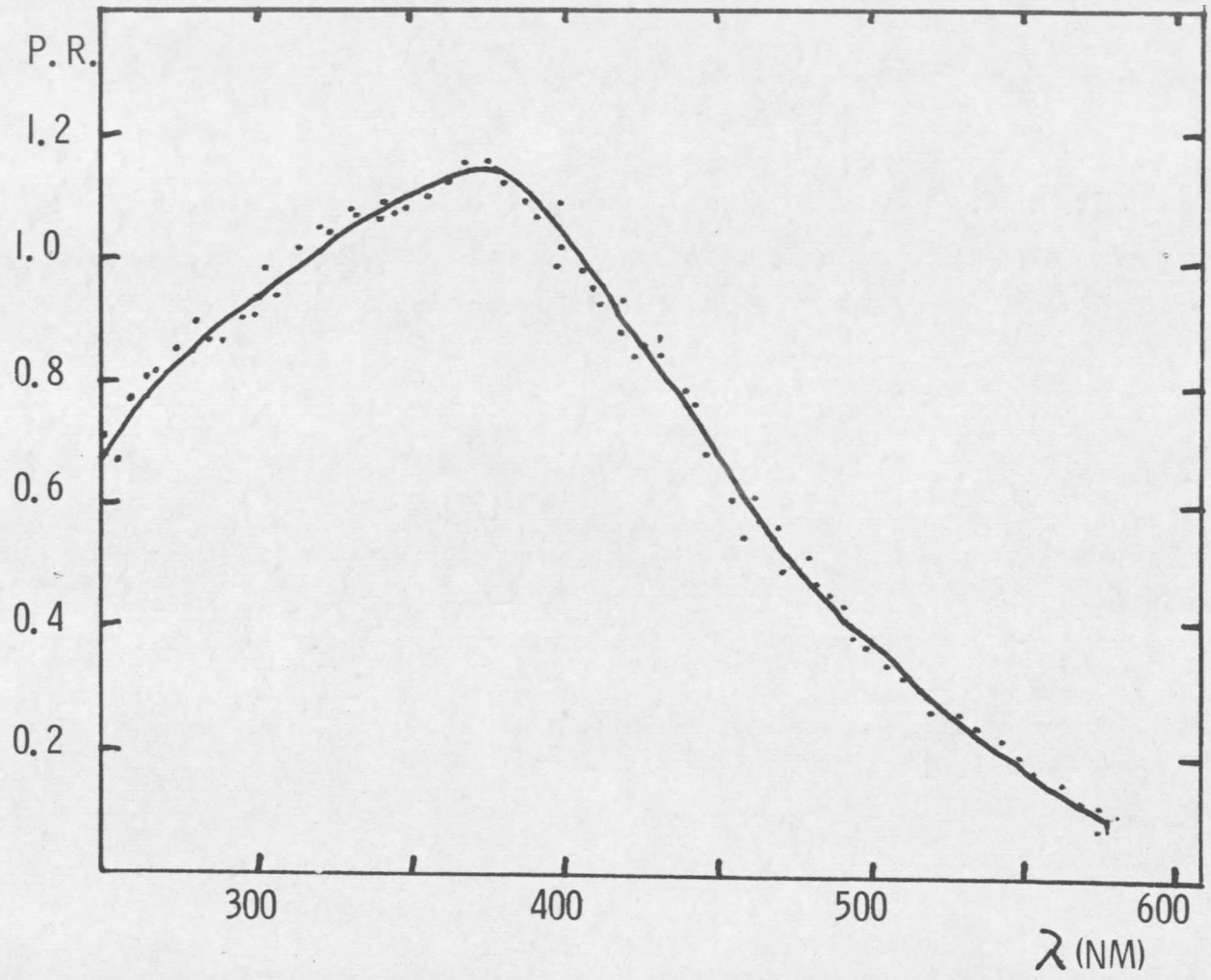

Figure 8. Phototube response curve.

monochromator was changed to correspond to that of the emission monochromator.

Experimental Techniques

1. Absorption spectroscopy. All absorption measurements, with the exception of chemical actinometry determinations, were made with the Cary 14 double beam absorption spectrophotometer.

a. The steel dewar and supracil cell were used throughout; the aluminum collar and plate attached to the steel dewar allowed the apparatus to be lowered into the sample compartment of the spectrophotometer.

b. All solutions were made up to have an initial optical density at the absorption maximum of from 0.5 to 0.8 O.D. units at room temperature.

c. A baseline of cell plus solvent was determined prior to any absorption measurement.

d. All spectral scans were made at a scan rate of 10 Å/sec.

e. Freshly prepared solutions were allowed to stand for a period of time and the O.D. at the maximum checked periodically until no further change in absorption was evident, insuring complete dissolution had occurred.

f. A Beer's law determination was made for those solutes, e.g., guanine, which are known to aggregate at higher concentrations

g. Spectral scans were made at room temperature and at reduced temperatures to observe the effects on the spectra due to solvent contraction, variation in the Boltzmann distribution, and hypochromism due to increased interaction in the dinucleotide cases. The low temperature spectra were used to compare with fluorescence excitation spectra taken at the same temperature-viscosity conditions.

h. Spectra taken at room temperature were compared with published spectra, when available, as a check on the purity of the solutes.

i. Spectra used for quantitative measurements were scanned only for 5 nm intervals, and stop-scan absorption measurements were taken at the beginning and end of these intervals throughout absorption envelope.

j. For low temperature measurements, the solution was allowed 15 minutes (to equilibrate), after the desired temperature was indicated on the potentiometer. Dry air was blown on the outer surfaces of the dewar windows to prevent fogging.

k. After periods of photochemical production, achieved by placing the dewar with enclosed cell and solution in the photolysis apparatus previously described and subjecting the cooled solution to high intensity UV excitation by the high pressure Hg lamp, the dewar was replaced in the Cary 14 sample compartment and the spectral scan remade over the original scan to elicit changes resulting from the photochemistry.

1. Air in the reference compartment provided a referencing medium

2. Luminescence spectroscopy. The luminescence apparatus as previously described was used for all luminescence determinations.

a. The Xenon lamp source was ignited and allowed 0.5-1.0 hr warm-up prior to use.

b. The rhodamine B quantum counting solution contained in the stoppered 1 cm silica cell was placed in the sample cell holder and the optical block translated in an X-Y manner until a maximum response was obtained on the fluorimeter. The emission monochromator being set to 620 nm, and the excitation monochromator set to 320 nm with slitwidths of 1.0 mm and 1.0 mm or 3.0 mm and 3.0 mm

depending on the subsequent experiments to be performed. Phototube voltage set to 1040 volts. An observed response of 3.50 for a Y gradient setting of 1 mV/in. and a sensitivity of 3 and 0.3 for the respective slitwidths was taken to be the standard response. The excitation monochromator was then varied from 220 nm to 320 nm and the scan recorded to give a measure of the I_0 in this spectral region.

c. Solutions, whose luminescence properties were to be studied, were made by diluting the stock solutions used in absorbance work, so that the optical density for a 6 mm pathlength, at the absorbance maximum was 0.20 O.D. units. Then by viewing only the front half of the sample cell, an effective O.D. of 0.10 was obtained. Inner filter effects were thus minimized and the expression for absorbed intensity $I_a = I_0(1 - 10^{-C\ell})$ could be simplified to $I_a = I_0 2.3\ C\ell$ without introducing an error of greater than 10%.

d. The quantum counting cell was replaced with the steel dewar and enclosed sample cell, the orientation such that 90° luminescence could be observed. The exit slit to the excitation monochromator was closed to prevent photochemistry production during the preliminary cooling period.

e. The cooling mechanism was set in place and activated; the $N_2(g)$ flow rate being reduced as the desired temperature was approached. Care was taken not to cool below the desired temperature as the glass formed was subjected to cracking on warming. On reaching the desired temperature, a period of 15 minutes was allowed for the solution to stabilize, prior to any luminescence measurement. Dry air was blown on the exterior dewar windows to prevent moisture condensation. A visual observation of the sample solution through the dewar windows prevented experiments being done with cracked glasses.

f. Luminescence spectra to be used for quantum yield determinations were obtained by exciting at the wavelength of the absorbtion maximum, through 1.0 mm slits, and allowing the emission monochromator to scan the emitted light. A scan from 250 nm to 500 nm at 25 nm/in. on the X axis of the recorder was sufficient for most molecules studied.

g. The exciting light wavelength was then changed at 10 nm intervals through the absorption envelope, the fluorescence maximum was made to be the normalization point by varying the sensitivity, and luminescence scans were made at each excitation wavelength. An invariance in

the shape of the luminescence curve was taken to mean the absence of emitting impurities. This was found to be the case for all monomers having a good signal to noise ratio. For some dinucleotides, a variation in shape is to be attributed to a variable ratio of excimer to monomer concentration which is wavelength dependent.

RESULTS AND DISCUSSION

While the original evidence showed photochemical production in both ApG and ApA, it was established early in the research that the photochemistry occurring in ApG was due to photoalteration of the GMP moiety alone. GMP alone would give the characteristic evidence for the photochemistry, whereas AMP alone exhibited no spectral change when irradiated.

ApA showed only minor alteration in its absorbance properties on photolysis, making analysis by this technique difficult. For this reason, the ApA photochemical phenomenon was set aside rather early in the research, and has not been investigated further. However, it remains an intriguing problem, especially since, as found, AMP does not show similar effects.

As a consequence, this writing is concerned principally with the photophysics and photochemistry of molecules containing, or are the derivatives of, guanines.

1. Absorption monitored photochemistry.

a. Guanine Base, Nucleoside, Nucleotide.

Guanine, guanosine, and suanosine monophosphate (GMP) all gave the same evidence for photochemistry, qualitatively and quantitatively, when subjected to intense UV excitation

by the high pressure Hg light source. The photolysis apparatus was the Absorption Monitored Photochemical Generator described in the experimental section. The solvent used was a G-60 or G-70, buffered to pH 7; and the temperature, -110°C.

A typical set of absorption spectra taken after periods of photolysis is shown in Figure 9. The molecule undergoing the photochemical change in this case was guanosine.

The clearly defined isobestic points at 287 nm and 235 nm give evidence for two interconverting species.

The absorption scan taken after 90 minutes irradiation is representative of the absorption spectrum of the low temperature photoproduct, assuming complete photoconversion has occurred. The fact that a doubling of excitation dosage by increasing the photolysis period to 180 minutes results in no significant absorbance changes is in favor of this. Fluorescence excitation spectra and fluorescence polarization studies (to be discussed later) support the correctness of this viewpoint. The molar extinction coefficients then, for the low temperature photoproduct, as measured by comparison to the known value for guanosine of $\epsilon_{252} = 13.7\times10^{2}$ would be 8.3×10^{3},

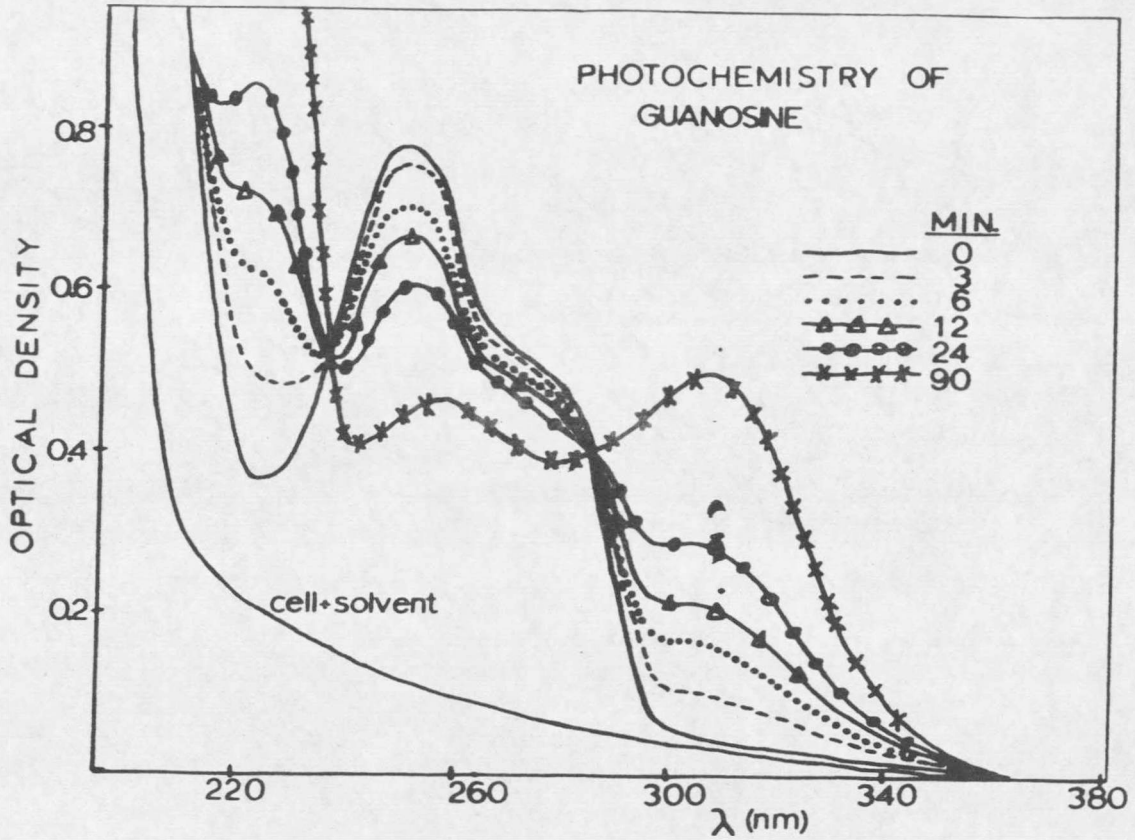

Figure 9. Absorbance changes in guanosine after periods of UV photolysis.

3.7×10^3, and 19.4×10^3 at 305, 265, and 225 nm, respectively.

An extended period of photolysis of ApG (photolysis period of >60 minutes) and examination of the absorbance spectrum after this time, showed that subtracting away the absorbance of the photoproduct based on the ϵ's obtained in the GMP complete conversion, resulted in an absorbance spectrum equivalent to that expected for initial AMP content. The absorbance at 305 nm provided the relative measure of the absorbances for the photoproduct in the 230 nm to 290 nm region.

It is of particular significance that the photoproduct has a strong transition at a lower energy than the first excited singlet of guanine, or, for that matter, any of the normal nucleic acid components. This means that the photoproduct once produced, can be excited independently of the parent guanine, or any other portion of a nucleic acid polymer, by exciting at wavelengths longer than 300 nm.

The low temperature product is thermally unstable as the spectral features revert to those of the parent molecule on allowing the solution to warm to room temperature. Occasionally, this reversion did not appear to go

to completion, which indicated some residual low temperature product, or perhaps another product formed from the low temperature species.

Photolysis of the solution at room temperature for periods of up to 30 minutes elicited no absorbance changes.

Photochemical quantum yields were not attempted in the absorption monitored mode as accurate intensity values were not available for the Hg lamp, and the irradiation was not nearly monochromatic. Hence, photochemical yields were measured relative to the GMP monomer case, as described below.

b. Other purines, GMP containing dinucleotides. Relative photochemical quantum yields by means of absorption spectroscopy were determined by observing the increase in the absorption due to the photoproduct at 305 nm after a period of 15 minutes excitation by the high pressure Hg source. Solvent and temperature conditions were the same as in A above, and the initial optical density, 0.50-0.60, at the parent maximum.

The expression describing the increase in photoproduct concentration with time of irradiation is,

$$\frac{d[\text{Product}]}{dt} = I_{ab}\ \Phi_{PC}.$$

The relation used to determine the apparent relative yields based on the fraction of light absorbed by the GMP present was:

$$\Phi(1)^{\text{Rel}}_{\text{PC}} = \left(1 + \frac{\epsilon_i C_i \ell}{\epsilon_G C_G \ell}\right) \times \frac{[1 - 10^{-(\epsilon_i C_i + \epsilon_G C_G)\ell}]^{-1}}{(1 = 10^{-\epsilon_G C_G \ell})^{-1}} \times \frac{\Delta A_{305}}{\Delta A_{305}(\text{GMP})}$$

where:

$\epsilon_i C_i \ell$ = absorbance of any absorbing species other than GMP at the absorption maximum,

$\epsilon_i C_i \ell$ = absorbance of GMP at the absorbing maximum,

$1 - 10^{-(\epsilon_i C_i + \epsilon_G C_G)\ell}$ = fraction of the incident light absorbed at the parent absorption maximum (252 nm),

ΔA_{305} = change in absorbance at 305 nm for the period of excitation.

In reduced form, the relation is the absorbance change at 305 nm, normalized by the fraction of incident light absorbed by the GMP moiety at 252 nm.

$$\Phi(1)^{\text{Rel}}_{\text{PC}} = \frac{\Delta A_{305}}{\frac{\epsilon_G}{\epsilon_G + \epsilon_i} \cdot f_{ab}^{\text{Tot}}} = \frac{\Delta A_{305}}{f_{ab}^{\text{GMP}}}$$

Normalized to the GMP value

Also calculated was the relative photochemical yields based on the fraction of the incident light absorbed at 252 nm and normalized to the GMP value.

$$\overset{\text{Rel}}{\underset{\text{PC}}{\Phi(2)}} = \frac{\Delta A_{305}}{f_{ab}^{\text{Tot}}}$$

The pertinent experimental data and the calculated values for (1) and (2) are collected in Table 5. The molecules in this compilation are GMP and a number of GMP containing dinucleotides. The column headings in the table have the following meanings:

A_{252}^{Tot} = the absorbance of the solution, prior to photolysis, at 252 nm,

$\frac{\epsilon_G}{\epsilon_G + \epsilon_i}$ = fraction of absorbance due to GMP at 252 nm, when in a dinucleotide, (For the dinucleotides, the concentrations are necessarily equal; and the nucleotides are assumed to be independently absorbing.)

f_{ab}^{Tot} = the fraction of the incident light absorbed at 252 nm $(1 - 10^{-(\epsilon_G + \epsilon_i)C\ell})$,

ΔA_{305} = the O.D. change observed at 305 nm as the result of photolysis,

$\Phi^{Rel}_{PC}(1)$ = as defined above

$\Phi^{Rel}_{PC}(2)$ = as defined above

Table 5. Φ^{Rel}_{PC} of dinucleotides via absorption mode

	A^{Tot}_{252}	$\frac{\epsilon_G}{\epsilon_G+\epsilon_i}$	f^{Tot}_{ab}	ΔA_{305}	$\Phi^{Rel}_{PC}(1)$	$\Phi^{Rel}_{PC}(2)$
GMP	0.535	1.00	0.708	0.185	1.00	1.00
ApG	0.590	.48	0.743	0.185	1.99	0.95
GpA	0.630	.48	0.765	0.210	2.19	1.05
CpG	0.515	.70	0.694	0.055	0.43	0.30
GpC	0.530	.70	0.704	0.070	0.54	0.38
GpU	0.565	.58	0.727	0.094	0.85	0.49
dGpT	0.525	.58	0.701	0.195	1.83	1.06
GpG	0.580	1.00	0.737	0.195	1.01	1.01

A repetition of the experiments did not show a variation of more than 15% for any determination, indicating the precision of the measurements.

Examination of the relative yields shows some rather striking results.

1. The dinucleotides ApG and GpA have a nearly two-fold increase in photochemical yield based on the fraction of light absorbed by the GMP portion of the molecule. In terms of Φ_{PC} based on light absorption by the molecule as a whole, the indication is that the light absorbed by the AMP is as effective in producing GMP photochemistry as that light absorbed by the GMP portion.

2. GpT shows a yield enhancement almost equal to that of ApG or GpA.

3. The CMP and UMP containing dinucleotides, on the other hand, exhibit an opposite effect. The relative photochemical yields are substantially reduced in these cases.

It should be noted that the use of the 252 absorbance maximum of GMP was used for the calculations of I_{ab} because there is a bright line of the high pressure Hg lamp in this wavelength region (~248 nm); however, there are additional intense lines in the region of 270-290 nm, which were present, and for those dinucleotides having a significantly different ϵ's in this region, an analysis of Φ_{PC}^{Rel} based in I_{ab} (252 nm) would not be accurate.

Experiments conducted with other purine molecules; AMP, xanthine, hypoxanthine, and caffeine under the same

condition as the guanine molecules were subjected to, showed little or no evidence of photoalteration.

c. pH dependence. To determine the effect of pH on the relative photochemical yields of ApG, the solvent mixture of G-70 had added to it, dropwise amounts of either concentrated NaOH or concentrated H_2SO_4 until the desired pH was obtained. The initial volume of solvent used for a determination was 10 ml, so that the addition of up to 10 drops of concentrated acid or base would not substantially alter the alcohol:water composition of the solvent. The pH was read to the nearest pH unit with Hydronium Ion Paper. The ApG was added to a portion of the pH adjusted solvent and the concentration was adjusted by dilution until the O.D. at 252 nm was near 0.5. The photolysis was conducted in the same manner as was previously done for ApG dissolved in G-70 and buffered to pH 7.

The results show that the photochemical yield as evidenced by the ΔA_{305}, remains nearly the same down to pH 5; while at pH $\leq$ 3, the photochemical yield drops to one-third that at the higher pH's.

d. Alcohol dependence. To determine the necessity of the glycol component in the solvent, in addition to

its role in the formation of an aqueous glass at reduced temperatures, various alcohols were substituted for the ethylene glycol in the solvent mixture. Alcohols used were; methanol, glycerol, 1,2 propanediol, and 1,3 propanediol. The diols and glycerol were mixed in the same 7:3 alcohol:water, V/V portions as had been used previously for G-70. Methanol-water mixtures were made in a 12:1, V/V proportion because of the reduced viscosity of methanol as compared with glycols.

Both diols and glycerol solvent mixtures provided an environment conducive to GMP photochemistry as evidenced by the characteristic spectral changes produced when GMP was subjected to irradiation in the solvent mixtures described (at reduced temperatures).

The methanol-water solvent mixture did not promote GMP photochemistry even when the temperature was reduced to successively colder temperatures to mimic the viscosity conditions present when G-70 was the solvent mixture. Only when ethylene glycol was added to the solvent mixture in amounts of 20% of the total volume did the GMP photochemistry resume on irradiation.

It would appear then that a diol component is a requirement for the guanine photochemistry at reduced temperatures.

e. Temperature-viscosity dependence. A variation of the temperature of the GMP solution where G-70 was the solvent, and the measurement of the relative photochemical yields under these conditions, provided the results shown in Figure 10. The data points for this set of experiments are circled ⊙ . Also shown in this same figure are results obtained when glycerol was substituted for ethylene glycol in the solvent mixture and GMP photolysis conducted at the indicated temperature. Data points for this experimental set are enclosed in boxes ⊡ .

A comparison of the two data sets indicate a viscosity dependence for the yield, as the glycerol-water solvent mixture is much more viscous than the ethylene glycol-water solvent mixture at any temperature above the temperatures where both solvents are rigid glasses. (Quantitative viscosity measurements were not made; but the macroscope differences in viscosity can be readily observed on a qualitative, and semi-quantitative, basis by the resistance to intrusion into the particular solvent mixture of a stiff wire). As the glycerol-water mixture forms a

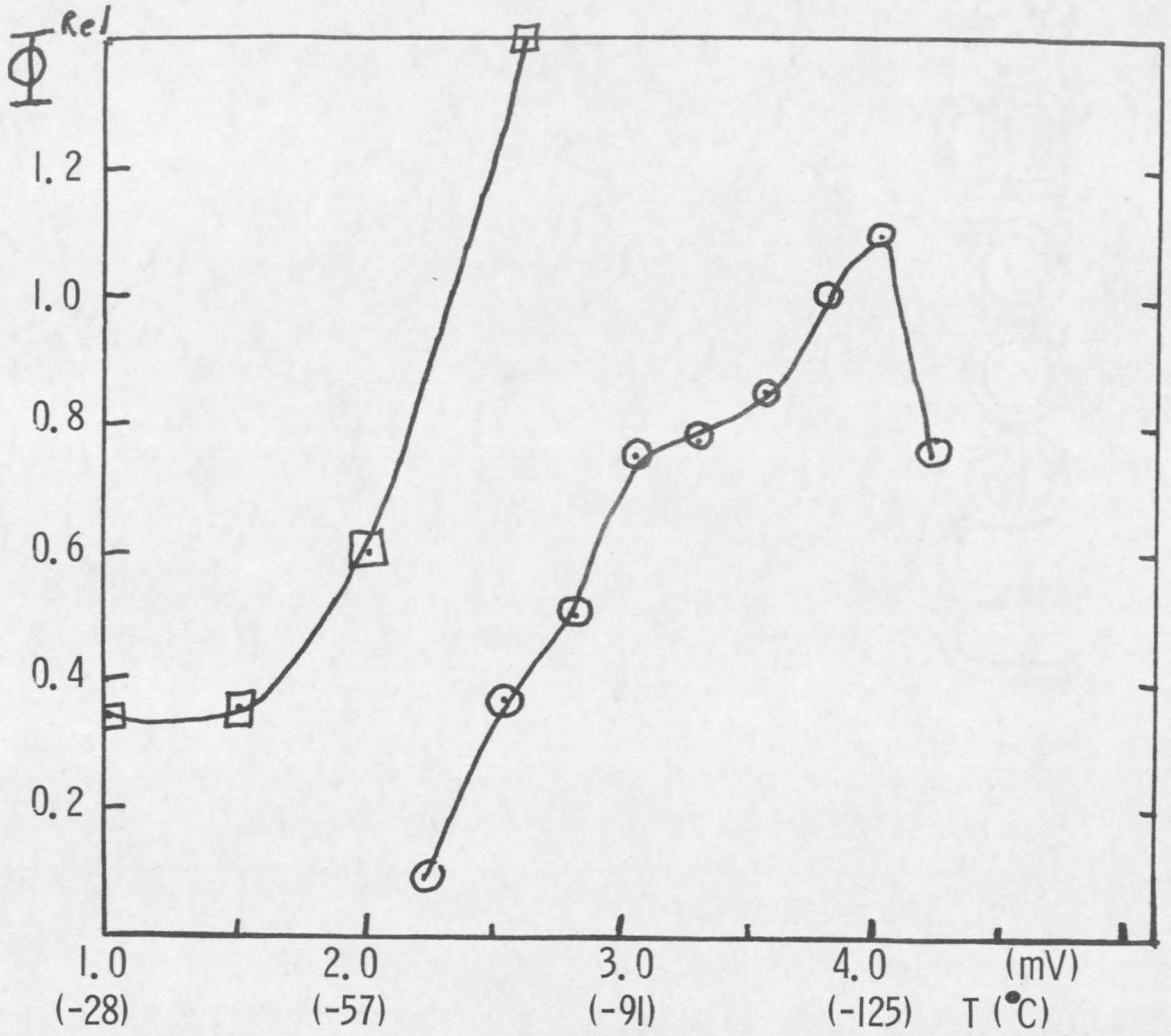

Figure 10. Temperature-viscosity dependence of GMP photochemistry. , G-70 solvent. , glycerol-water solvent.

rigid glass at considerably higher temperatures than the G-70, it was not deemed advisable to cool this mixture below about -70°C for fear of fracturing the supracil quartz cell.

The curve generated by the data points for the case where the G-70 solvent is the medium for the GMP photochemistry appears somewhat irregular, and a discussion of its shape will be deferred to a later section when luminescence data can be added for clarification.

f. Metal ion dependence. The addition of metal ions to the solution in nearly equimolar amounts with the disssolved GMP, 1×10^{-4} M, caused a severe reduction of the photochemical yield in some cases. Evidence for complex formation was also seen in some cases in the low temperature absorption spectra previous to photolysis. The relative photochemical quantum yields, and the ratios of the observed absorbances at 250 and 280 nm, 250 and 270 nm, prior to irradiation, are listed in Table 6. The metals were obtained as the nitrate salts and were used without additional purification. Photolysis time was 10 minutes, temperature of -112°C.

Complex formation, then, between the GMP chromophore and paramagnetic ions such as Cu^{2+}, Ni^{2+}, and Co^{2+}

causes a substantial reduction in photochemical yield. Zn^{2+}, although showing an indication of complexation, has no effect on the photolysis yield. Zn^{2+} is a diamagnetic ion. A repeat of the Mg^{2+} case gave a value of 1.00 for the photochemical yield.

Table 6. Effect of M^{n+} on GMP Φ_{PC}

M^{n+}	Na^{+}	Mg^{2+}	Ca^{2+}	Zn^{2+}	Mn^{2+}	Cu^{2+}	Ni^{2+}	Co^{2+}
Φ_{PC}^{Rel}	1.00	0.87	0.97	1.06	1.00	0.06	0.14	0.24
A_{270}/A_{250}	0.68	0.70	0.68	0.66	0.70	0.61	0.63	0.65
A_{280}/A_{250}	0.59	0.59	0.60	0.63	0.61	0.63	0.65	0.65

The literature values for A_{270}/A_{250} and A_{280}/A_{250} are 0.685 and 0.595, respectively (27).

Similar experiments conducted using ApG as the absorbing chromophore and the introduction of the metal ions Na^{+}, Ca^{2+}, Zn^{2+}, Co^{2+}, Ni^{2+}, and Cu^{2+} into the solutions showed that only Cu^{2+} was effective in reducing the photochemical yield. $\Phi_{PC}^{Rel} = 0.34$.

A review of metal-nucleic acid interactions has been published (28); and a more recent discussion of the possible causative or preventative roles of metal ions in cancer formation is also available (29). Previous

information as indicated in these reviews* pointed to an interaction of the Cu^{2+} ion with both the phosphate and base portions of the GMP molecule. Ni^{2+} and Co^{2+} have been thought to bind only at the phosphate and with a k_F of an order of magnitude less than that of Cu^{2+}. The results of the experiments performed in this investigation tend to favor the larger k_F with Cu^{2+}, but what may be of more significance is the apparent requirement that all three of the ions Cu^{2+}, Ni^{2+}, and Co^{2+} be situated in the vicinity of the base portion of the molecule to demonstrate the large effects on the photochemical yields. Luminescence yield values for these complexes, to be discussed in a later section, are complimentary to the photochemical yield results.

2. Luminescence monitored photochemistry and spectroscopy studies.

a. GMP photochemistry. Equally dramatic effects occur in the luminescence when GMP undergoes photolysis at reduced temperatures. An example of this is shown in Figure 11 which shows the fluorescence from a solution

---

*Pertaining to aqueous solution and room temperature.

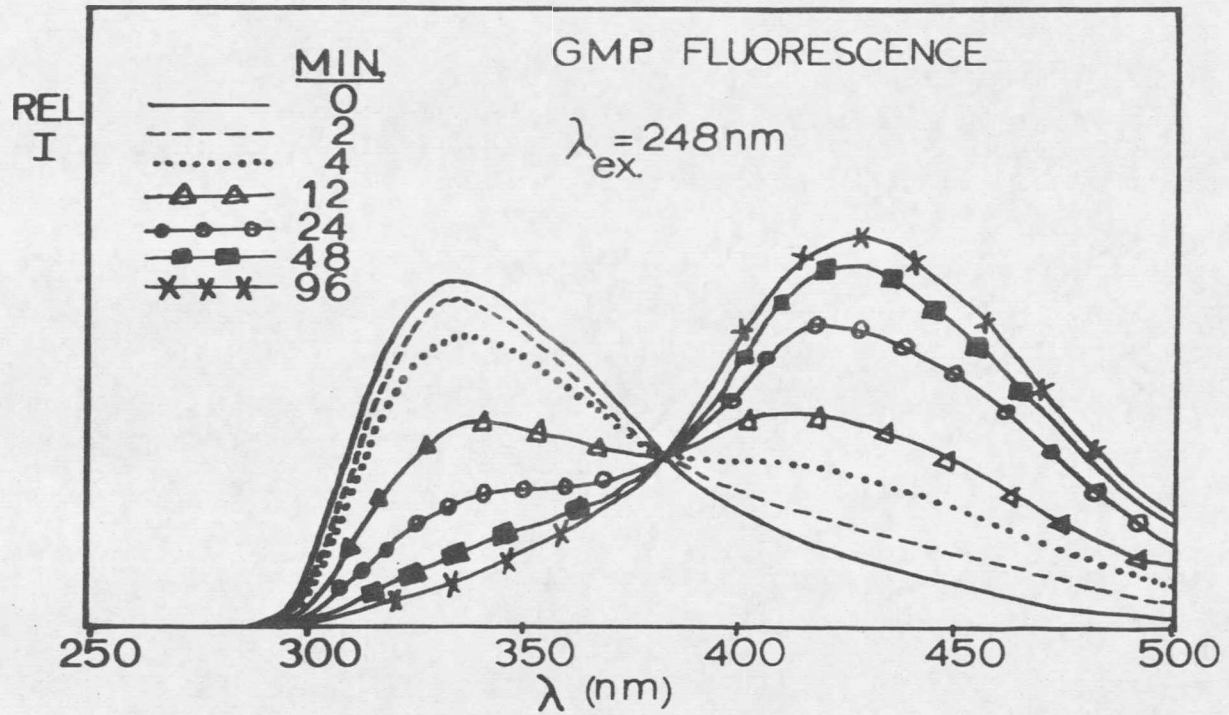

Figure 11. Fluorescence changes of GMP with time of UV photolysis.

of GMP in G-70 at -110°C, while being irradiated with 248 nm light. It is seen that as the time of irradiation increases, the fluorescence due to the GMP, which has a maximum at 328 nm, decreases, while a new fluorescence with a λ^{F}_{max} at 418 nm increases. The presence of the isotylbic point indicates that only two species may be involved in the transformation.

After irradiation at 248 nm, excitation at wavelengths between 305 and 350 nm yields the 418 nm fluorescence, whereas only the very weak fluorescence from the solvent was observed before irradiation. This is illustrated in Figure 12 and is the result of the low temperature photoproduct having its first transition in this region.

Drobnik and Augenstein (30) have reported observing a fluorescence characteristic of that of the photoproduct from solutions of deoxyguanosine in ethylene glycol-water at approximately -100°C, and have attributed it to aggregation of the deoxyguanosine molecules, not to photochemistry. The process reported here does not occur in the dark, so that it is likely that these workers inadvertently left their excitation monochromator slits open while cooling the solution.

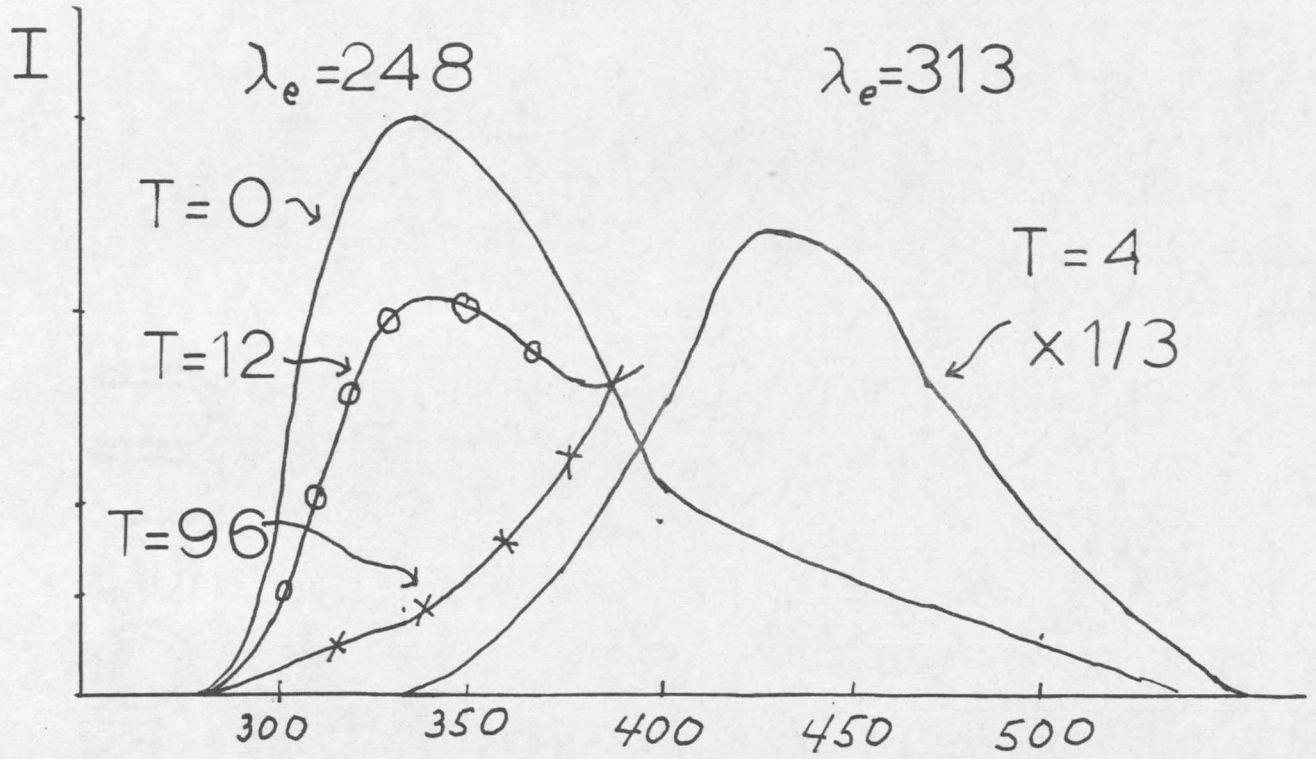

Figure 12. Changes in the fluorescence spectrum of GMP on photolysis. T = time of photolysis.

The advantage of examining the photochemical evidence in the luminescence mode is that an order of magnitude less concentrated solutions may be used, and a signal may be produced which is characteristic only of the photoproduct, i.e., excitation at λ's > 300 nm results in the exclusive fluorescence response of the photoproduct, once formed in small amounts.

b. Intensity dependence, acetone sensitization, and photochemical quantum yield, or GMP.

(1) Intensity dependence. Certain types of photochemical and photophysical processes are known to have other than a first-order dependence on the intensity of the exciting light, I_0, e.g., alkylbenzene-sensitized decomposition of hydrocarbon solvents as the results of triplet-triplet absorption following singlet-singlet absorption and intersystem crossing (31). An experiment was performed to determine if a similar non-linear dependence of I_0 was operative for the GMP photochemistry.

A 10 minute 250 nm excitation of a 0.2 O.D. solution of GMP in G-70 was made in the luminescence apparatus at -110°C. The decrease in the parent fluorescence and the increase in the 418 nm fluorescent maximum peak (excitation λ = 313 nm) were noted.

The method was repeated, except that a light chopper was placed in the excitation beam. The chopper blade was of a construction that provided equal periods of light passage and light blockage, thus causing I_0 to be reduced by a factor of 0.5 for the excitation period.

The results showed that the photochemical yield, as evidenced by both the reduction in parent fluorescence and the product fluorescence growth, was halved by a halving of I_0. Two repetitions of the experiment gave a precision of 10%, with the signal to noise ratio of the fluorescence being 20:1. The I_0 dependence for the photochemistry proved to be first order for the excitation intensities used.*

(2) Acetone sensitization. Energy transfer experiments designed to determine the photoreactive spin state of GMP, using acetone as the donor molecule, are termed photosensitization, to differentiate from the energy transfer experiments conducted for the intramolecular case, i.e., dinucleotides.

The principle behind the method is illustrated in Figure 13. Acetone has a lower energy transition for its

---

*This analysis is correct only if the $^3\tau$ is $> 10^{-3}$ sec., the chopping frequency.

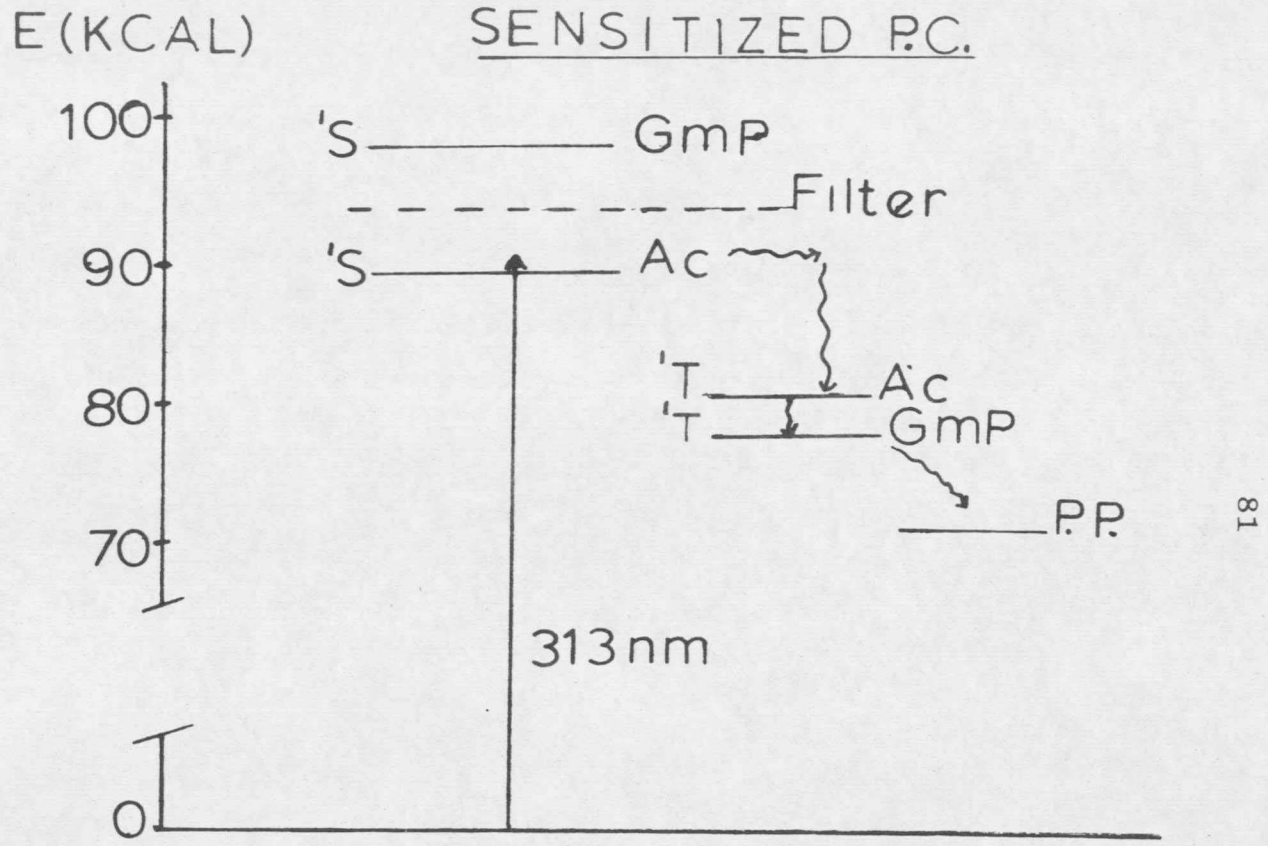

Figure 13. Acetone sensitization.

first excited singlet state than does GMP. Consequently, irradiation with 313 nm light will populate ^1S of acetone exclusive of ^1S of GMP. The intersystem crossing yield of acetone is near unity (0.95) so that the excitation is transferred with high efficiency to ^1T of acetone. While acetone has the lower energy singlet, GMP has the lower energy triplet state. Thus, there exists the possibility of triplet energy transfer from acetone to GMP, if the molecules are in close proximity. The experiment performed to detect photochemical production by GMP under these conditions is described below.

The solvent was made to be H_2O:$(CH_3)_2CO$: EG, 3.5: 1.0:7.5, V:V:V, with GMP as solute.

An optically dense (O.D. > 2.0 at 250 nm) solution of GMP + CMP was used as a chemical filter to additionally insure that there was negligible probability of population of ^1S of GMP.

The excitation monochromator was set to provide a mean excitation wavelength of 313 nm with slit widths of 3 mm and 3 mm. With the reciprocal linear dispersion of 3.3 nm/mm for the monochromator, the half-band width of excitation was then near 10 nm. The luminescence monochromator was set to 418 nm, the F_{max} of the photoproduct.

After cooling to -110°C and opening the shutter of the excitation monochromator, the characteristic fluorescence response of the GMP photoproduct was seen to grow in with time of excitation. Exclusive of any other effects such as hydrogen abstraction of the solvent by acetone, the indication is that the photoreactive spin state of GMP, for the observed photochemistry, is that of the triplet state.

(3) Φ_{PC} of GMP. A 0.20 O.D. (λ = 265 nm, ℓ = 6 mm) solution of GMP (EG:H_2O, 7:3, V:V, pH 7, T = 110°C) was irradiated at the absorption maximum with excitation monochromator slit widths of 3.0 mm and 3.0 mm for a period of 5 minutes. The decrease in the fluorescence maximum was taken to be the measure of the photochemical production.

The relation used to calculate the quantum yield was

$$\Phi_{PC} = \frac{\text{moles pp}}{\bar{I}_a}$$

where:

moles pp = moles of photoproduct produced for the period of excitation, taken to be equal

to the number of moles of GMP destroyed as measured by the decrease in the fluorescence signal at 330 nm.

$\bar{I}_a$ = the average number of Einsteins (moles of photons) absorbed by the parent compound for the excitation period, $I_0 2.3\ \bar{C}\ell$.

For an initial [GMP] of 2.22×10^{-5}, a reduction of 7.3% in the parent fluorescence, an irradiated volume of 0.09 cm , $I_0 = 3.40\times10^{-8}$ Einsteins for the 5 minute excitation time and beam size as taken from the actinometry results, and $\bar{C}\ell$ of 0.09 viewing the front half of cell, the yield value becomes:

$$\Phi_{PC} = \frac{1.4\times10^{-10} \text{ moles pp}}{6.6\times10^{-9} \text{ Einsteins}} = 2.1(\pm0.5)\%$$

c. Photochemical kinetics and dinucleotide photochemistry. To augment the photochemical quantum yield determination, as described above for GMP for a single excitation period, additional experiments were performed in the luminescence mode wherein measurements of the decrease in parent fluorescence, and the increase in photoproduct

fluorescence were taken at repeated intervals for an excitation period of up to 60 minutes. Not only GMP was investigated, but a set of GMP containing nucleotides were also investigated in similar fashion. The relative rates were determined by plotting:

(1) $\log F_{325}^{265}$ vs. t(min)

where:

F_{325}^{265} = the fluorescence response in arbitrary intensity units, when viewing the emitted light at 325 nm while the exciting light is set at 265 nm,

t(min) = the period of excitation time elapsed previous to reading F_{325}^{265}

(2) $\log[F_{425}^{313}(\infty) - F_{425}^{313}(t)]$ vs. t(min)

where:

$F_{425}^{313}(\infty)$ = the estimated fluorescence response when viewing the emitted light at 425 nm and exciting at 313 nm, after complete photoconversion of GMP moiety present. The response observed in the simple GMP

nucleotide case, for a given percentage conversion, was the standard used,

$F_{425}^{313}(t)$ = the observed response viewing at 425 nm, exciting at 313 nm, after a photolysis period at 265 nm.

The results are graphed in Figure 14 and Figure 15 and tabulated in Table 7. Each determination was performed two times. In Figure 14, data points are plotted for single determination. In Figure 15, the slope is the average obtained from the two runs. The absolute rates for GMP have an experimental variation of about 15%. Only a single kinetics experiment was made on dGpT. $k_p^{(Rel)}$ and $k_{pp}^{(Rel)}$ refer to the relative rate constants for the decrease in parent fluorescence and increase in photoproduct fluorescence, respectively, as determined from the plots of (1) and (2). Also included is a listing of relative photochemical quantum yields, Φ_{PC}^{Rel} (1), obtained from absorption monitored data, Table 5.

The values of k_p and k_{pp} for GMP agree to within 10%, so that it is established that photoproduct formation is occurring at the same rate as the loss of the parent GMP in the simple nucleotide case. A discussion of some

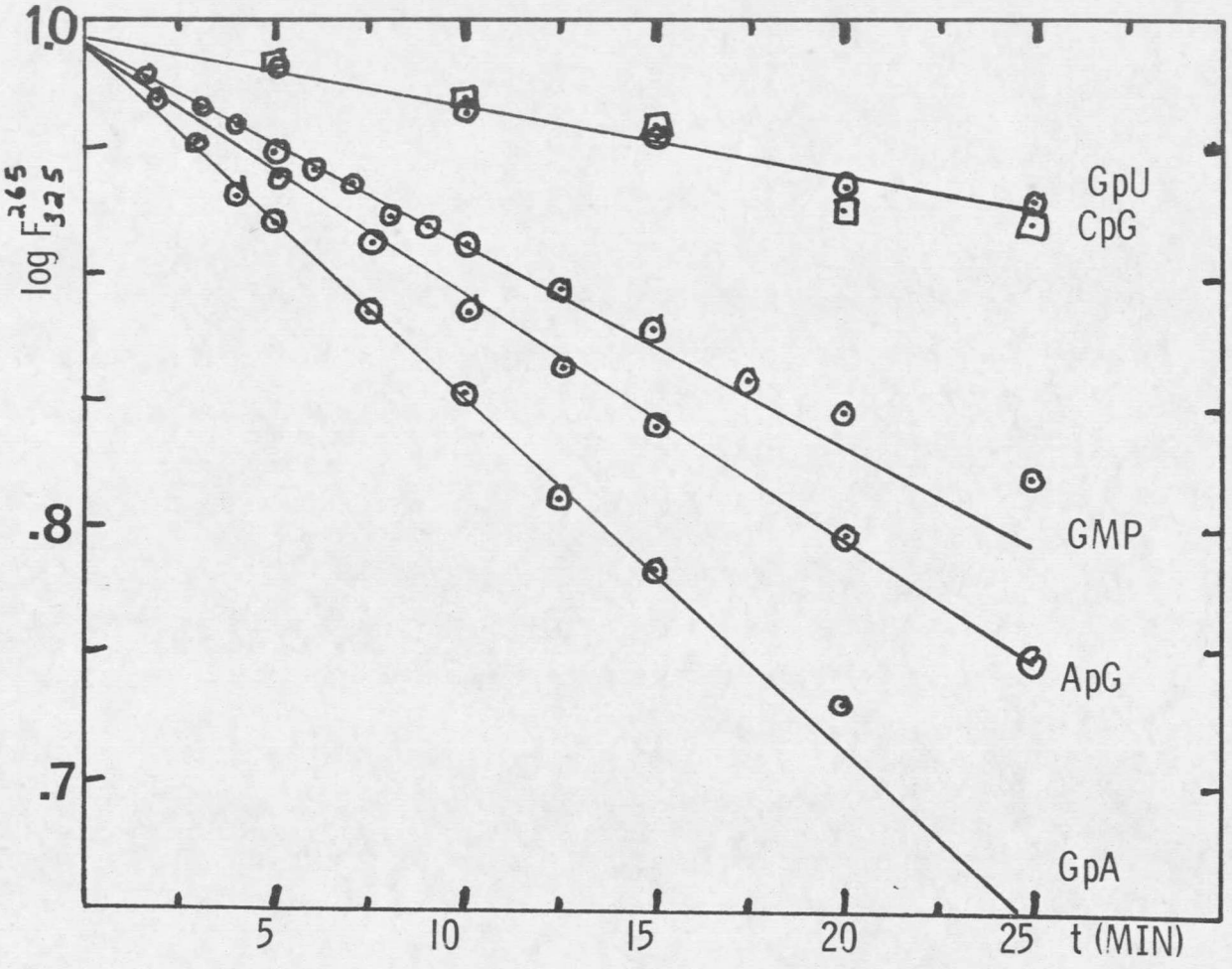

Figure 14. Decay of parent fluorescence with time of photolysis.

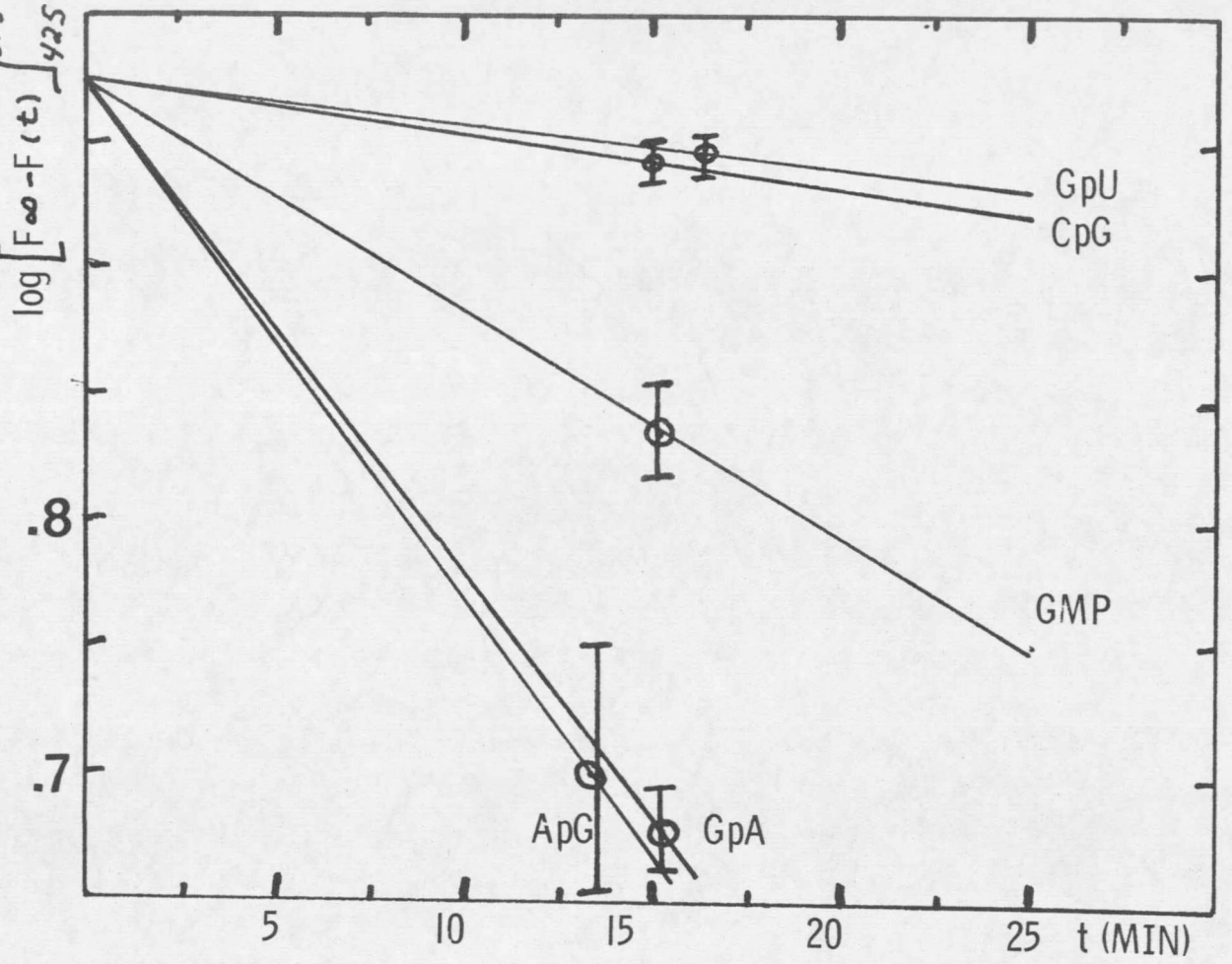

Figure 15. Photoproduct increase with time of photolysis, as an average of two determinations.

of the other apparent discrepancies for the dinucleotide cases will be deferred to a later section after amplifying photophysical data has been presented and discussed. It is seen from the data to this point that the rate of parent decay is not simply related to the growth of photoproduct in all dinucleotides, and there are severe discrepancies between k_{pp} and $\Phi^{Rel}_{PC}(1)$ in a few cases, notably GpU and dGpT.

Table 7. Photochemical relative rates via luminescence

	k_p(Rel)	k_{pp}(Rel)	$\Phi^{Rel}_{PC}(1)$
GMP	1.00	1.00	1.00
ApG	1.30 ±0.13	2.20 ±0.38	1.99
GpA	1.80 ±0.06	2.00 ±0.16	2.19
CpG	0.30 ±0.06	0.22 ±0.05	0.43
GpU	0.30 ±0.12	0.16 ±0.03	0.85
dGpT	1.00	0.95	1.83

d. Photochemical action spectra and luminescence excitation spectra. It is a recognized rule that photochemical and photophysical quantum yields should be independent of the wavelength of excitation. This is true because of the rapid rates of internal conversion for most molecules studied (32). The depopulation of the higher

electronic states to the ground state thus occurs only from the lowest vibrational levels of the ^1S and ^1T electronic levels. Photodissociation is recognized as being an exception. It had been reported, however, that certain of the nucleic bases, notably uracil, had a wavelength dependence in the rate of intersystem crossing and subsequently in the formation of photodimers (33). For this reason, a photochemical action spectrum was determined for GMP, using the I_0 values as obtained from the actinometry studies to correct for the variation of Xenon lamp intensity with wavelength of excitation. The photolysis was conducted at 10 nm intervals in the absorption band, with time of photolysis of 10 minutes at each λ_{ex}. A separate sample was used for each determination. The measured response, F_{425}^{313}, was taken to be the measure of photoproduction. The action spectrum generated as the result of these experiments did not coincide with the absorption spectrum as would be expected in the relation.

$$\frac{d(Prod)}{dt} = \Phi_{PC} I_0 2.3 \epsilon(\lambda_i) C\ell$$

with Φ_{PC} taken to be a constant. Rather, Φ_{PC} was indicated to be wavelength dependent, being substantially

larger in the long λ region of the absorption band. Since it was recognized that the actinometry values might not be accurate enough for this type of a determination, the I_0(rel) results for the Xenon lamp as generated by the Rhodamine B technique were used to correct I_0 for the action spectrum. The recalculated spectrum was nearer that of the absorption spectrum but the effect remained.

It was then decided that photochemical action spectra should be generated for the GMP containing dinucleotides as well. It was also thought necessary to produce luminescence excitation spectra for all of the molecules involved since a variation of Φ_{PC} with wavelength would likely have an underlying variation of one or more photophysical Φ's as the cause.

The spectra for the molecules of interest are shown in Figures 16 to 30. Fluorescence excitation spectra were recorded by setting the emission monochromator to the fluorescence maximum of the molecule and varying the wavelength setting of the excitation monochromator. Excitation monochromator slit widths were 1.0 mm and 1.0 mm. It was determined the photochemical alteration was not a factor for the duration of any determination. Phosphorescence excitation spectra were obtained in similar fashion and as

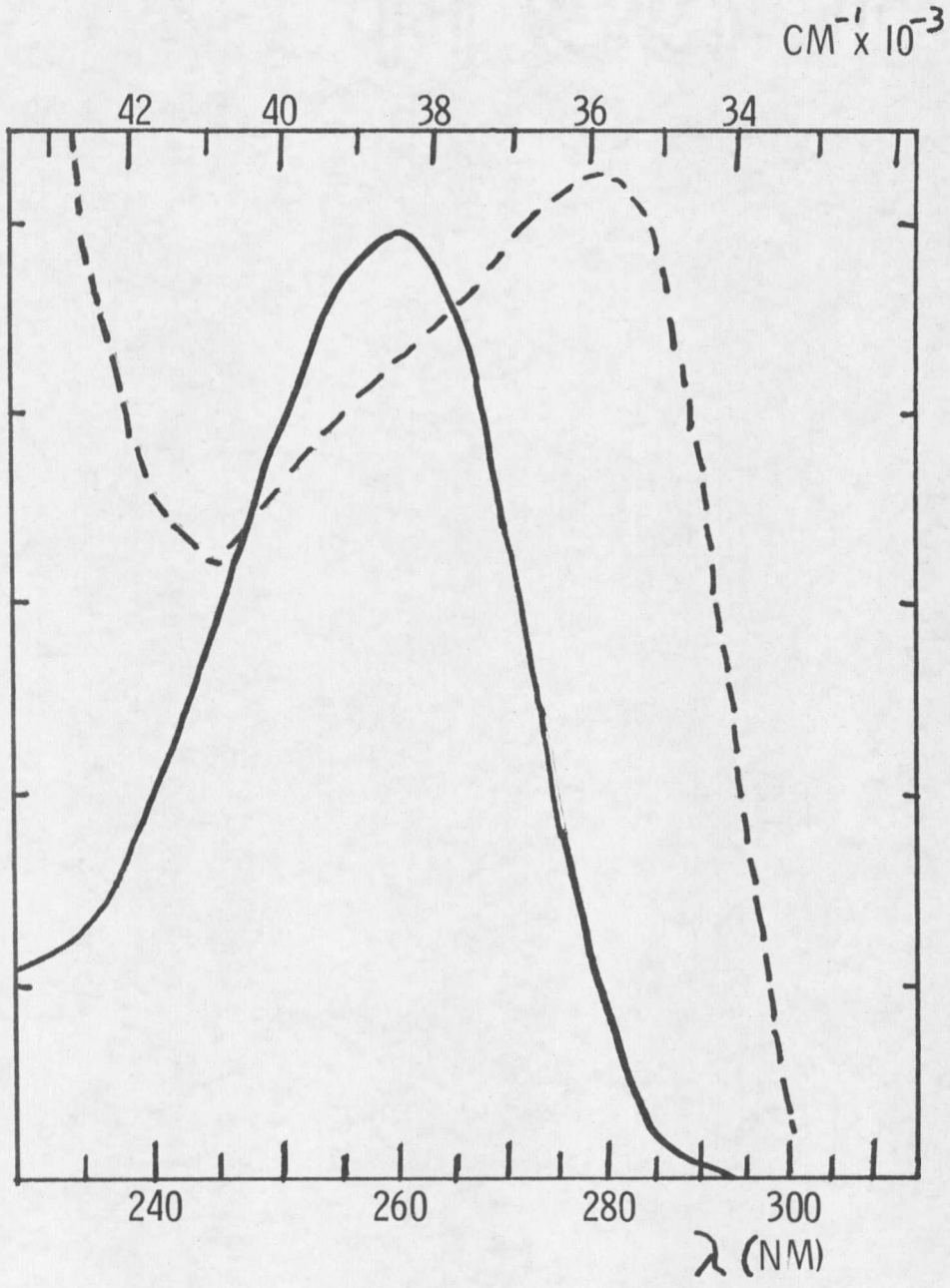

Figure 16. AMP spectra; ——— absorption, ----- fluorescence excitation.

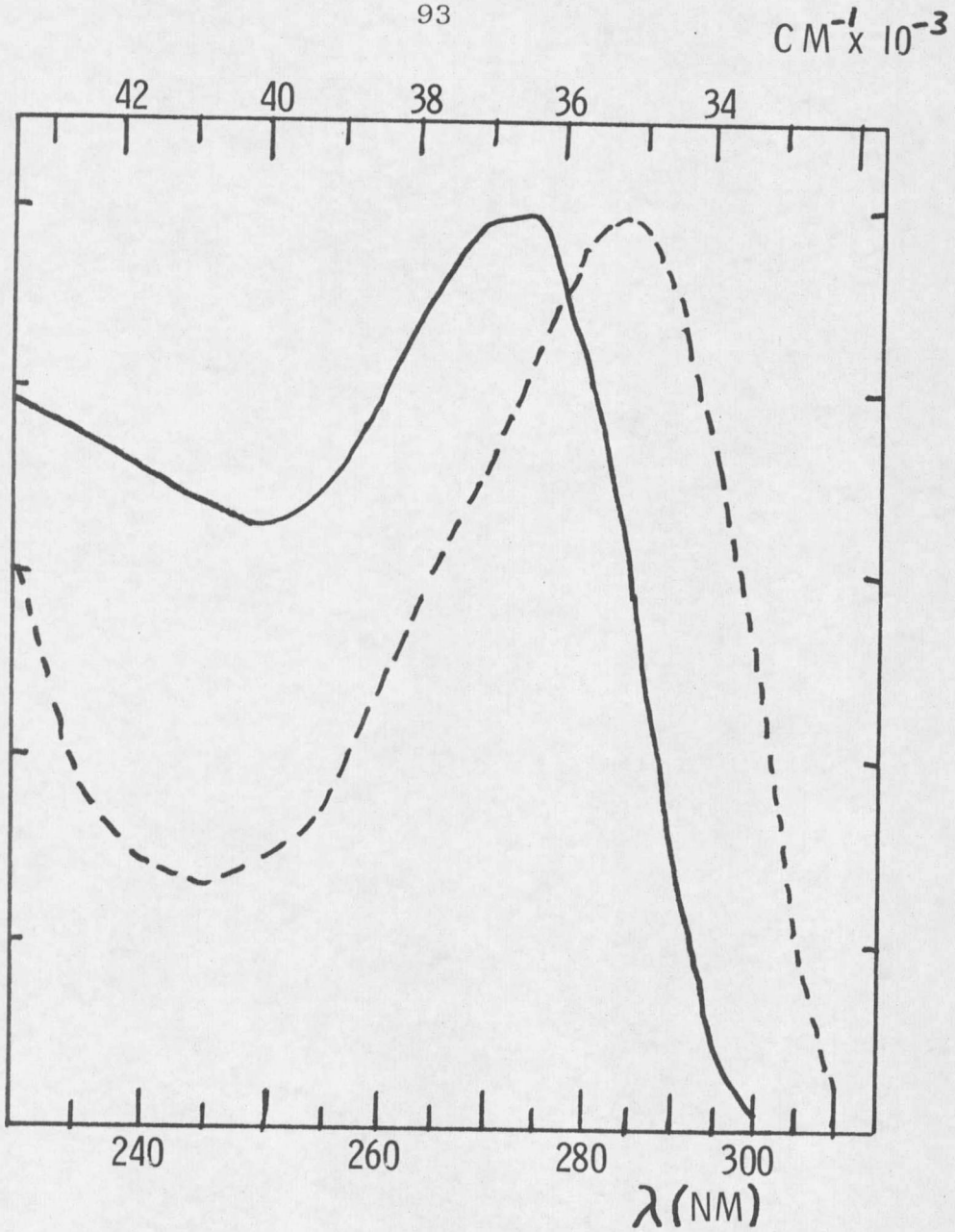

Figure 17. CMP spectra; ——— absorption, ----- fluorescence excitation.

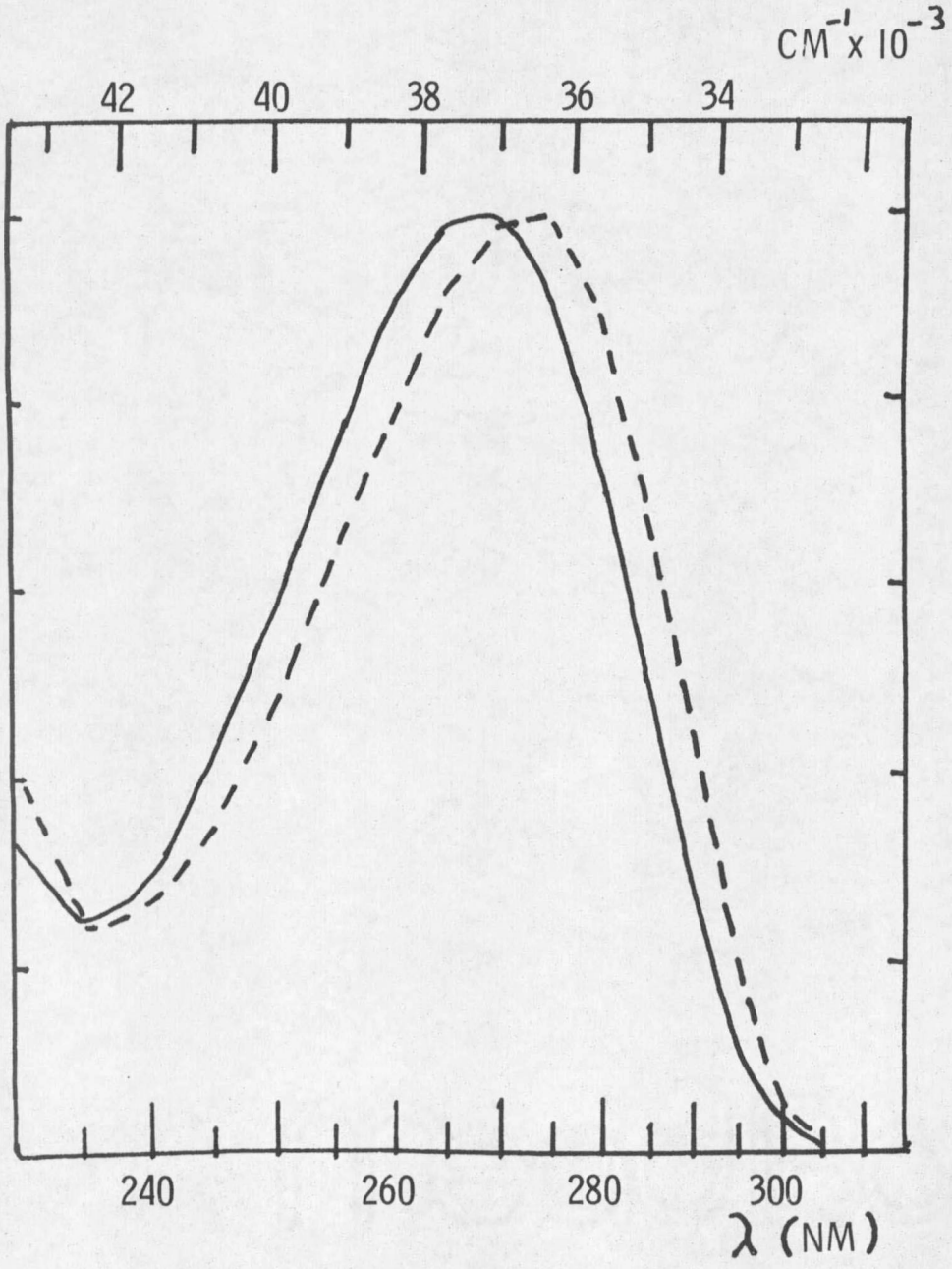

Figure 18. TMP spectra; ——— absorption, ----- fluorescence excitation.

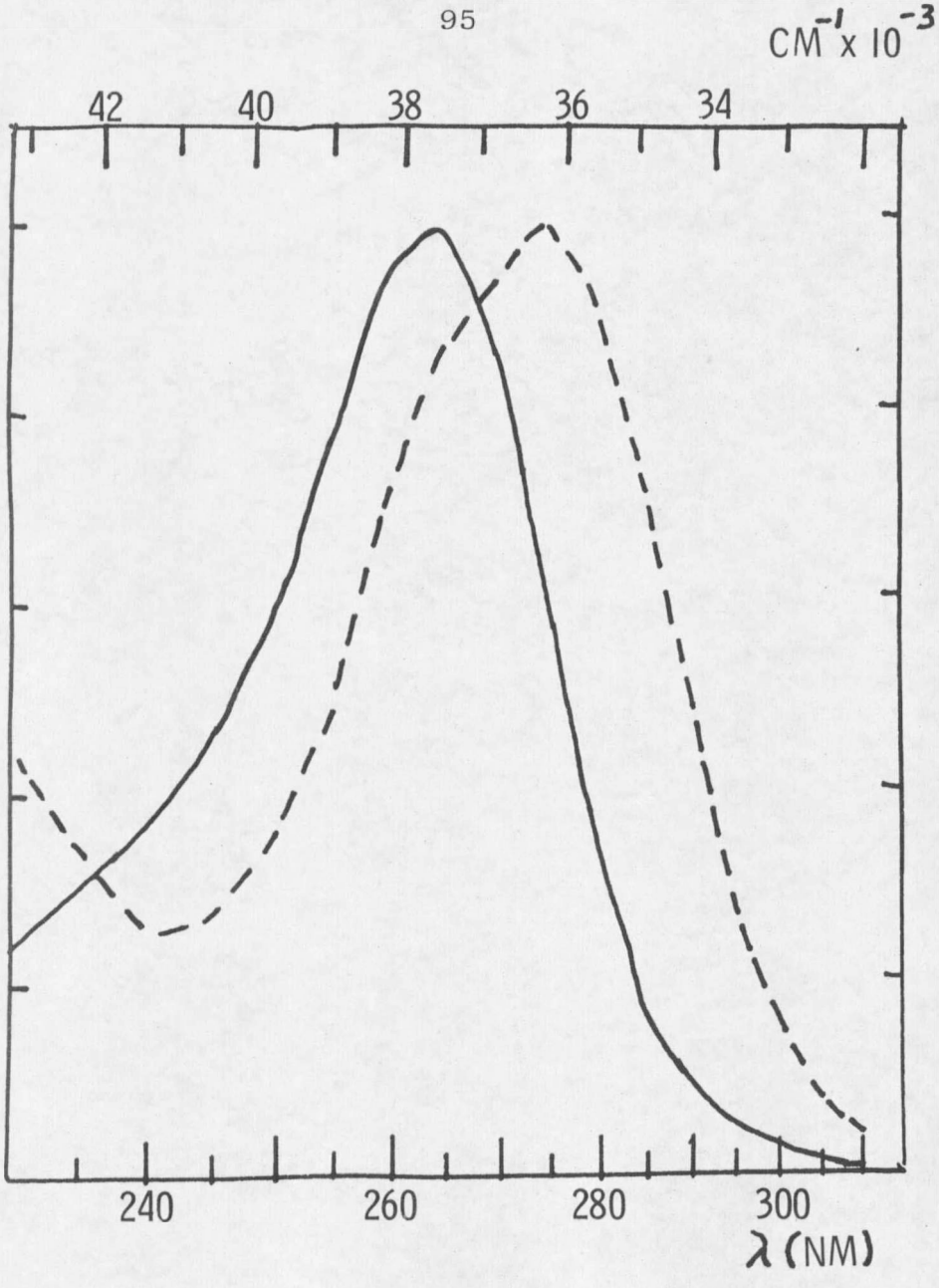

Figure 19. Purine spectra; ——— absorption or phosphorescence excitation, ----- fluorescence excitation.

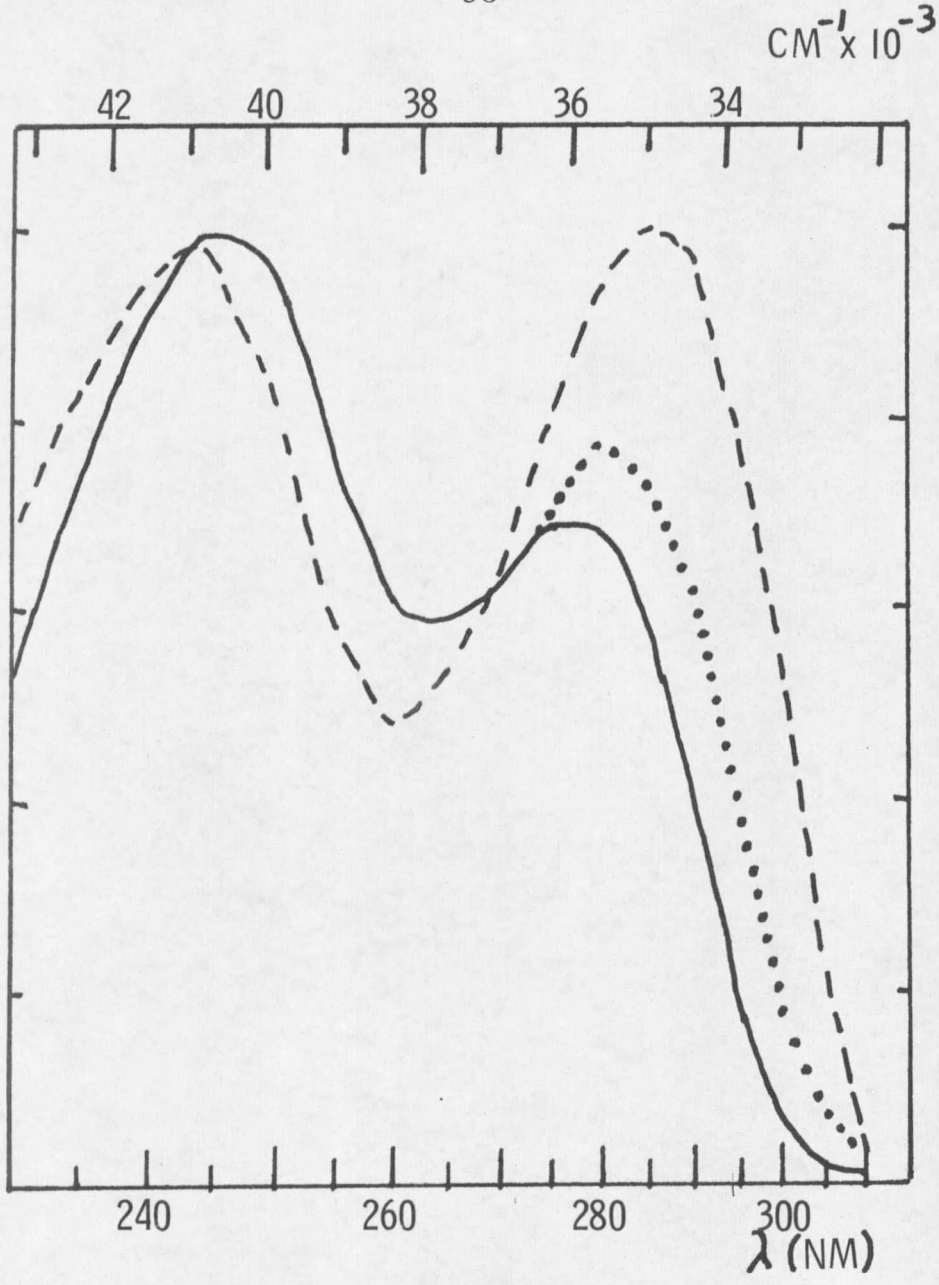

Figure 20. Guanine spectra; ——— absorption, ----- fluorescence excitation, ····· phosphorescence excitation.

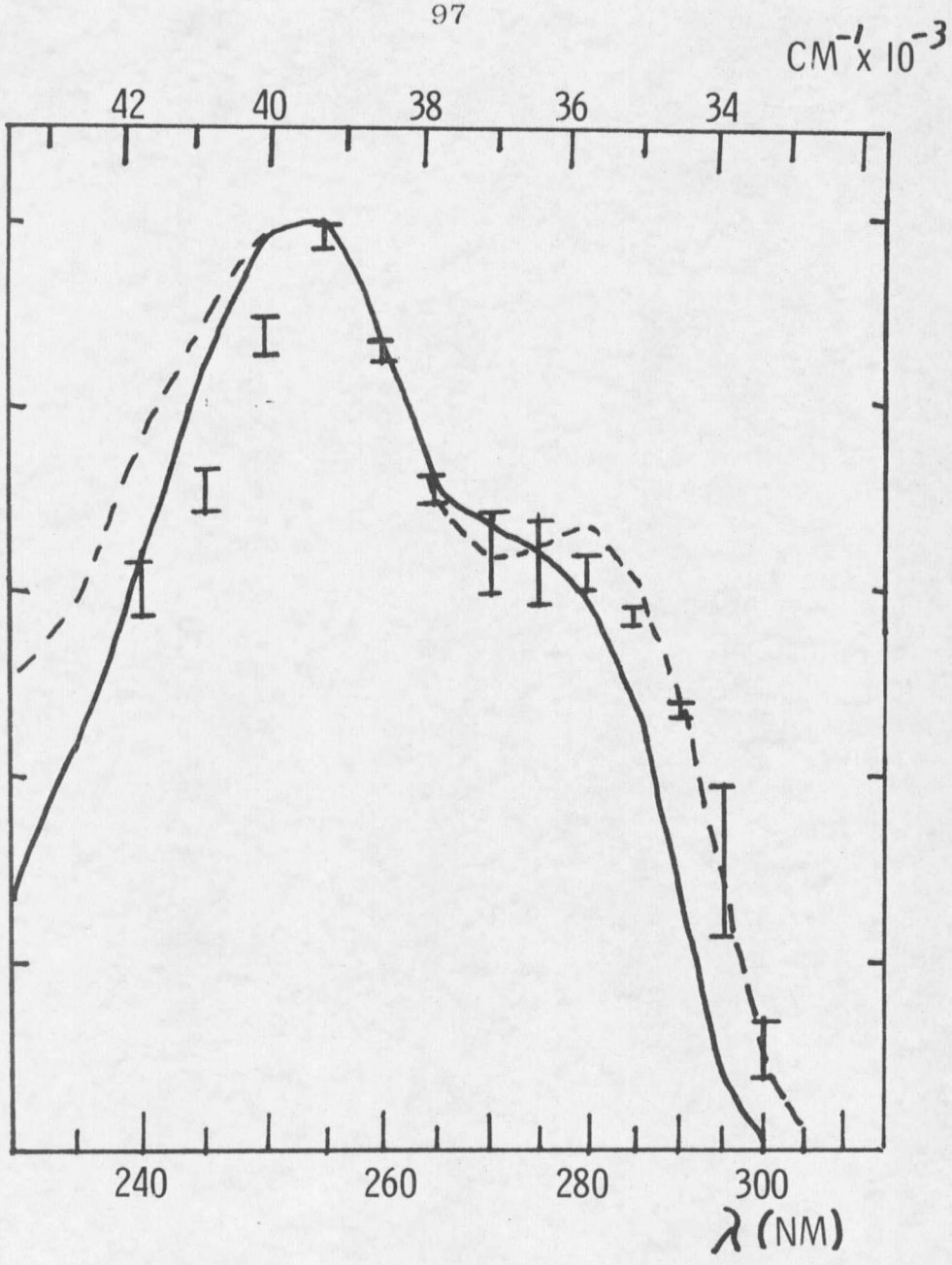

Figure 21. GMP spectra; ——— absorption, ----- fluorescence or phosphorescence excitation, ⊥⊥ photochemical action.

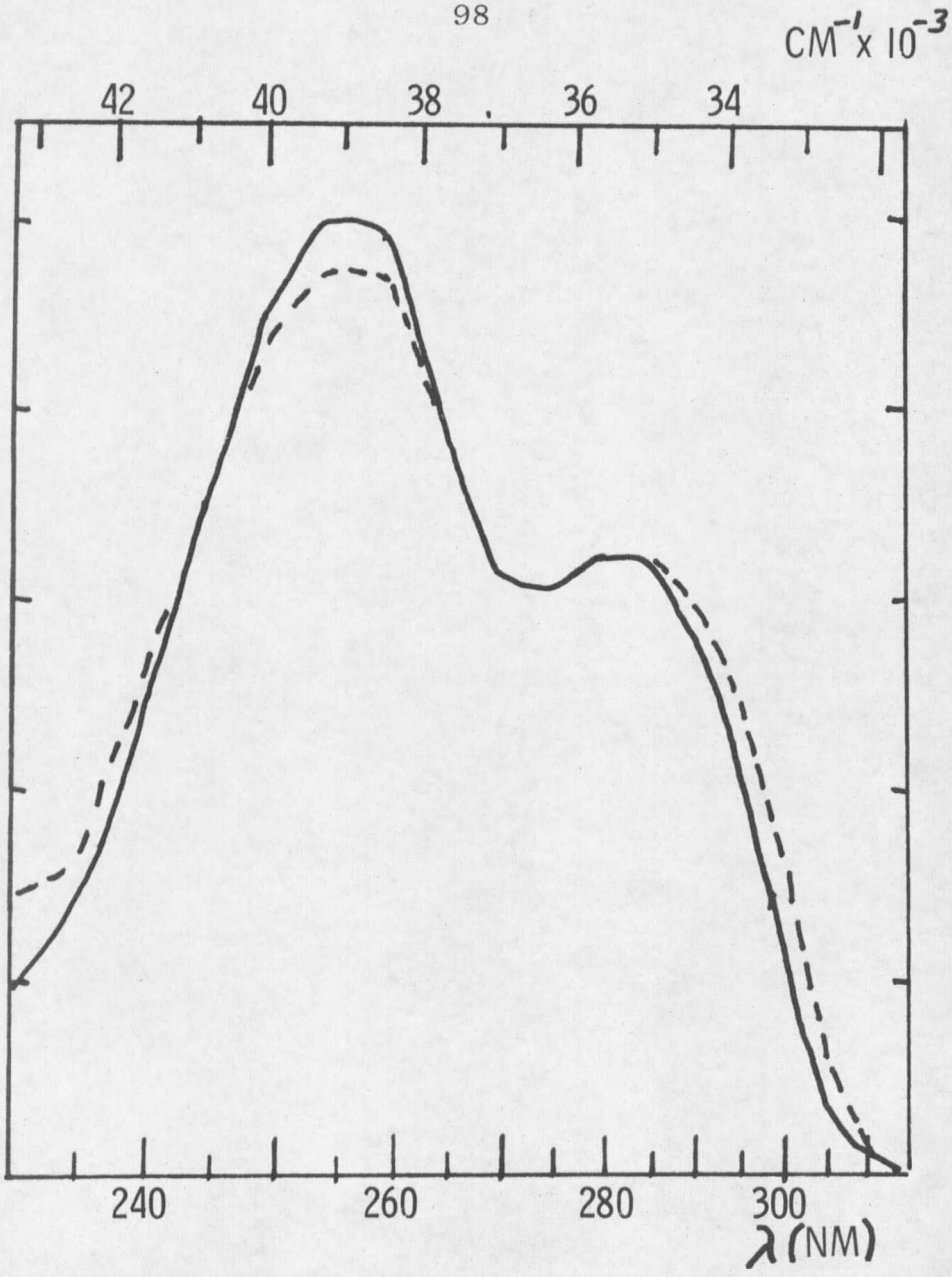

Figure 22. GMP spectra (pH 2); ——— absorption, ----- fluorescence excitation.

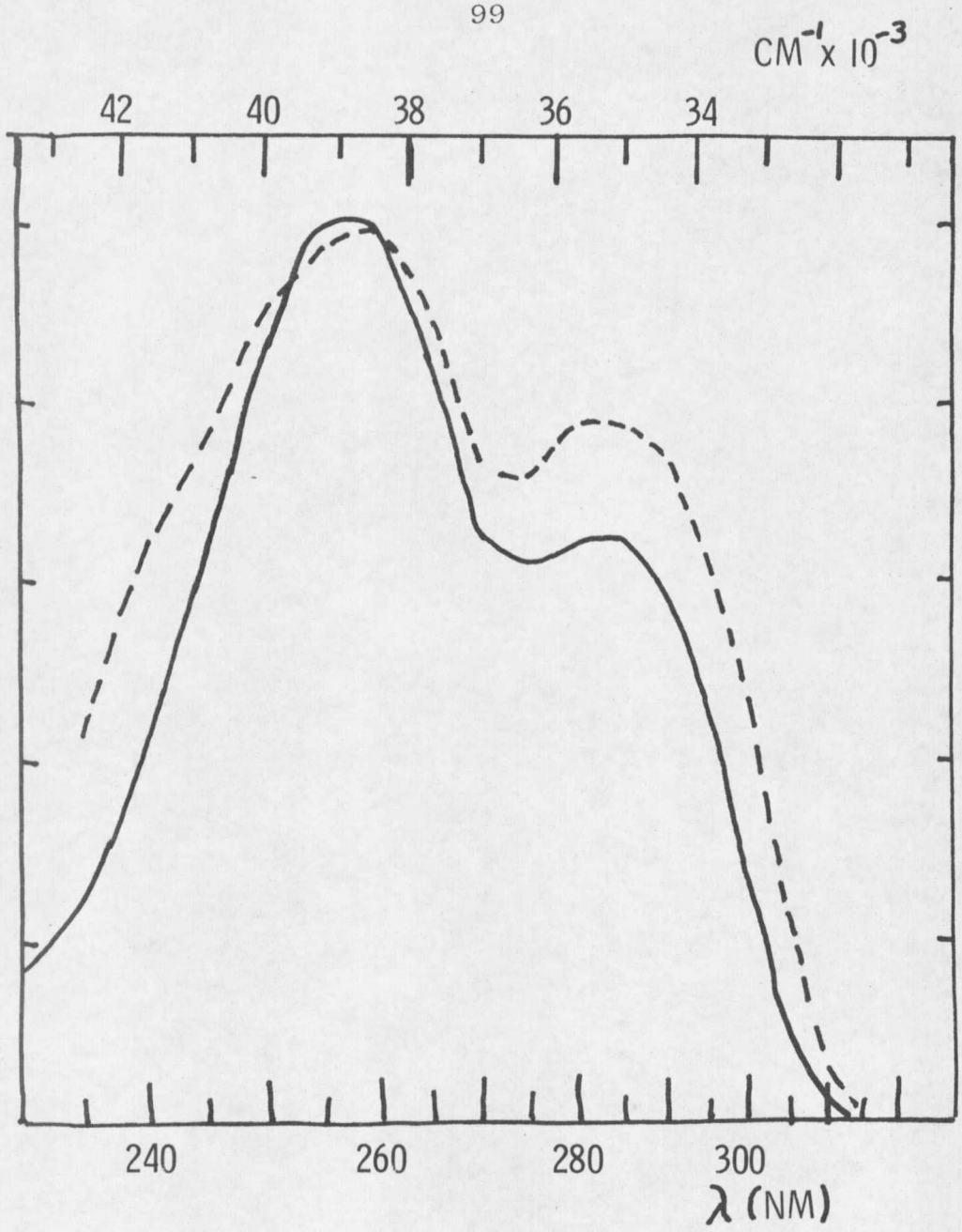

Figure 23. 7-Methylguanosine spectra; ——— absorption, ----- fluorescence or phosphorescence excitation.

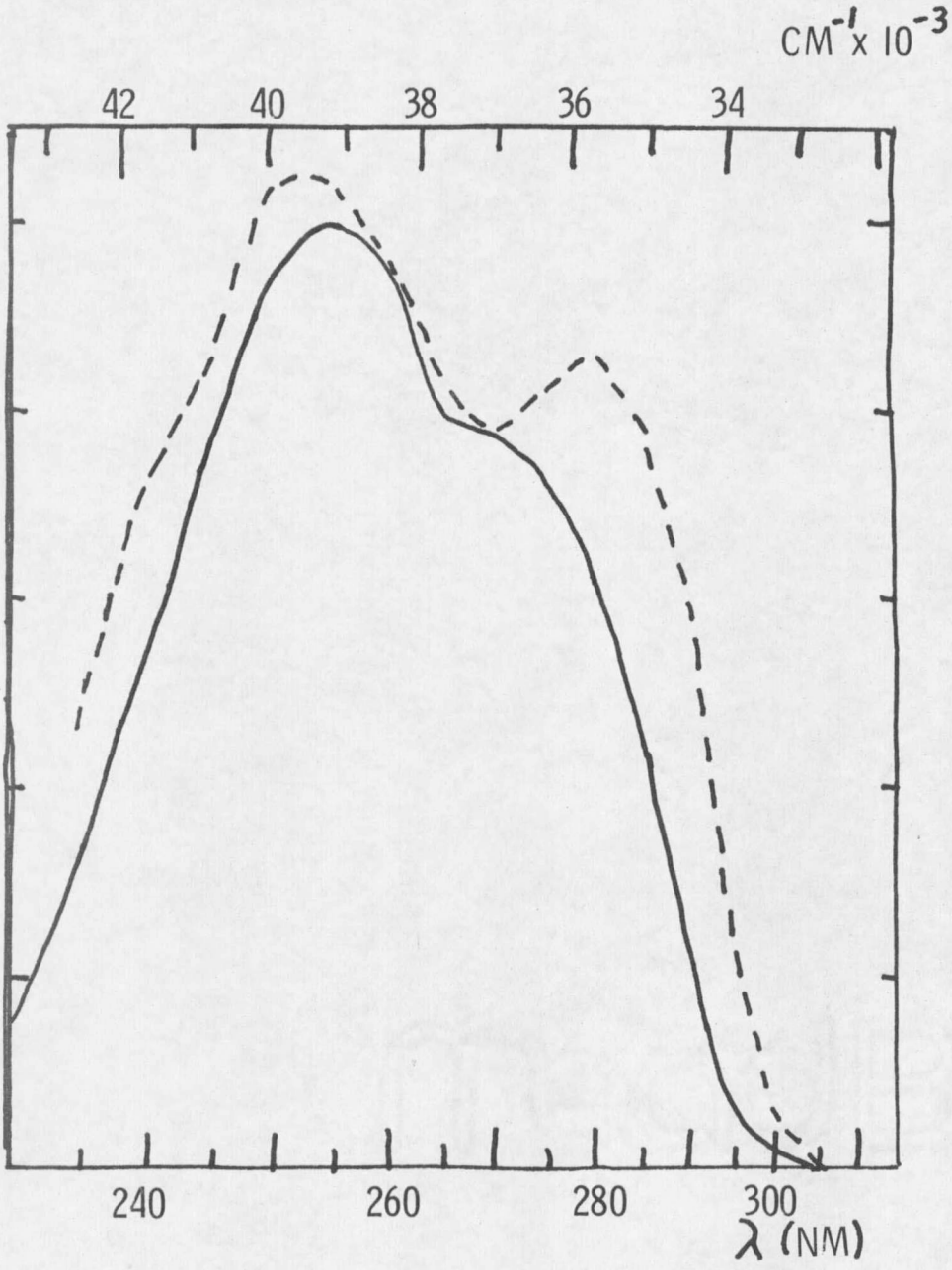

Figure 24. 1-Methylguanosine spectra; ——— absorption, ----- fluorescence or phosphorescence excitation.

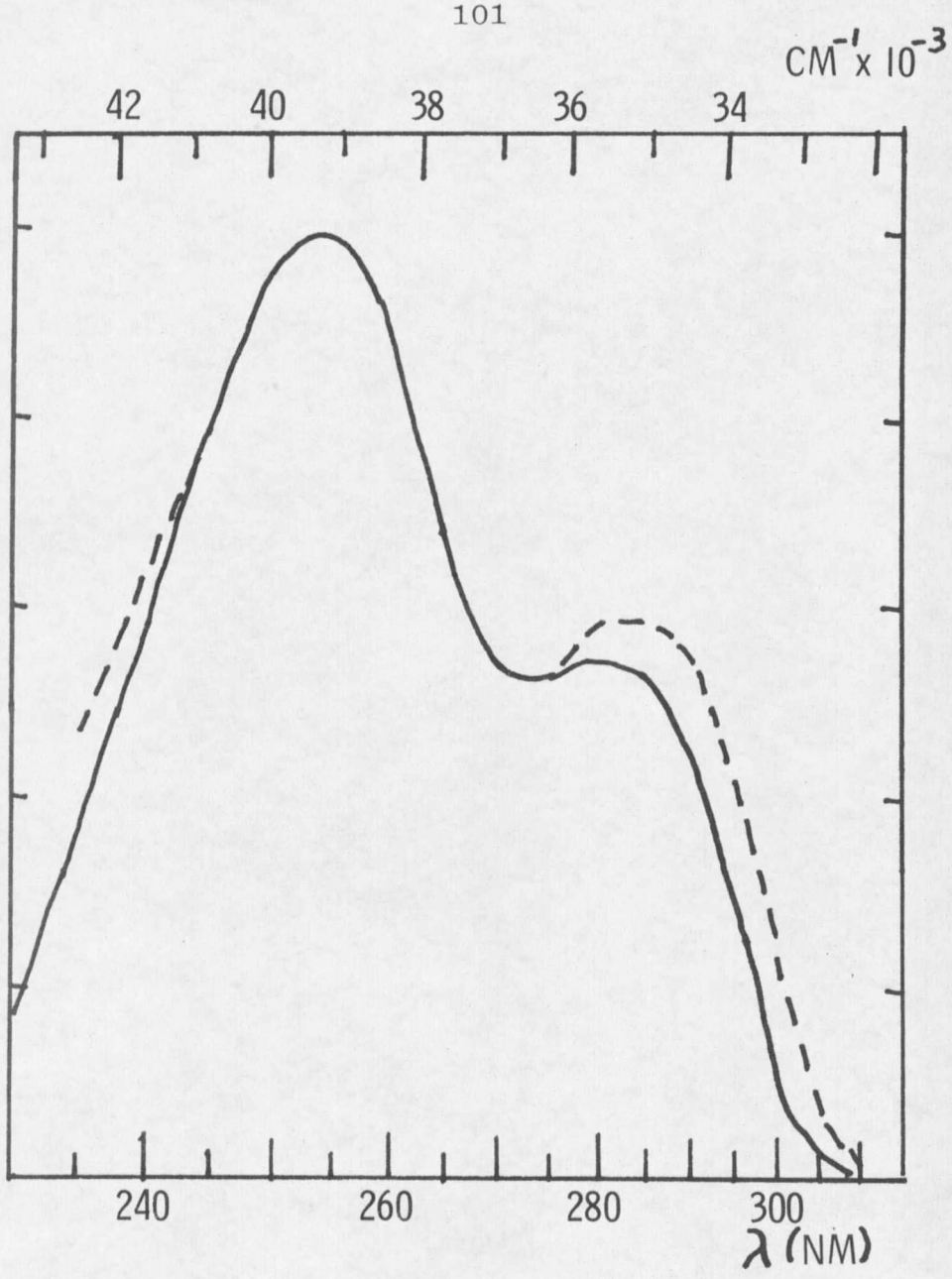

Figure 25. N_2-Dimethylguanosine spectra; ——— absorption, ----- fluorescence or phosphorescence excitation.

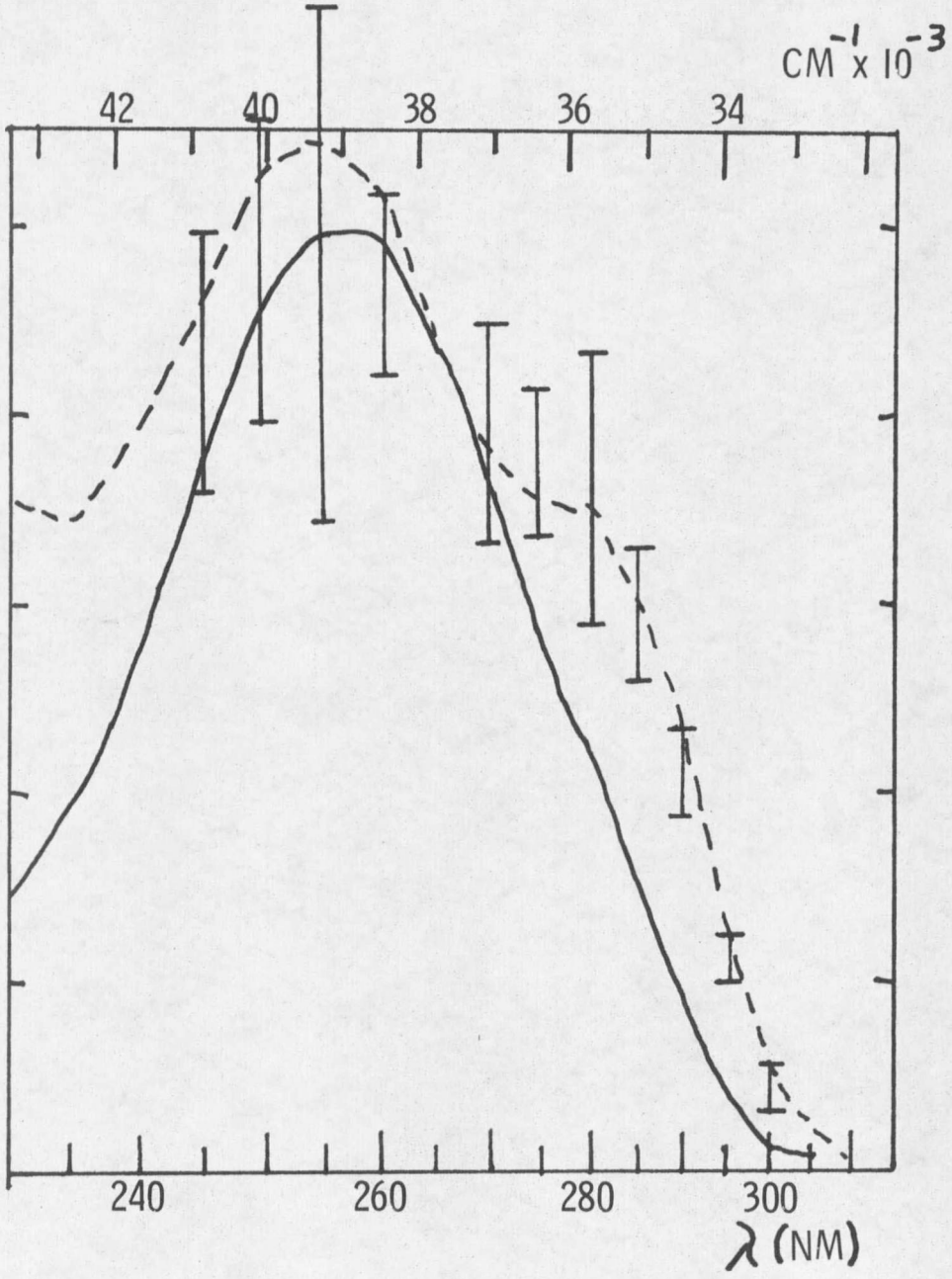

Figure 26. ApG spectra; ——— absorption, ----- fluorescence or phosphorescence excitation, ⌶⌶ photochemical action.

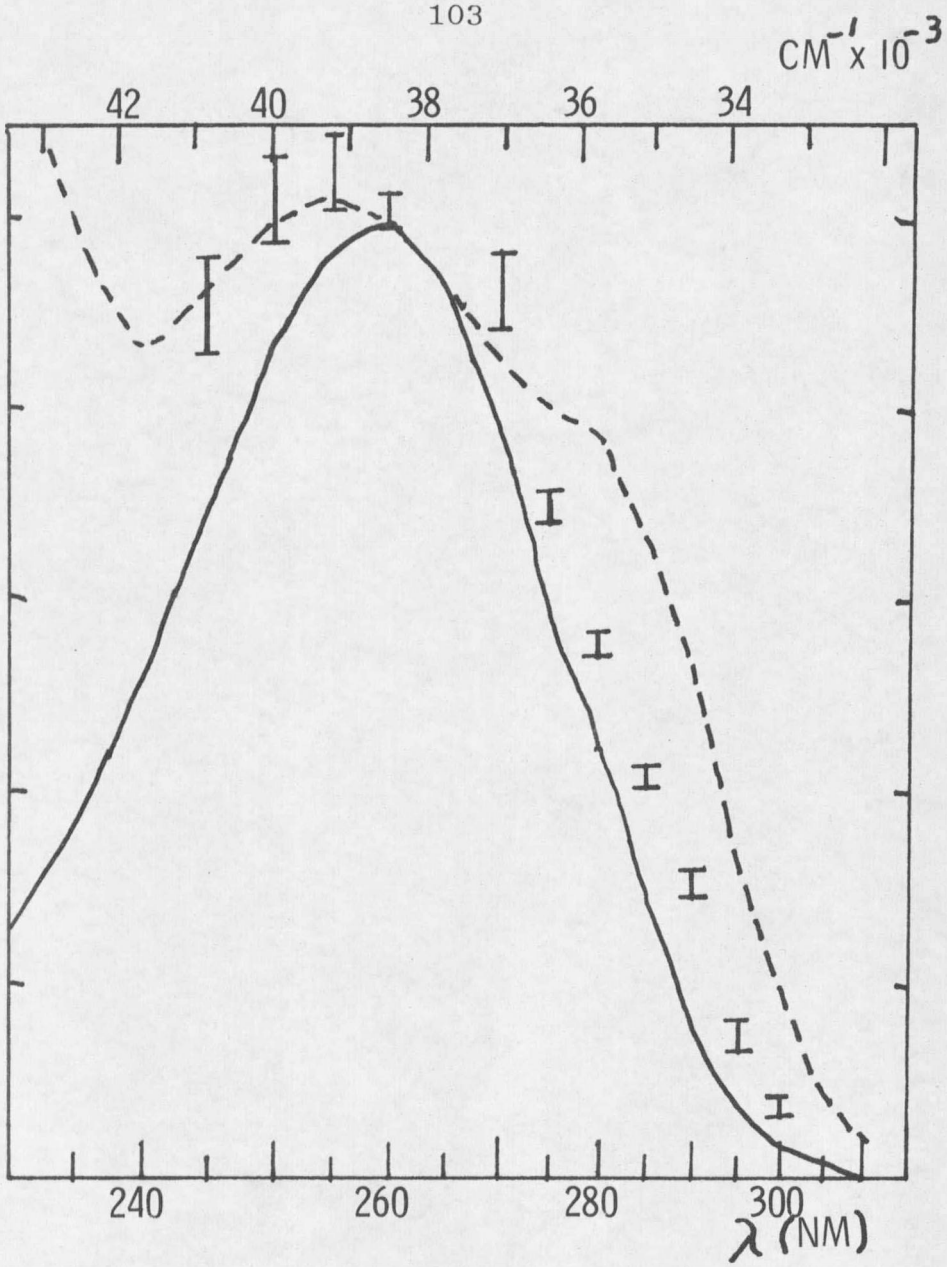

Figure 27. GpA spectra; ——— absorption or phosphorescence excitation, ----- fluorescence excitation, I I photochemical action.

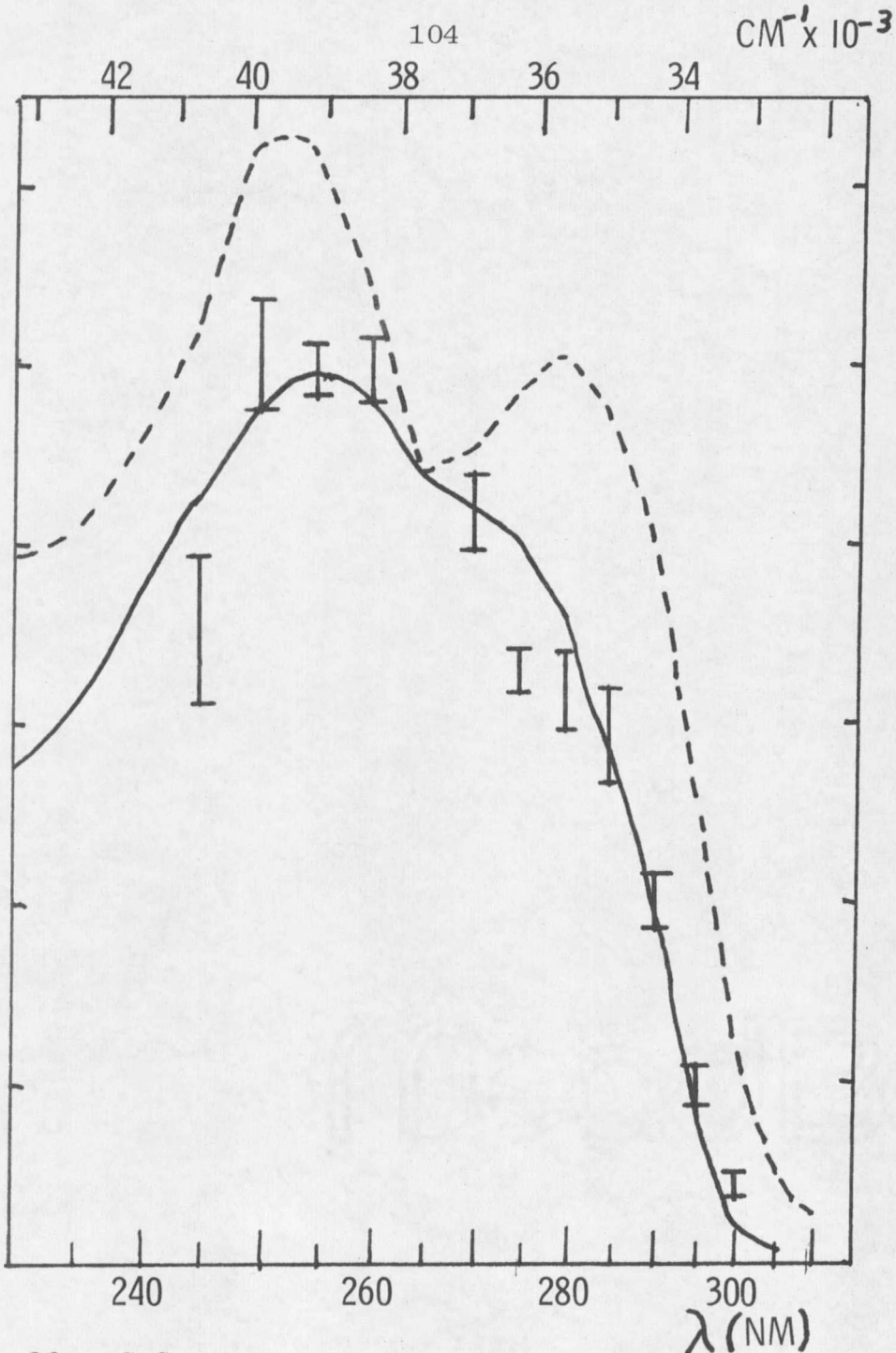

Figure 28. CpG spectra; ——— absorption, ----- fluorescence and phosphorescence excitation, ⊥⊥ photochemical action.

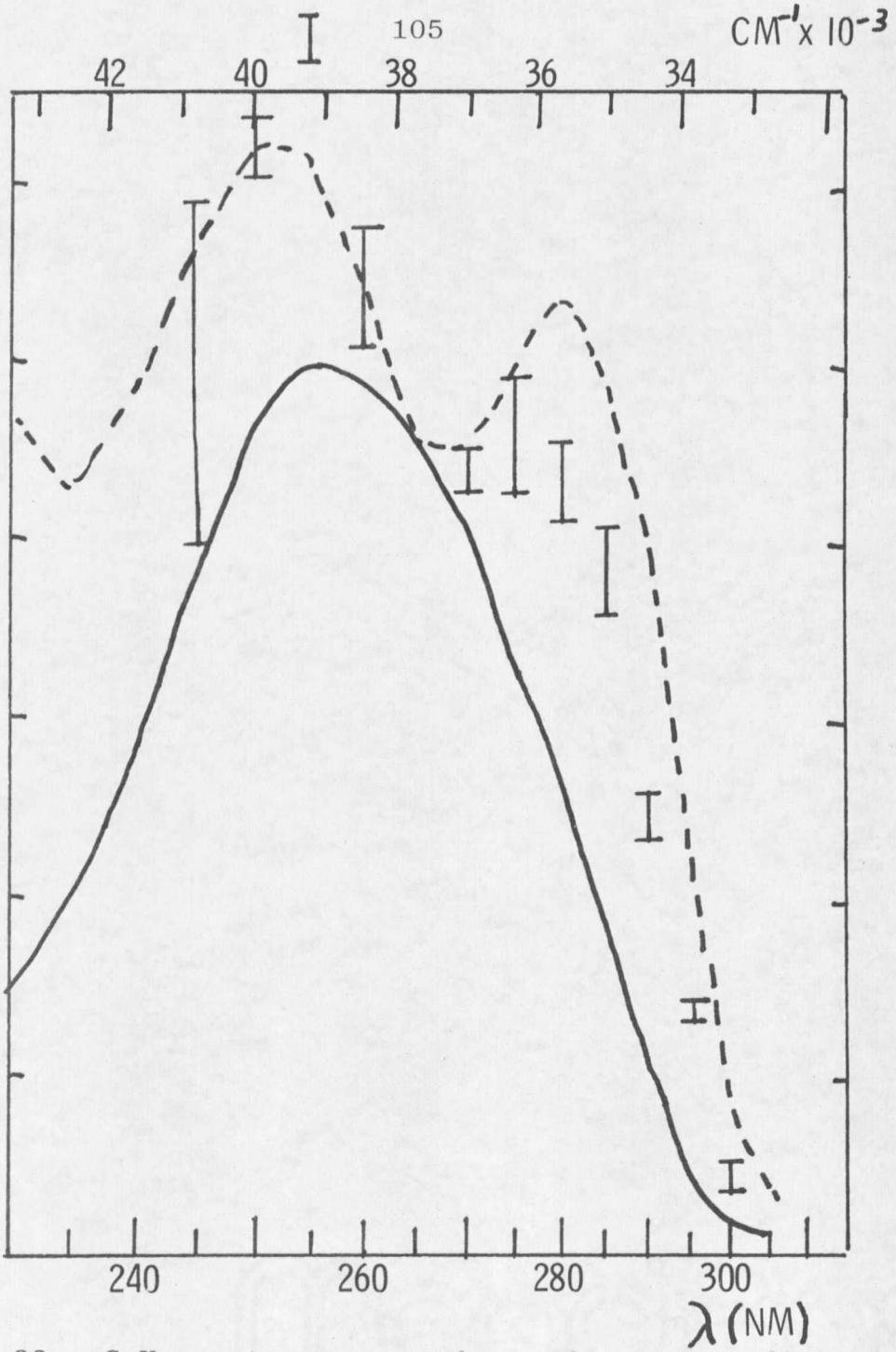

Figure 29. GpU spectra; ——— absorption, ----- fluorescence excitation, ⌶⌶ photochemical action.

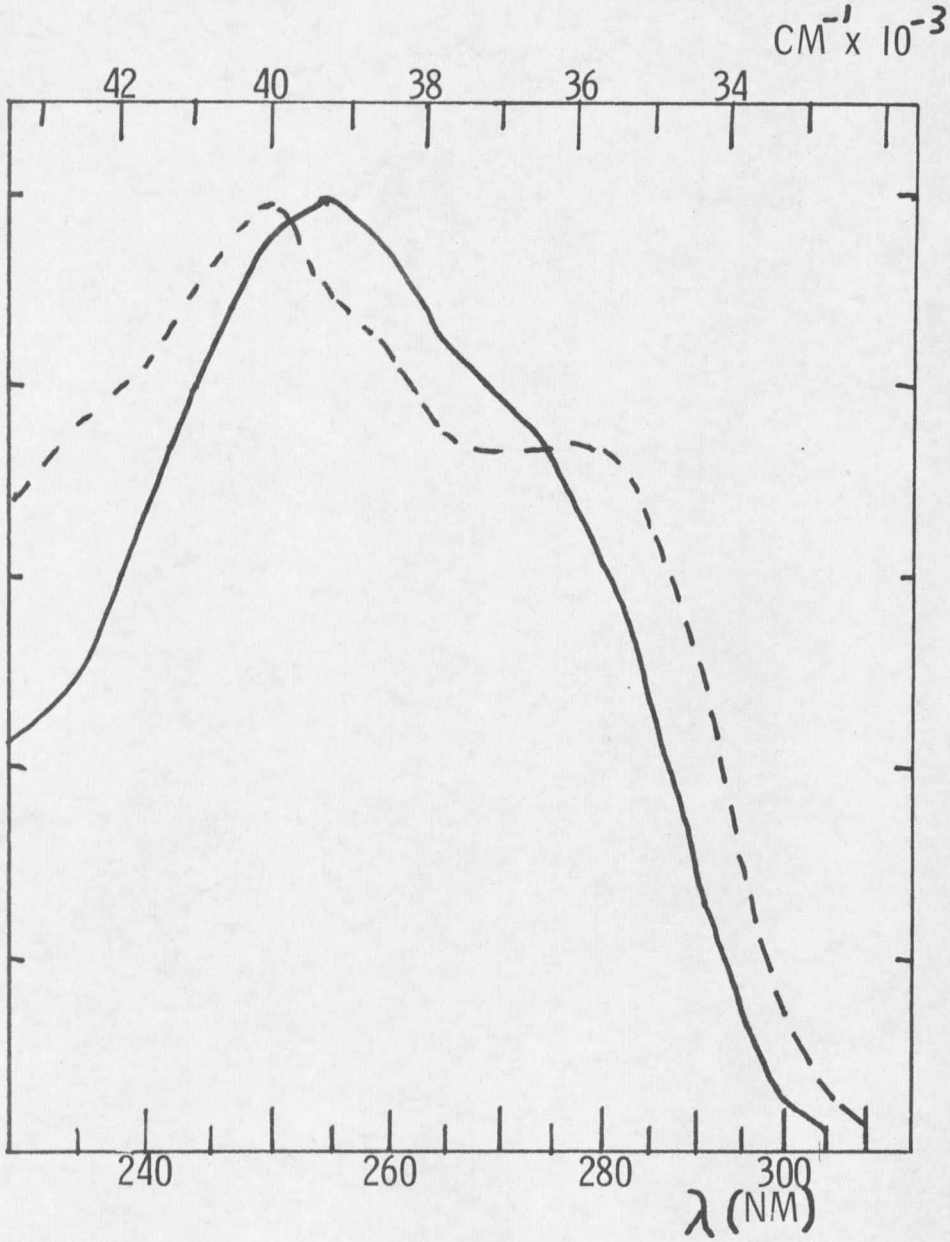

Figure 30. GpT spectra; ——— absorption, ----- fluorescence or phosphorescence excitation.

indicated in the figures agree with the fluorescence excitation spectra in most cases. Where not indicated, the phosphorescence quantum yields were too small to obtain good results for the excitation spectra. The excitation spectrum for AMP must be considered as only roughly correct due to the low fluorescence quantum yield. The absence of UMP excitation spectrum is due to its having a very low fluorescent quantum yield. Absorption spectra shown are those taken at low temperature (-110°C). Normalization of spectra is at 265 nm.

The results of the luminescence excitation spectra indicate that there is a variation in luminescent yield with wavelength of excitation for all chromophores investigated. The purine and GpA phosphorescence excitation spectra are the exceptions which help to prove the rule.

A proposed explanation for these effects is that the quantum yield variation in the monomer cases is due, at least in part, to a variable internal conversion rate from the various vibronic excited states directly to vibronic levels of the ground state. This, of course, is contrary to accepted theory wherein the internal conversion must take place only from the lowest vibronic level of the first excited states. A variation of Φ_F with λ_{ex}

such as exhibited has been attributed to the presence of tautomeric forms (34); but since the methylated guanosines show a similar effect, this explanation would seem to be precluded for GMP. Molecules such as GpA, GpU, GpC, and GpT which show a variation in their fluorescence spectrum shapes depending on λ_{ex} might be expected to have such $\Phi_F(\lambda_{ex})$ dependencies. The variation in shape of the fluorescence spectra seen was that when exciting at different λ's and normalizing the spectra on the monomer maximum, the fluorescence response in the region of excimer fluorescence (~400 mm) was some 25% greater when exciting at 260 nm than when excitation was at 280 nm.

The photochemical action spectra are more difficult to analytically evaluate because of the precision error evident, but the following qualitative observations are made:

(1) The action spectra follow the luminescence excitation spectra in the GMP, ApG, and GpU cases, indicating that the variation in action as a function of λ_{ex} reflects the variation in internal conversion rate at the singlet level.

(2) The photochemical action spectra follow the absorption and phosphorescence excitation spectra for

GpA at λ's longer than 260 nm, indicating an invariance in intersystem crossing yield in this spectral region. Additional comment will be offered on these matters in later sections.

e. Luminescence quantum yields. While excitation spectra provide evidence for variable luminescence quantum yields, it is also of importance to know what the yields are quantitatively. To this end, fluorescence and phosphorescence yield determinations were conducted.

All quantum yield values were determined as relative to that of quinine bisulfate in 0.1 N H_2SO_4. The literature value is reported to be $\Phi_F = 0.55$ (35). The relation used to obtain the relative yields was:

$$\frac{\Phi_i}{\Phi_{QBS}} = \frac{I_0(\lambda_{ex}^{QBS})}{I_0(\lambda_{ex})_i} \times \frac{(\epsilon C\ell)_{QBS}}{(\epsilon C\ell)_i} \times \frac{(\int F(\lambda)d\lambda)_i}{(\int F(\lambda)d\lambda)_{QBS}}$$

where:

Φ = luminescence quantum yield,

$I_0(\lambda)$ = relative intensity of the exciting light at the wavelength of excitation,

$\epsilon C\ell$ = optical density of the solution at the wavelength of excitation,

$\int F(\lambda)d\lambda$ = the area under the corrected luminescence curve.

(1) The $I_0(\lambda)$ values were taken from the rhodamine B quantum counting experiment.

(2) The optical densities, $\varepsilon C\ell$, were made to be equal to 0.20 O.D. in all cases.

(3) The observed luminescence curves were corrected by use of the phototube response curve, and the value of the integral $\int F(\lambda)d\lambda$ obtained by a computer calculation which made a summation of 5 nm intervals of the corrected luminescence curve.

(4) To test the method, three relative fluorescence quantum yields were determined for molecule which fluoresce in the same region as the nucleic acids. The results obtained as compared with the literature values are:

	Φ_F(Determined)	Φ_F(Literature)
Tyrosine (in H_2O)	0.15	0.14[36]
Tryptophan (in H_2O)	0.15	0.15[36]
Salicylic Acid (in H_2O)	0.29	0.28[37]

The values obtained for the molecules of interest in this study are listed in Table 8. The λ_{ex} was 265 nm in all cases. The phosphorescence spectra were extracted from the total luminescence spectra obtained at -137°C by subtracting out the fluorescence curves in relation to the shape obtained at the warmer temperature, -112°C. The phosphorescence comes at long enough wavelengths that no overlap of fluorescence and phosphorescence occurred in the region of the fluorescence maxima.

Table 8. Luminescence quantum yields

	Φ_F	Φ_P
Guanine	0.051	--
1Me-Guanosine	0.020	0.015
N^2-Guanosine	0.067	0.053
7Me-Guanosine	0.48	--
GMP	0.029	0.022
ApG	0.033	0.043
GpA	0.023	0.18
CpG	0.011	0.009
GpU	0.013	0.010
GpT	0.024	0.012
AMP	~0.002	~0
CMP	0.013	0
UMP	~0.001	0
TMP	0.036	0

Repeats of these experiments showed a variability of 15-20% in the yields.

Since ApG and GpA show a fluorescence quantum yield nearly equal to that of GMP, as well as having similar photochemical yields, an energy transfer effect at the singlet level is suggested, from A to G. GpT is also seen to have similar results. The acknowledged singlet energy levels for the nucleotides are AMP > UMP > TMP > GMP > CMP. For CpG, the Φ_F is quite near that of CMP, so that it would be permissible to attribute a singlet level transfer from GMP to CMP as the cause. GpU might be considered as if the GMP and UMP portions of the molecule were acting independently, as the Φ_F and Φ_p could be derived from light absorption of the GMP part of the molecule alone. The Φ_p's of ApG and GpA offer little that would aid the analysis. The luminescence yields of the methylated guanosines are not particularly clarifying in terms of the GMP photochemistry either, unless the Φ_p's of the 1Me and N^2 cases are indicative of a difference in k_{ISC} for the two molecules. Certainly then, while energy-transfer might be implicated by some of the luminescence and photochemical yields, more information is needed to this point.

Luminescence yields were also attempted for some of the situations where metal ions were added in equimolar amounts to GMP. The results are shown in Table 9 as luminescence yields relative to GMP without added M^{n+}. The relative photochemical yields, as previously given from the absorption monitored mode, are listed for comparison.

Table 9. GMP Φ_F with M^{n+} added.

	GMP	$+Mg^{2+}$	$+Ca^{2+}$	$+Cu^{2+}$	$+Co^{2+}$	$+Ni^{2+}$
Φ_{PC}	1.00	0.87	0.97	0.06	0.24	0.14
Φ_F	1.00	0.65	0.72	0.08	0.14	0.11

The absorbance of the GMP solutions used was 0.1 at 250 nm for the 6 mm path length.

Considering the precision of the Φ_F measurements to be ±20%, the qualitative agreement between the relative Φ's indicates quenching at the singlet level and/or paramagnetic intersystem crossing enhancement in terms of reducing the photochemical yield. The phosphorescence signals produced on further cooling were too weak to be analyzed with any confidence.

f. Triplet lifetimes, $^3\tau$. To establish the nature of the lowest occupied triplet state in

dinucleotides containing GMP, triplet lifetime studies were made on all of the nucleotides, XMP, and on all dinucleotides, XpG, GpX.

(1) A solution of the molecule whose $^3\tau$ was to be determined was cooled to a temperature low enough to promote phosphorescence, -137°C.

(2) Excitation was made at the absorption maximum.

(3) After determining the shape of the total luminescence curve with the fluorimeter and observing the wavelength of maximum phosphorescence response, the emitting monochromator was set to this wavelength and the output of the photometer connected to the Y axis input of a storage oscilloscope.

(4) The sensitivity of the oscilloscope and the slit widths of the excitation monochromator were adjusted to obtain the maximum observable response on the display scope scale.

(5) The scope sweep period was adjusted to a time scale which would allow the recording of at least one triplet decay period of the molecule in question.

(6) The exciting light was blocked with a mechanical shutter and the luminescence decay recorded on the storage scope.

(7) A photograph of the stored trace was taken with the Polaroid camera attachment.

(8) Plots were made of log phosphorescence vs. time, and $^{3}\tau$ determined by finding the time required for the phosphorescence signal to be reduced to 1/e of the initial phosphorescence signal.

A semilog plot of the results is shown in Figure 31 and the $^{3}\tau$ values are given in Table 10. The nucleotides CMP, UMP, and TMP have no detectable phosphorescence under these conditions.

It is evident that all of the molecules having a phosphorescence signal show a single exponential decay from their triplet states, with the exception of GpT. The decay curve of GpT can be resolved into two components; a longer lived component which has a decay constant equal to that of GMP, and a component which has a decay constant representative of TMP. The observed lifetimes are also consistent with what other investigators have indicated, that the phosphorescence originates solely from the nucleotide component having the lowest energy triplet; again

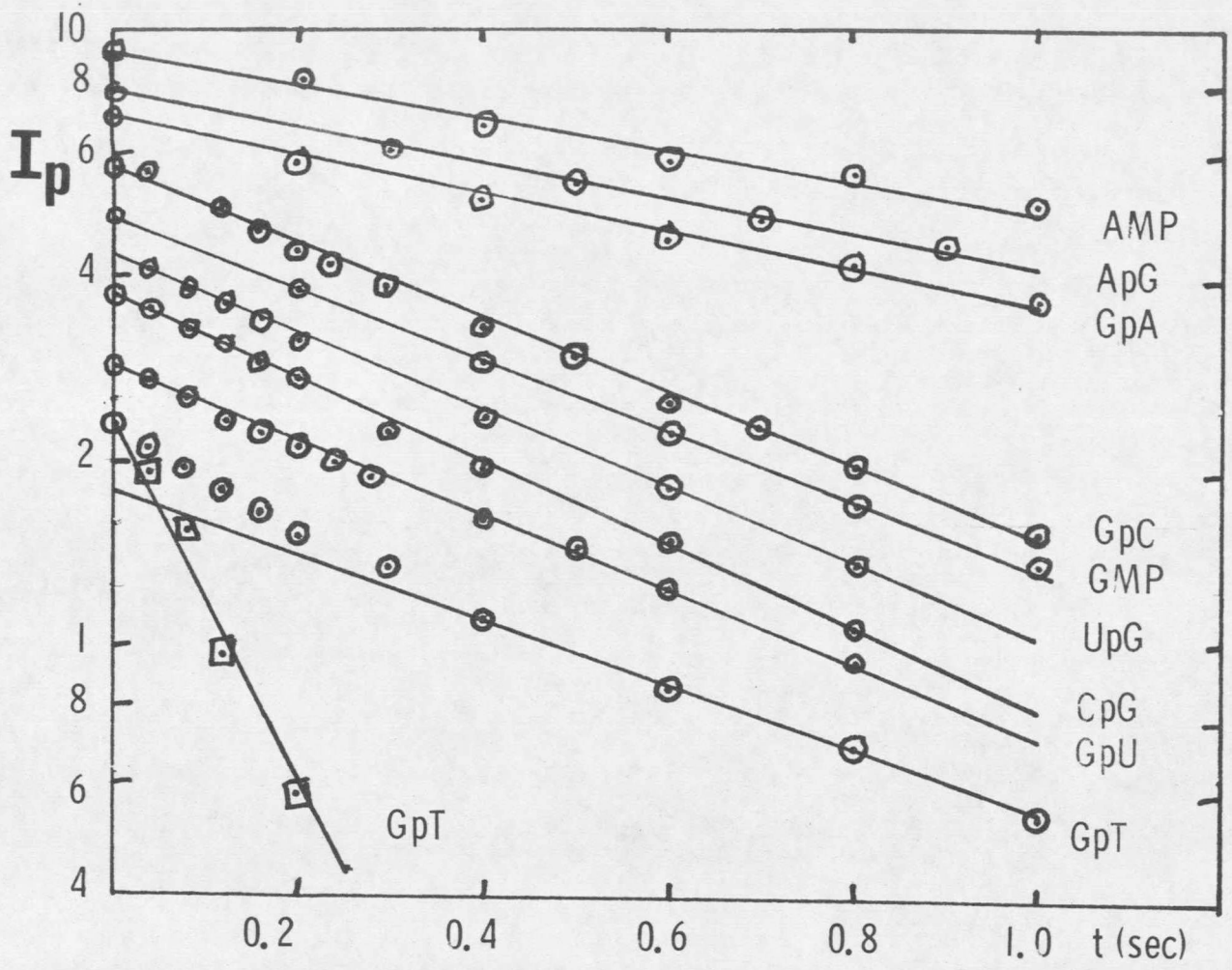

Figure 31. Semilog plot of phosphorescence decay.

GpT is an exception. The reported order of triplet energy levels for the nucleotides is CMP > UMP > GMP > AMP > TMP (38). Much has been made of the observation that TMP has the lowest triplet and, as a consequence, is a low energy trap for triplet excitation, causing much of the known photoalteration of nucleic acid polymers to result from TMP photochemistry (39). Either the GpT dinucleotide is not stacked sufficiently under the present conditions to allow triplet transfer or perhaps the triplet energies of TMP and GMP are sufficiently close in the experimental situation so that there is no preferential low energy state. Of course, in the ApG and GpA cases, it must be that the rate of photochemistry of GMP is competitive with the triplet transfer to AMP.

Table 10. Triplet lifetimes.

	$^3\tau$(sec)		$^3\tau$(sec)
AMP	1.4	GpT(ℓ)	0.70
ApG	1.4	GpT(s)	0.14
GpA	1.4		
GMP	0.72		
CpG	0.62		
GpC	0.65		
UpG	0.69		
GpU	0.70		

g. Dinucleotides vs. nucleotide mixtures. The results with the dinucleotides at low concentration have indicated that the presence of a second nucleotide in the same molecule causes major changes in photochemical and photophysical quantum yields from what would be expected if the two nucleotides acted independently. The previously discussed experiments made comparison between the dinucleotides and individual nucleotides. Here is presented the results of experiments designed to show directly the difference between dinucleotides and equimolar mixtures of the appropriate nucleotides. There is an advantage here in that higher concentrations may be used resulting in a larger luminescence signal. This is possible since one is only interested in comparisons and both solutions have nearly the same absorbance properties. Transmittance effects were taken into account for the excitation spectra.

The dinucleotides were made up to have an O.D. of 0.80 at 255 nm in the buffered G-70, the cell pathlength being 6 mm. The equimolar mixtures of nucleotides were made to have the same 0.80 O.D. at 255 nm. The proper portion of each nucleotide required was determined from the relation $A^{255}_{Tot} = \epsilon^{255}_{G} C\ell + \epsilon^{255}_{x} C\ell$. Knowing the values for A^{255}_{Tot}, ϵ^{255}_{G}, ϵ^{255}_{X}, and ℓ it was possible to solve for

C; and then equal volumes of solutions having O.D.'s of $2\epsilon_G^{255} C\ell$ and $2\epsilon_x^{255} C\ell$ were mixed to give the equimolar mixture of the GMP and XMP nucleotides.

The following experiments were performed at -110°C in the luminescence mode for the dinucleotides and equimolar nucleotide mixtures:

(1) The fluorescence signal at 325 nm when exciting at 255 nm, F_{325}^{255}, was recorded as a measure of the Φ_F's.

(2) Photolysis was conducted for 10 minutes at λ_{ex} = 255 nm, and the F_{425}^{313} recorded as a measure of the Φ_{PC}'s.

(3) Fluorescence excitation spectra were recorded uncorrected, and the difference spectra determined and corrected for lamp intensity and transmittance factors, to measure the differences in Φ_F as a function of λ_{ex} for the two systems.

The data and comparisons for (1) and (2) are given in Table 11. The results from (3) are illustrated in Figures 32 to 38. All recorded information is for the same instrumental settings and I_0's.

The results shown in Table 11 indicate a good relationship between the increase or decrease in Φ_F when a

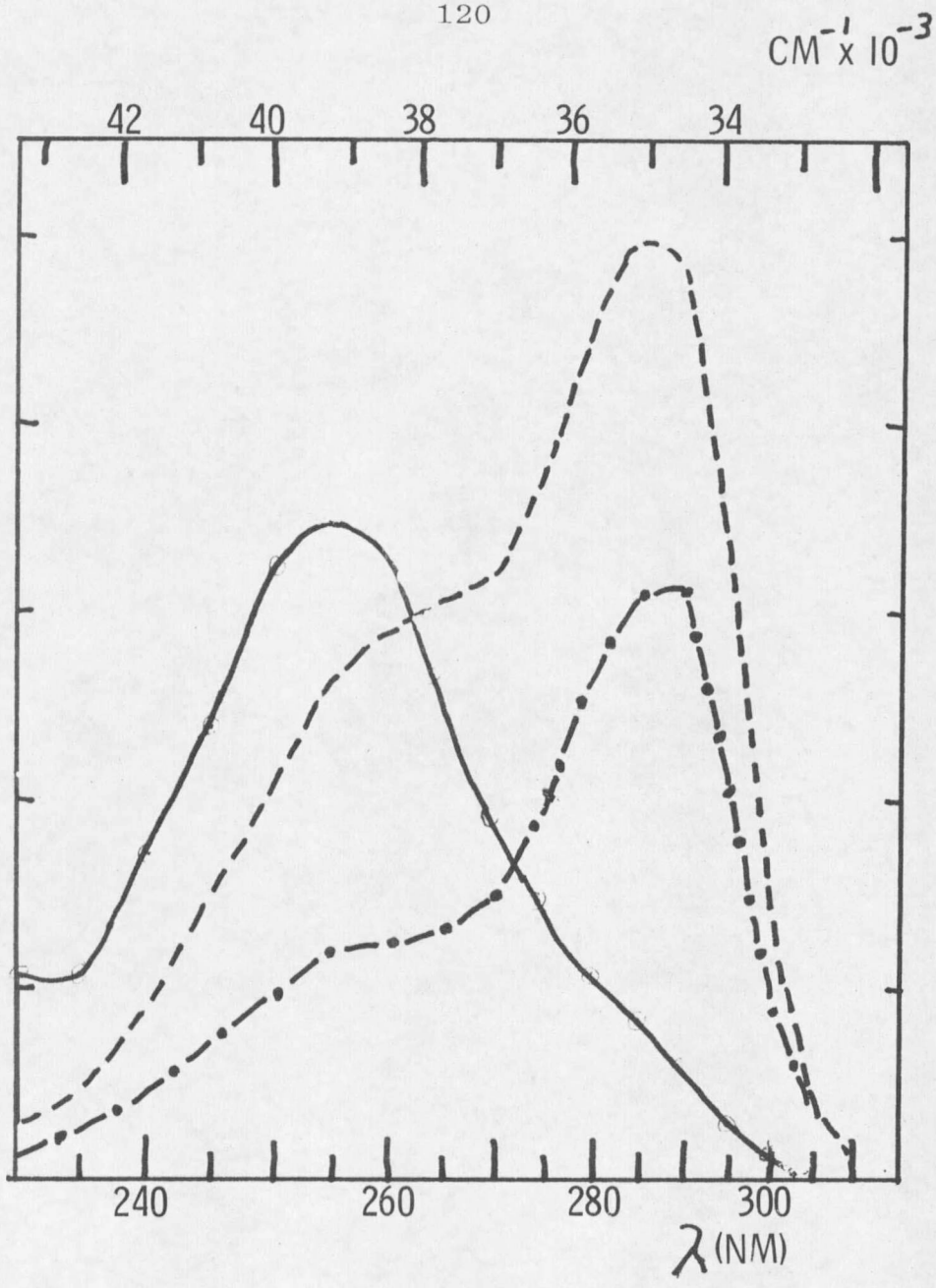

Figure 32. AMP + GMP vs. ApG; ----- fluorescence excitation ApG, •–•–• fluorescence excitation AMP + GMP, ——— corrected difference spectrum.

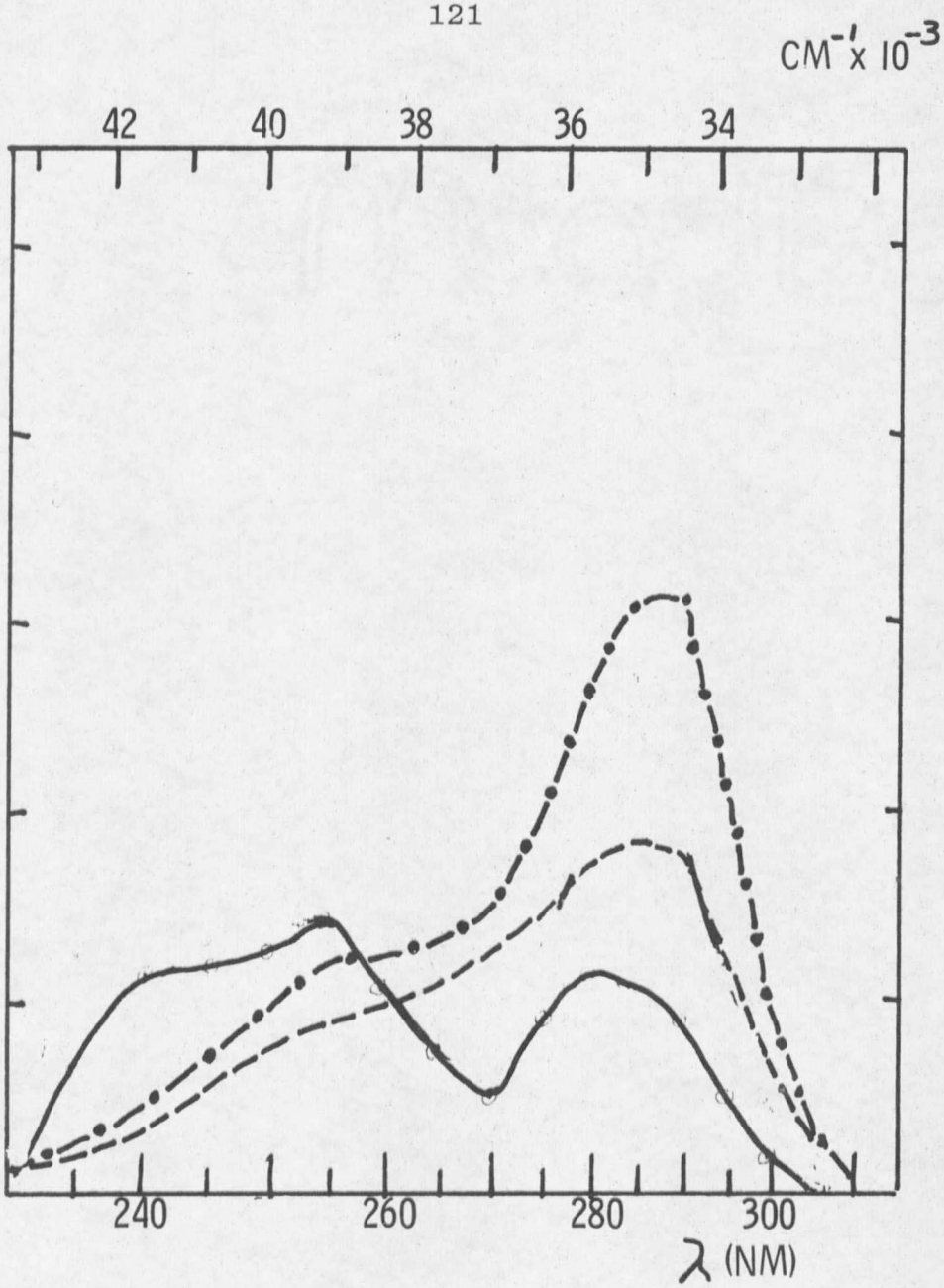

Figure 33. AMP + GMP vs. GpA; ----- fluorescence excitation GpA, • • • • • fluorescence excitation AMP + GMP, ——— corrected difference spectrum.

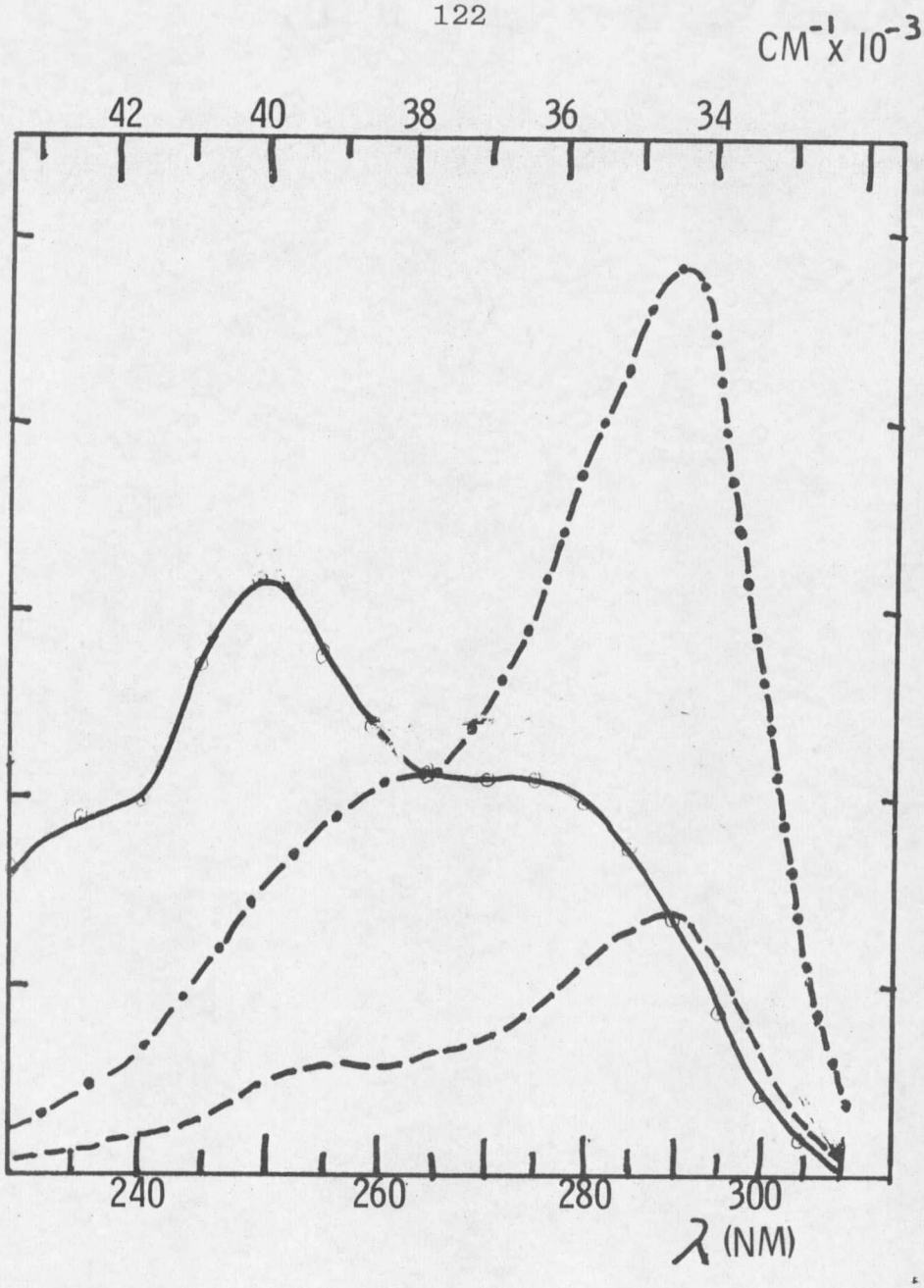

Figure 34. CMP + GMP vs. CpG; ----- fluorescence excitation CpG, • • • • • fluorescence excitation CMP + GMP, ——— corrected difference spectrum.

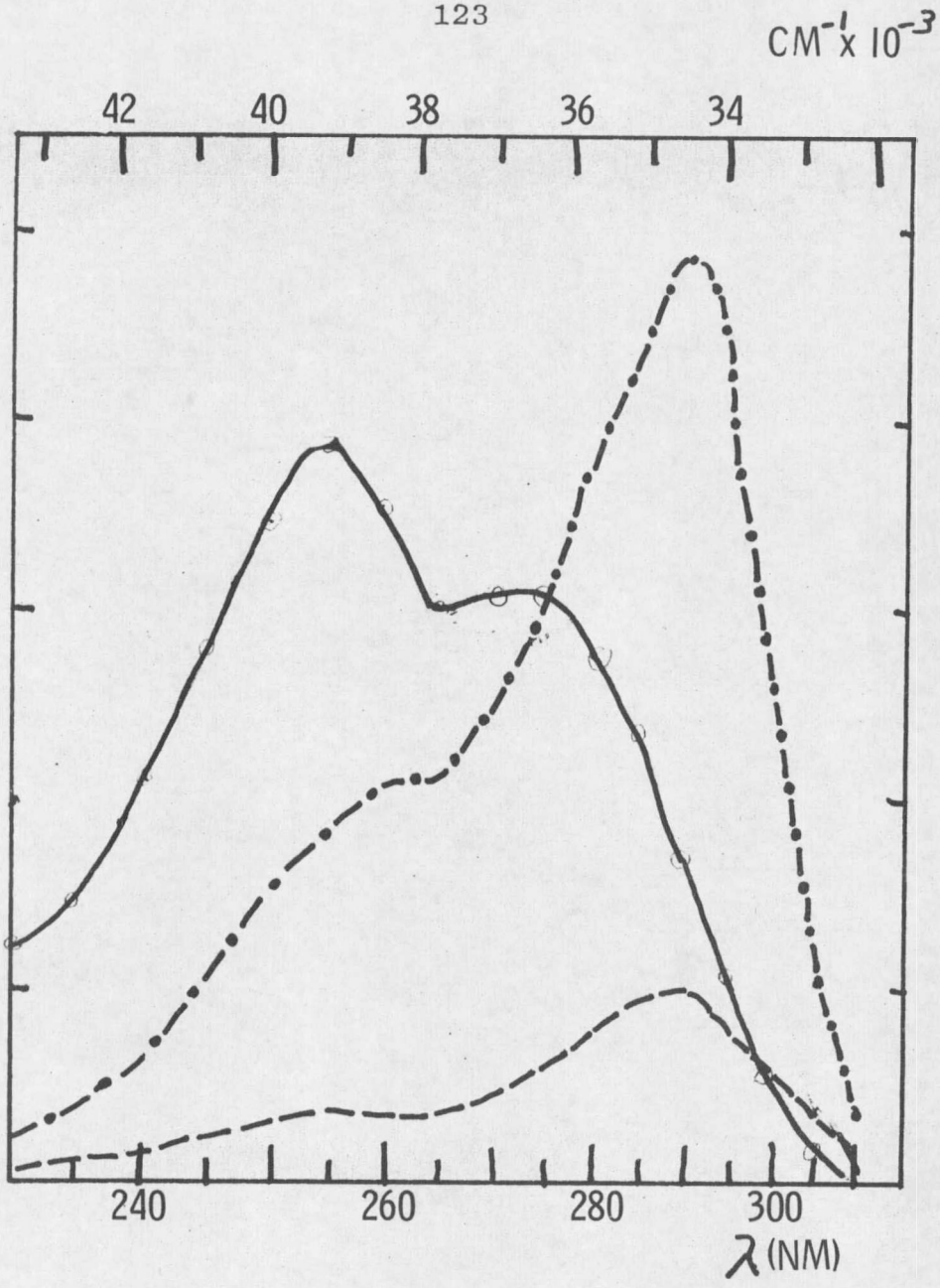

Figure 35. CMP + GMP vs. GpC; ----- fluorescence excitation GpC, · · · · · fluorescence excitation CMP + GMP, ——— corrected difference spectrum.

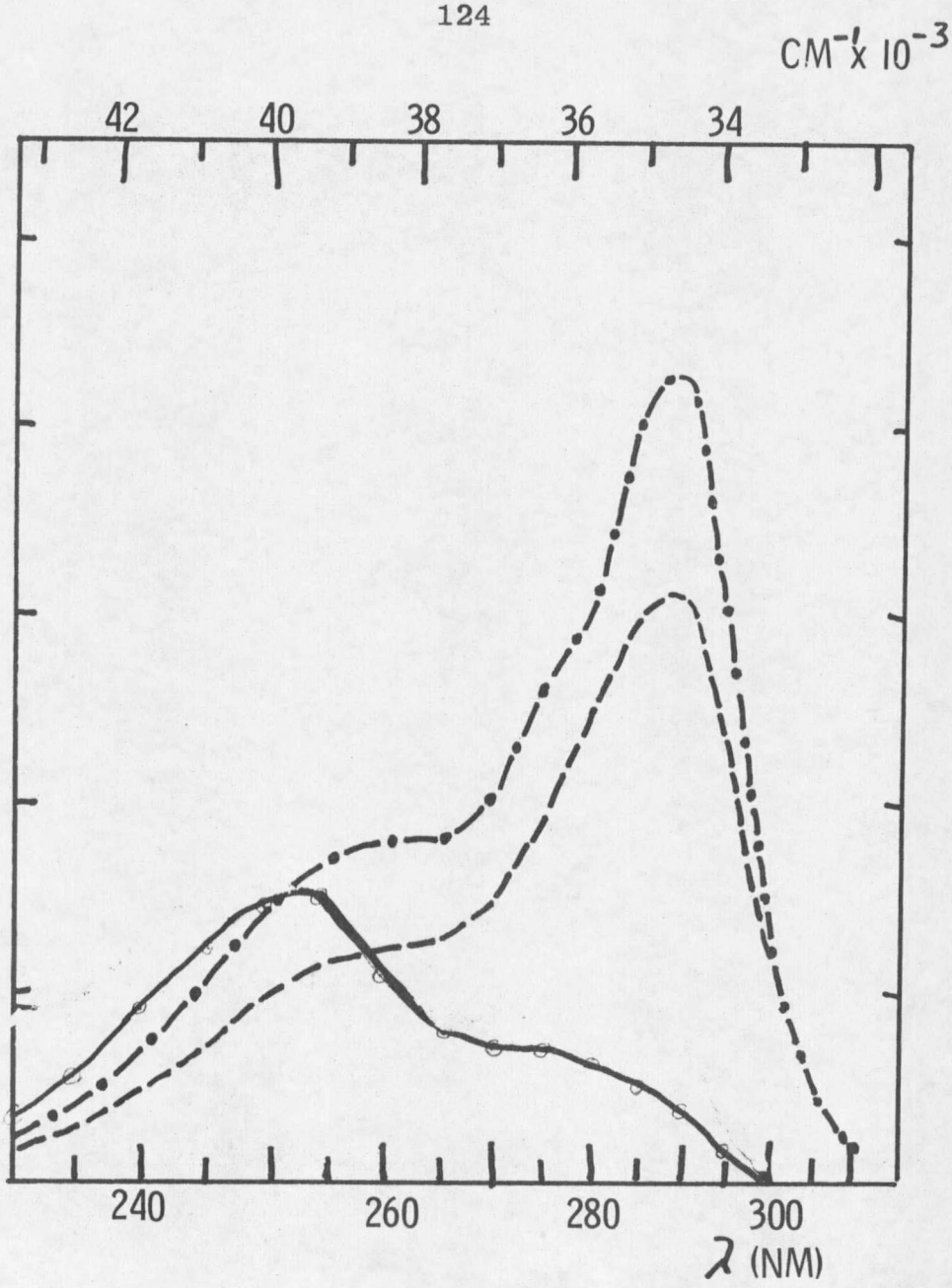

Figure 36. UMP + GMP vs. UpG; ----- fluorescence excitation UpG, • • • • • fluorescence excitation UMP + GMP, ——— corrected difference spectrum.

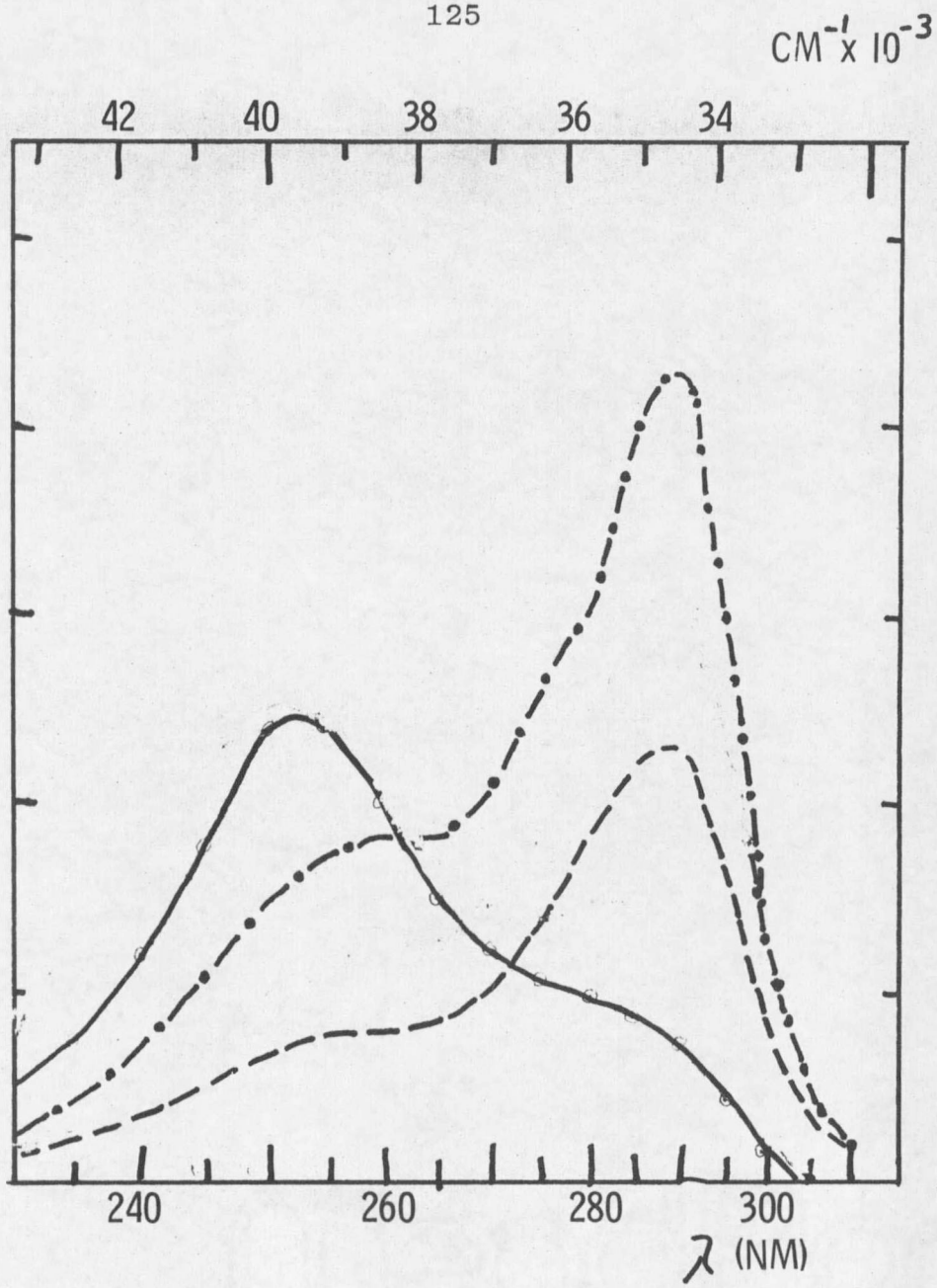

Figure 37. UMP + GMP vs. GpU, ----- fluorescence excitation GpU, • • • • • fluorescence excitation UMP + GMP, ——— corrected difference spectrum.

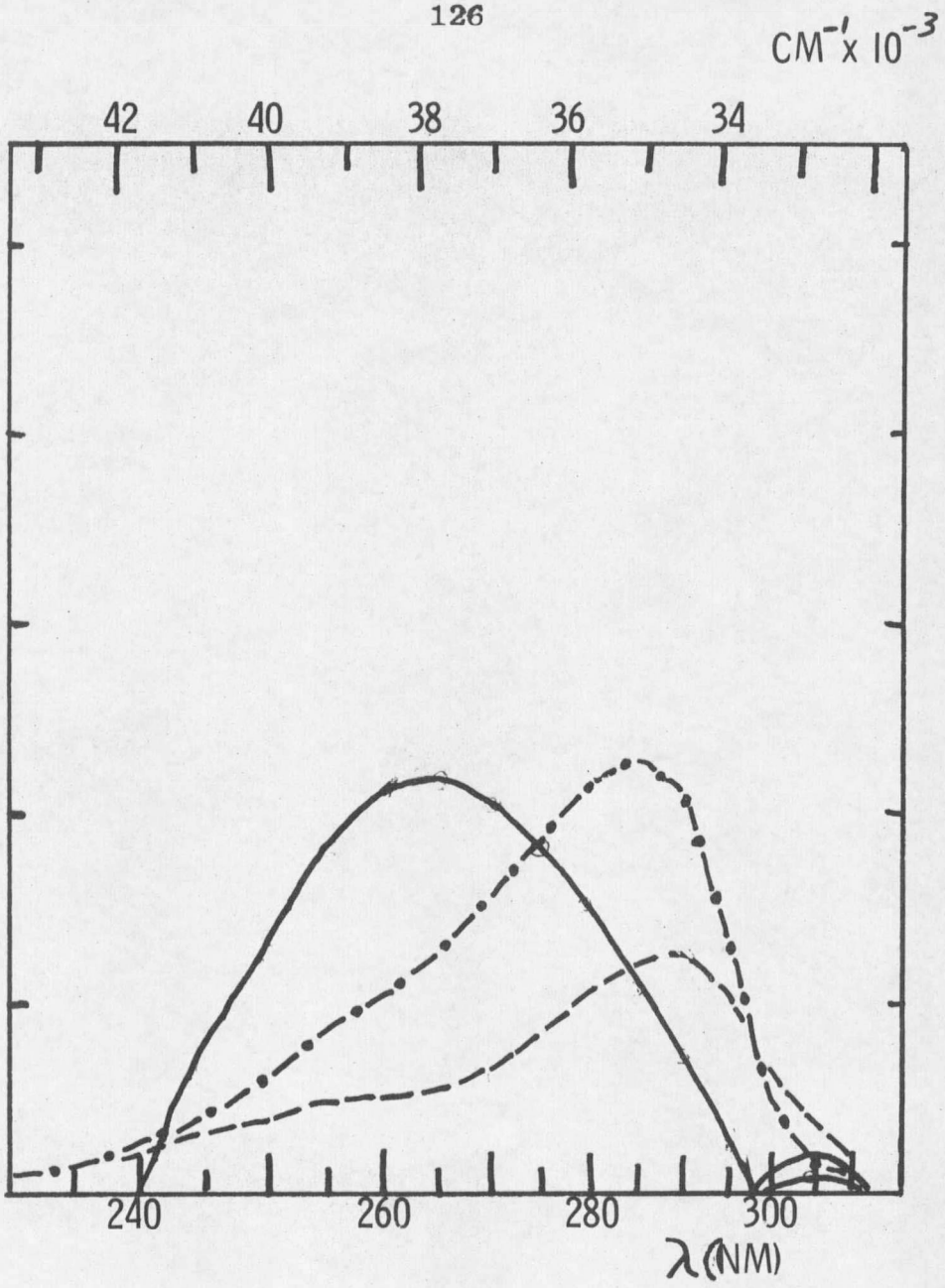

Figure 38. TMP + GMP vs. GpT; ----- fluorescence excitation GpT, • • • • • fluorescence excitation TMP + GMP, ——— corrected difference spectrum.

Table 11. Dinucleotide vs. monomer mixtures data.

$\%A^{255}$		F^{255}_{325}	$F^{255}_{325}(XpG)/F^{255}_{325}(X+G)$	F^{313}_{425}	$F^{313}_{425}(XpG)/F^{313}_{425}(X+G)$
48	GMP + AMP	1.75	--	16	--
48	ApG	4.20	2.5	35	2.2
48	GpA	1.60	0.95	34	2.1
70	GMP + CMP	3.0	--	31	--
70	CpG	0.83	0.25	4.5	0.15
70	GpC	0.41	0.15	5.0	0.16
58	GMP + UMP	2.60	--	21	--
58	UpG	1.80	0.70	7	0.33
58	GpU	1.25	0.48	10.5	0.50
58	GMP + TMP	3.60	--	22	--
58	GpT	2.10	0.61	15	0.68

dinucleotide is present as opposed to a nucleotide mixture, and the corresponding changes in Φ_{PC}. GpA might not seem to have such good agreement, but a reference to the Φ_F, as determined by the proper integration of the fluorescence (Table 8) shows that the value is not much less than that of ApG. The apparent discrepancy is likely due to GpA having a considerable excimer fluorescence at wavelengths greater than 350 nm so that the F_{325}^{255} is not a proper measure of its Φ_F. The UpG results cannot be explained away in a similar fashion.

The intensity corrected difference spectra of the fluorescent excitation spectra of the dinucleotides and equimolar nucleotide mixtures show specifically the variation of Φ_F with λ_{ex} that results on bringing the nucleotides in close proximity, as they are in a dinucleotide. Examination of the difference spectra provides the following observations.

(1) For CpG, GpC, UpG, and GpU, the spectra are similar to the absorption or fluorescence excitation spectrum of GMP. The values of A_{280}/A_{250} are 0.63, 0.80, 0.40, and 0.40 for the molecules difference spectra as listed, compared to values of 0.60 and 0.70 for the

absorption and fluorescence excitation spectra of GMP. This is indicative of singlet-singlet energy transfer from GMP.

(2) For GpT, the spectrum is strikingly like that of the absorption spectrum of TMP, indicating energy transfer from TMP to GMP.

(3) The ApG case is unique for the cases shown as it is the only situation for which the Φ_F is greater at all λ_{ex}'s for the dinucleotide than for the equimolar mixture of nucleotides. The corrected difference spectrum is similar to an AMP absorption spectrum, representative of energy transfer from AMP to GMP.

(4) The GpA spectrum is certainly the most unusual in its shape, showing no relation to the absorption spectrum of either GMP or AMP. However, excimer emission has been indicated to be λ_{ex} dependent for this molecule, which could account for the nature of the curve.

It has been implied here that some degree of singlet-singlet energy transfer is responsible for the various Φ's obtained for the dinucleotides. Certainly the results are suggestive of this mechanism in a number of cases. A theoretical evaluation of the possible rates of transfer for the GMP containing dinucleotides will be

presented in the next section, along with a discussion of the combined experimental results for each dinucleotide.

h. Optical properties of the low temperature product. The absorption and fluorescence excitation spectra of the low temperature photoproduct, normalized at 280 nm, are shown in Figure 39. Also indicated in the figure are the results of a fluorescence polarization study of the product made by the method of photoselection (40). The polarization study was conducted as follows:

(1) A sample of GMP in G-70 at -110°C was irradiated at 255 nm until no evidence of the parent compound was detectable by fluorescence measurement.

(2) Polarizers were attached to both the excitation and emission monochromators.

(3) The emission monochromator was set to the wavelength of the fluorescence maximum of the photoproduct.

(4) With the polarizer on the excitation monochromator oriented to pass light polarized in the vertical sense, the fluorescence response, $I_{//}$, was measured with the polarizer on the analyzing monochromator oriented to pass light polarized parallel to the exciting light. The analyzing polarizer was then rotated to pass light

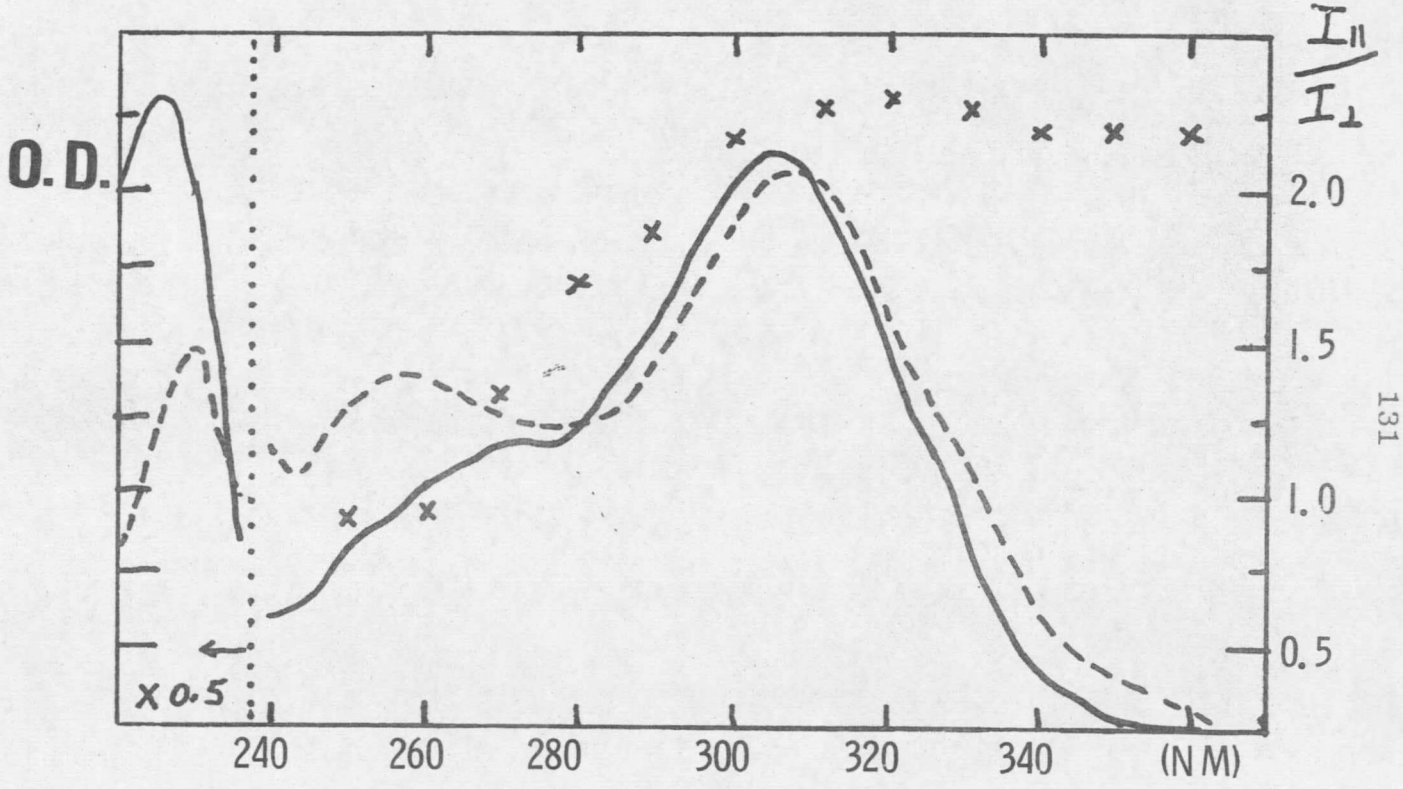

Figure 39. Low temperature photoproduct; ——— absorption, ----- fluorescence excitation, x x x polarization ratio $I_{\parallel}/I_{\perp}$.

polarized perpendicular to the exciting light and the fluorescence response, $I_{\perp}$, taken. This process was begun with exciting light of the wavelength of the lowest energy in the absorption envelope of the product, 360 nm, and repeated at 10 nm intervals down to 250 nm.

(5) A plot was made of the polarization ratio $I_{\parallel} / I_{\perp}$ vs. wavelength of exciting light.

The drop in the polarization ratio from 2.25 at 310 nm to a value of 0.98 at 260 nm indicates the existence of two transition moments approximately 60° to one another. This substantiates what was suggested in the absorption and fluorescence excitation measurements, that there was a second transition located in the vicinity of 260 nm.

The Φ_F for the product at -112°C as determined relative to QBS is 0.35. The O.D. for the measurement when exciting at 313 nm was estimated from the percentage decrease in the parent GMP fluorescence and the relative ε's of the GMP and product as estimated previously from the complete conversion via the absorption monitored mode. This value of Φ_F is then an order of magnitude greater than the Φ_F of the parent GMP, 0.029. On cooling to -137°C, the product showed no detectable phosphorescence.

The overlap of the absorption and fluorescence bands places the O-O band at 28.0×10^3 cm^{-1}, which is 6.0×10^3 cm^{-1} lower in energy than GMP. The Stokes shift, as estimated from the energy difference between the F_{max} and the absorption maximum of the low energy absorption moment, is 8.0×10^3 cm^{-1} as compared to a Stokes shift of 6.0×10^3 cm^{-1} for GMP.

A literature search revealed two compounds with similar optical properties, both purine derivatives; the so-called Y base (41) found in some t-RNA's, and the fluorescent derivative of adenosine, 1,N^6-ethenoadenosine (42). Both of these compounds have a structure which is the result of the formation of a third nitrogen heterocyclic ring system in guanine and adenine through the connection of the N_1 purine nitrogen and the exocyclic amine nitrogen by two carbon atoms. The reported structures are:

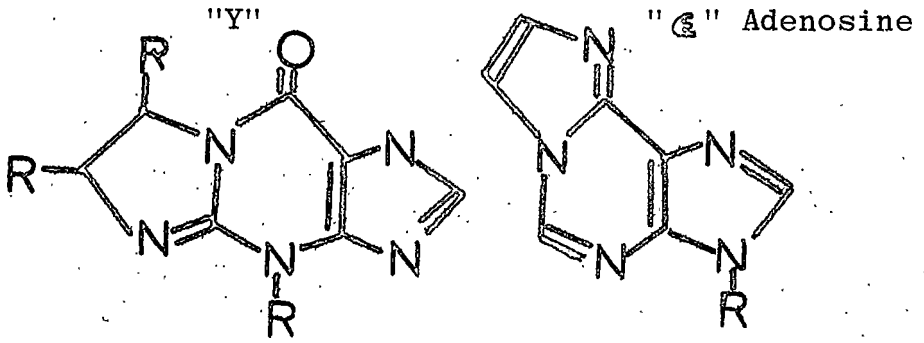

The optical properties, as compared to the low temperature GMP product, are given in Table 12.

The optical properties are similar enough to suggest a tricyclic structural form for the low temperature GMP product.

Table 12. Product, "Y", and "ϵ" optical properties

Cmpd	Absorption		Fluorescence	
	λ_{max}(nm)	$\epsilon \times 10^{-3}$	F_{max}(nm)	Φ_F
"ϵ"	258	5.0	415	0.44
(pH 7 at	265	6.0		
300°K)	275	6.0		
	294	3.1		
"Y"	236	23.5	409	0.5
(G-50 at	264	4.4		
80°K)	303	4.4		
GMP "P"	225	19.4	418	0.35
(G-70 at	265	3.7		
160°K)	305	8.3		

i. Temperature dependence and stable product formation. While the low temperature product of GMP was seen to be thermally unstable, as characterized by the disappearance of its identifying absorbance and fluorescence

properties when the photolized solution was allowed to warm to room temperature, there were on occasion optical effects which were suggestive of a minor amount of remaining product. As a consequence, a study was made of the temperature dependence of both the rate of product formation and the rate of product decay. The results of the variation of product formation rate as determined in the luminescence mode is shown in Figure 40. The varying GMP Φ_F is also given, along with the results previously obtained for product formation in the absorption monitored mode (Figure 10).

Good agreement is seen between the luminescence and absorption results for the temperature range -91°C to -137°C. The decrease in photochemical yield at temperatures below -120° could well be the result of decreased solvent mobility as emission from the triplet state becomes increasingly more efficient for GMP under these conditions. The product gave no indication of thermal decay under these temperature-viscosity ranges (-91°C to -137°C) as the product fluorescence remained constant with time, in the absence of irradiation of the parent.

The situation was changed significantly by altering the experimental temperature to -80°C. At this

temperature-viscosity, photolysis produced, in addition to the usual 418 nm fluorescence band, a second less intense band in the vicinity of 350 nm. Cessation of photolysis of the parent and observation of the product fluorescence produced a surprising effect; the 418 nm band was partially transformed with time into the 355 nm band. A very slow warming to room temperature had the result that the 355 nm band remained, although diminished in intensity and red shifted to 365 nm. Recooling to -80°C re-established the shape and intensity of the 355 nm band. The 418 nm band was absent at room temperature and when the solution was recooled at -80°C.

At slightly warmer photolysis temperatures, -57°C to -74°C, only the 355 nm band is produced, with decreasing efficiency and increased red shifting to near 360 nm. At room temperature, the efficiency of producing the 365 nm band is only 5% that at -80°C.

Preliminary results with the GMP dinucleotides and with soluble RNA indicate that all of these compounds show the characteristic GMP photoproduct fluorescence, when photosensitized with acetone in the presence of glycol at room temperature. The use of the product as a fluorescent probe in biological polymers is thus established.

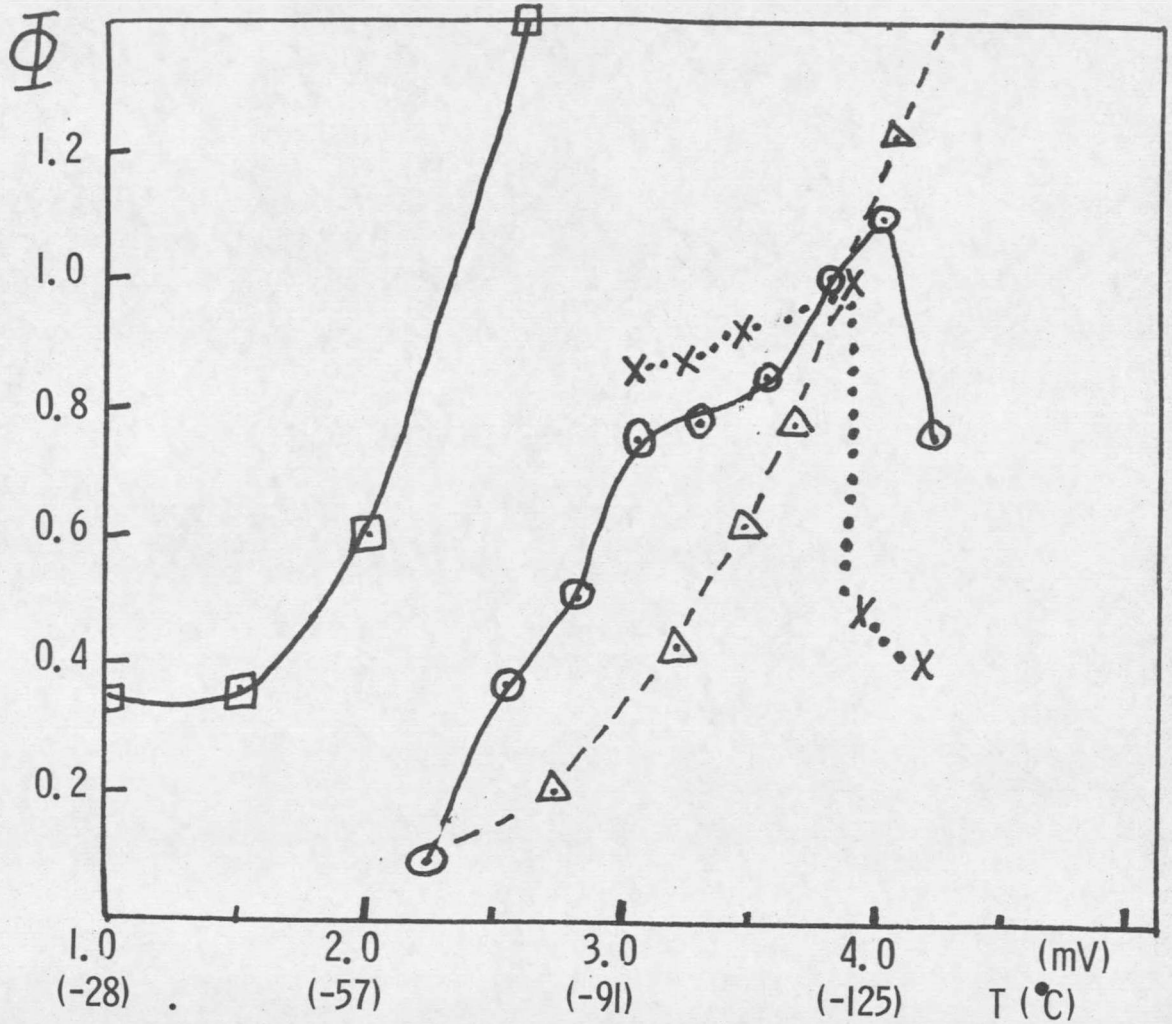

Figure 40. Relative Φ's of GMP vs. temperature; ▣ Φ_{PC} in 70% glycerol via absorption, ◎ Φ_{PC} in G-70 via absorption, x··x Φ_{PC} in G-70 via fluorescence λ_{ex}=255, △ Φ_F as measured by F_{325}^{255} in G-70.

3. Energy transfer, theoretical and experimental results.

a. Theoretical results. Gueron, Eisinger, and Shulman (13) have published the results of calculations designed to show the probability of singlet-singlet energy transfer, assuming dipole-dipole coupling for the nucleotides, based on the optical properties of the nucleotides at 77°K. Only ApA was correlated experimentally with the proposed theoretical results.

Here are presented the results of similar calculations for GMP containing dinucleotides under the conditions at which the photophysical and photochemical properties of these molecules was determined for this work. There is an advantage now for these calculations in that there has been published recently an X-ray structure of a GMP containing dinucleotide GpC (2), and the experimentally determined transition moment directions for the nucleic bases are now all available. Also rather than making certain approximation in the calculations, it was attempted to make reasonably complete integrations, etc.

This expectedly improved analysis, however, does not necessarily mean that this approach is totally accurate for the dinucleotides. Excimer formation is not

taken into account, nor is hypochromism, the reduction in absorptivity which results when two nucleotides are joined to form a dinucleotide. The possibility of excitation transfer by electron exchange is another factor which could be significant at the small distances which separate the nucleotides.

The relation used to predict the rates and efficiencies of singlet energy transfer is that derived by Förster for the very weak coupling interaction case of dipole-dipole coupling (43). This is a convenient expression of the phenomenon as the parameters are given in terms of experimental observables. The relation for the transfer rate is:

$$k_{D\to A} = \frac{9000K^2 \ell n\ 10}{128\pi^5 n^4 N \tau_0 R^6} \int \frac{F_D(\bar{\nu})\ \epsilon_A(\bar{\nu}) d\bar{\nu}}{\bar{\nu}^4}$$

where:

$k_{D\to A}$ = rate constant for transfer,

K = dipolar orientation factor,

= $\cos\theta - 3 \cos\omega_1 \cos\omega_2$, where θ is the angle between the transition moment vectors of both molecules, while ω_1 and ω_2 are the

angles between the respective vectors and the direction of R,

R = distance between donor and acceptor,

n = index of refraction of the intervening medium,

N = Avogadro's number,

$^1\tau_0$ = the natural radiative lifetime of the donor,

$\mathcal{E}_A(\bar{\nu})$ = molar extinction coefficient of the acceptor,

$F_D(\bar{\nu})$ = the spectral distribution of fluorescence normalized such that $\int F_D(\bar{\nu})d\bar{\nu} = 1$.

A modification of this formula gives an expression which relates to the efficiency of the transfer. This is done by assuming a distance R_0 wherein the rate of energy transfer is equal to the rate of all other depopulation pathways of the donor singlet state, i.e.,

$$k_{D\rightarrow A} = \sum_i k_i, \text{ when } R = R_0.$$

Also since $\sum_i k_i = 1/^1\tau$, and $^1\tau = \Phi_F\, ^1\tau_0$;

$$R_0^6 = \frac{9000K^2 \Phi_F \ln 10}{128\pi^5 n^4 N} \int \frac{F_D(\bar{\nu}) \mathcal{E}_A(\bar{\nu}) d\bar{\nu}}{\bar{\nu}^4}$$

where Φ_F is the fluorescence quantum yield of the donor molecule.

The integral term is referred to as the "overlap integral" between the donor fluorescence and the acceptor absorption and shall be termed J. It has units of $mole^{-1}$ cm^3.

In order to obtain the $k_{D\rightarrow A}$ values for the GMP containing dinucleotides from the spectral and crytallographic data, it was first necessary to calculate $^1\tau_0$ values for the nucleotides. This was done from the Strickler and Berg relation (44) which is a modification of Einstein's relation for the natural radiative lifetimes for atoms. The Strickler and Berg relation for $^1\tau_0$ of molecules is

$$\frac{1}{^1\tau_0} = 2.88 \times 10^{-9} n^2 <\bar{\nu}_F^{-3}>_{AV}^{-1} \frac{g\ell}{g_u} \int \mathcal{E} \, d \ln \bar{\nu},$$

where:

n = the index of refraction of the medium (1.4 for G-70),

$\langle \bar{\nu}_F^{-3} \rangle_{AV}^{-1}$ = the reciprocal of the mean value of $\bar{\nu}^{-3}$ in the fluorescence spectrum,

g_ℓ/g_u = the ratio of the degeneracies in the upper and lower states (assumed here to be unity),

ϵ = the molar extinction coefficient at $\bar{\nu}$ in the region of the lowest transition for the molecule.

The results for the nucleotides as determined by the above relation are given in Table 13.

Table 13. Calculated $^1\tau_0$ values for the nucleotides by the Strickler-Berg relation.

	$\langle \bar{\nu}_F^{-3} \rangle_{AV}^{-1}$ $\times 10^{-13}$	$\int \epsilon \, d \ln \bar{\nu}$ $\times 10^{-3}$	$^1\tau_0$ (sec) $\times 10^9$
GMP	2.97	1.218	4.8
AMP	3.25	1.886	2.8
CMP	2.97	1.030	5.7
UMP	3.17	0.943	5.8
TMP	2.97	0.902	6.5

The values of $\bar{\nu}_F$ were estimated from the literature values of $\bar{\nu}_F^{max}$ at 77°K. The ϵ values were taken from the low temperature (-110°C) values obtained for this work.

Where there was large overlap from a higher energy transition in the absorption spectrum, an attempt was made to make the lowest absorption band gaussian in shape on a wave number scale. The fluorescence polarization study on guanine by Callis (45) was particularly helpful in resolving the low energy band for GMP.

The $^1\tau_0$ values listed here agree reasonably well with those calculated by Gueron, Eisinger, and Shulman (13), except for GMP. Their values based on oscillator strengths and suitable averages of λ_F(cm) and λ_A(cm) were given as 3, 12, 5.5, 4.5, and 4.5 nsec for the $^1\tau_0$'s of AMP, GMP, CMP, TMP, and UMP, respectively. The discrepancy in the GMP case is likely due to their having underestimated the oscillator strength for the low energy band.

The dipolar orientation factor K for the dinucleotides was determined by, 1) considering that the conformations of the GMP containing dinucleotides were the same as that obtained by Day, Seeman, Rosenberg, and Rich (2) in their X-ray structural analysis of the GpC molecule; 2) the use of current reports of the experimentally determined transition moment directions in the nucleic bases: Cytosine, Callis, and Simpson (46), Lewis and Eaton (47); 9-methyladenine, Stewart and Davidson (48); 9-ethylguanine,

Callis and Simpson (49); 1-methyluracil, Eaton and Lewis (50); 1methyl thymine, Stewart and Davidson (51); 3) the dipoles were placed in the center of the six membered ring in all cases.

The values obtained for the θ, ω_1, ω_2 angles in the $K = \cos\theta - 3\cos\omega_1\cos\omega_2$ expression and the resultant K^{+2} values for the low energy moments are listed in Table 14. There exists an ambiguity for the directions of the low energy moments in guanine. For that reason, two data sets are listed for each molecule, the first listed is that considering the direction of the guanine moment to be +44° and the second set for the guanine transition direction of -14°. The ω_1 and ω_2 values are the angles that the GMP and XMP moments, respectively, make with R vector.

The final factor needed to calculate the rate constant for transfer $k_{D\rightarrow A}$ was J, the overlap integral. The integration was accomplished by a computer method where an area approximation was made at 5 nm intervals, the $F_D(\bar{\nu})$ was phototube response corrected.

The $k_{D\rightarrow A}$ values obtained are listed in Table 15 along with the necessary parameters K^2, $^1\tau_0^{-1}$, and J. The value of n is taken to be unity since no solvent intervenes stacked bases. R is 4Å.

Table 14. Postrelaxation orientation factors.

XpG	θ	ω_1	ω_2	K^2
ApG	22°	89°	82°	0.844
"	36°	75°	82°	0.491
CpG	11°	89°	82°	0.964
"	46°	49°	82°	0.177
UpG	3°	89°	86°	0.863
"	60°	49°	86°	0.132
GpA	80°	77°	74°	0.0001
"	22°	89°	74°	0.832
GpC	63°	72°	68°	0.011
"	9°	78°	68°	1.51
GpU	67°	72°	72°	0.011
"	10°	78°	72°	0.627
GpT	34°	72°	76°	0.365
"	23°	78°	76°	0.591

For the calculation of the R_0 distances, the Φ_F's used were those accumulated for this work at -110°C. The K^2 and J values used were those previously listed. The 1 and 2 subscripts for the R_0 values in Table 16 refer to the +44° and -14° directional cases for the low energy GMP moment.

All of the results listed below for the very weak coupling analysis have as an implicit assumption that the energy transfer occurs after vibrational relaxation to

Table 15. Postrelaxation energy transfer rates.

XpG	K_1^2	K_2^2	$\times 10^{-8}$ $^1\tau_0^{-1}$	$\times 10^{16}$ J	$\times 10^{-12}$ $_1k_{D\rightarrow A}(sec^{-1})$	$\times 10^{-12}$ $_2k_{D\rightarrow A}(sec^{-1})$
XMP = Donor, GMP = Acceptor						
ApG	0.844	0.491	3.50	4.12	26.2	15.2
GpA	0.0001	0.832	3.50	4.12	0.003	25.8
CpG	0.964	0.177	1.75	0.46	1.67	0.30
GpC	0.011	1.54	1.75	0.46	0.017	2.67
UpG	0.863	0.132	1.72	3.47	11.1	1.68
GpU	0.011	0.627	1.72	3.47	0.14	8.04
GpT	0.365	0.591	1.55	1.25	1.53	2.45
GMP = Donor, XMP = Acceptor						
ApG	0.844	0.491	2.1	0	0	0
GpA	0.0001	0.832	2.1	0	0	0
CpG	0.964	0.177	2.1	0.73	3.18	0.58
GpC	0.011	1.54	2.1	0.73	0.036	5.07
UpG	0.863	0.132	2.1	0.20	0.77	0.12
GpU	0.011	0.627	2.1	0.20	0.010	0.56
GpT	0.365	0.591	2.1	0.54	0.88	1.44

K_1^2, K_2^2, $_1k_{D\rightarrow A}$, and $_2k_{D\rightarrow A}$ refer to the cases where the transition moment for the GMP is at 1(+44°) and 2(-14°).

the lowest vibrational level of the first excited singlet of the donor molecule. Considering the magnitude of the rate constants for transfer (e.g., 10^{13} sec^{-1} for ApG), and R_0 distances obtained as compared to the R distance of 4.0 A which should apply to the stacked nucleotides, the possibility that transfer could happen prior to vibrational relaxation was not discounted.

Table 16. Calculated R_0 distances in XpG dinucleotides. Units of R_0 are Å.

	XMP = Donor			GMP = Donor		
XpG	$\times 10^2$ Φ_D	R_{0_1}	R_{0_2}	$\times 10^2$ Φ_D	R_{0_1}	R_{0_2}
ApG	0.2	6.3	5.7	2.9	0	0
GpA	0.2	1.4	5.0	2.9	0	0
CpG	1.3	6.1	4.6	2.9	7.5	5.7
GpC	1.3	2.9	6.6	2.9	3.6	8.1
UpG	0.1	5.5	4.0	2.9	5.9	4.4
GpU	0.1	2.6	5.2	2.9	2.9	5.6
GpT	3.6	7.3	7.9	2.9	6.1	6.6

In order to evaluate the pre-relaxation transfer rates, the following calculations were made: the J overlap integral was recomputed, where the donor fluorescence spectrum was blue-shifted by the amount $\bar{\nu}_{ex} - \bar{\nu}_{0-0}$, $\bar{\nu}_{ex}$

being the wave number of excitation and also the wave number of the minimum energy of fluorescence assumed to occur, ν_{0-0} represents the wave number of 0-0 band as determined from experimentally observed post relaxation fluorescence. The K orientation factors were refigured for the transition moments of the donor and acceptor molecules at the energy of the excitation.

Rather than attempt to assess the pre-relaxation rates at all excitation energies, the situation where excitation was at 250 nm was taken to be a representative case. At this wavelength of excitation, the second band of guanine is almost completely dominant. The transition moment direction for this moment is nearly perpendicular to the moment in the low energy band, with a direction of either +95° or 115 relative to the N , C axis (47). In the other bases, either the low energy band remains clearly dominant at this wavelength, or if the second band makes a significant contribution the transition moment direction is little changed from that of the low energy moment, e.g., cytosine. Therefore, it was considered necessary to only redetermine ω_1, the angle that the GMP moment makes with the R vector, and θ, the angle between the

moments, ω_2 was not redetermined for the pre-relaxation $K^{2'}$.

The pertinent angles and the $K^{2'}$ values are listed in Table 17 for transfer between the GMP containing dinucleotides occurring prior to vibrational relaxation and with a λ_{ex} of 250 nm. Also included is J' the overlap integral for the pre-relaxation transfer.

As in the post-relaxation case, the two fold ambiguity in the GMP transition moment direction requires two sets of data for each dinucleotide, in Table 17 the first data set listed for a dinucleotide refers to the situation where the GMP moment is at +115° relative to the N_3, C_6 axis and the second set is where the GMP moment is at +95°.

To assess the change in rate of transfer resulting from pre-relaxation, as opposed to post-relaxation, transfer, the factors obtained by the changed K' and J terms in the two cases are listed separately, and as a product, in Table 18.

The calculated pre-relaxation energy transfer rate constants $k'_{D\to A}$ as determined by the product $f^* \cdot k_{D\to A}$ are given in Table 19. The $k'_{D\to A}$ values for the ApG cases where GMP was the donor were calculated directly from the

Förster relation using the $K^{2\prime}$ and J' values in the place of K^2 and J.

Table 17. Pre-relaxation orientation and overlap factors, λ_{ex} = 250 nm.

XpG	θ	ω_1	ω_2	$K^{2\prime}$	$J'(\times 10^{16})$ XMP=Donor	$J'(\times 10^{16})$ GMP=Donor
ApG	85°	70°	82°	0.003	23.6	7.90
"	73°	71°	82°	0.024	23.6	7.90
CpG	83°	50°	82°	0.021	25.6	12.3
"	63°	58°	82°	0.054	25.6	12.3
UpG	69°	48°	86°	0.047	18.1	7.50
"	48°	58°	86°	0.31	18.1	7.50
GpA	30°	74°	74°	0.41	23.6	7.90
"	53°	72°	74°	0.12	23.6	7.90
GpC	40°	88°	68°	0.53	25.6	12.3
"	63°	83°	68°	0.17	25.6	12.3
GpU	42°	86°	72°	0.46	18.1	7.50
"	65°	83°	72°	0.10	18.1	7.50
GpT	75°	90°	76°	0.07	19.2	11.6
"	85°	83°	76°	~0	19.2	11.6

Table 18. Pre-relaxation correction factors.

XpG	$K^{2\prime}/K^2$	XMP=Donor $J^\prime/J$	GMP=Donor $J^\prime/J$	XMP=Donor f^*	GMP=Donor f^*
ApG	3.5×10^{-3}	5.7	∞	2.0×10^{-2}	∞
"	4.9×10^{-2}	5.7	∞	0.28	∞
CpG	2.2×10^{-2}	56	17	1.1	0.37
"	0.30	56	17	17	5.1
UpG	5.4×10^{-2}	5.2	38	0.28	2.0
"	2.3	5.2	38	12	87
GpA	4.1×10	5.7	∞	$2.3\ 10^{-2}$	∞
"	0.14	5.7	∞	0.80	∞
GpC	4.8×10	56	17	27	8.2
"	0.11	56	17	6.2	1.9
GpU	4.2×10	5.2	38	2.2	16
"	0.16	5.2	38	0.83	6.1
GpT	0.20	15	21	3.0	4.2
"	0	15	21	0	0

$f^* = (K^{2\prime}/K^2)\cdot(J^\prime/J)$

Table 19. Rate constants for pre-relaxation transfer.

	XMP = Donor			GMP = Donor		
XpG	$\times 10^{-12}$ $k_{D\rightarrow A}$	f^*	$k'_{D\rightarrow A}$	$\times 10^{-12}$ $k_{D\rightarrow A}$	f^*	$k'_{D\rightarrow A}$
ApG	26.2	2.0×10^{-2}	5×10^{11}	0		1×10^{11}
"	15.2	2.8×10^{-1}	4×10^{12}	0		8×10^{11}
CpG	1.67	1.1	2×10^{12}	3.18	3.7×10^{-1}	1×10^{12}
"	0.30	$1.7\times10^{+1}$	5×10^{12}	0.58	5.1	3×10^{12}
UpG	11.1	2.8×10^{-1}	3×10^{12}	0.77	2.0	2×10^{12}
"	1.68	$1.2\times10^{+1}$	2×10^{13}	0.12	87	1×10^{13}
GpA	3×10^{-3}	2.3×10^{-2}	7×10^{7}	0		1.4×10^{13}
"	25.8	0.8	2×10^{13}	0		4×10^{12}
GpC	1.7×10^{-2}	$2.7\times10^{+1}$	5×10^{11}	$3.6\ 10^{-2}$	8.2	3×10^{12}
"	2.67	6.2	2×10^{12}	5.07	1.9	1×10^{13}
GpU	0.14	2.2	3×10^{11}	0.01	1.6	2×10^{11}
"	8.04	0.8	6×10^{12}	0.56	6.1	3×10^{12}
GpT	1.53	3.0	2×10^{13}	0.88	4.2	4×10^{12}
"	2.54	~0	?	1.44	~0	?

Discussion of Results for the Dinucleotides

A compilation of the experimental data and theoretical energy transfer calculations pertinent to the GMP containing dinucleotides is given in Table 20. Figure 41 shows the energy order of XMP's at the singlet and triplet levels. A discussion of this information with regard to

Table 20. Combined results.

	$\Phi(1)^{Rel}_{PC}$	k^{Rel}_{p}	k^{Rel}_{pp}	$\frac{F^{255}_{XpG}}{F^{255}_{X+G}}$	$\frac{F^{313}_{XpG}}{F^{313}_{X+G}}$	FX	P.X	P.C.A.	F.X [XpG - (X+G)]	$f^{G\,255}_{ab}$	Φ_F
GMP	1.0	1.0	1.0	--	--	‡Ab	=F.X	~F.X	--	1.0	0.029
AMP	0	0	0	--	--	‡Ab	--	--	--	--	0.002
CMP	0	0	0	--	--	‡Ab	--	--	--	--	0.013
UMP	0	0	0	--	--	‡Ab	--	--	--	--	0.001
TMP	0	0	0	--	--	‡Ab	--	--	--	--	0.036
ApG	1.99	1.30	2.2	2.5	2.2	‡Ab	=F.X	~F.X	$\sim AMP_{ab}$ or GMP_{ab}	0.48	0.033
GpA	2.19	1.80	2.0	0.95	2.1	‡Ab	=Ab	~Ab	?	0.48	0.023
CpG	0.43	0.30	0.22	0.25	0.15	‡Ab	~F.X	~Ab	$\simeq GMP_{ab}$	0.70	0.011
GpC	0.54	--	--	0.15	0.16	--	--	--	$\sim GMP_{ab}$	0.70	--
UpG	--	--	--	0.70	0.33	--	--	--	$\sim GMP_{ab}$	0.58	--
GpU	0.85	0.30	0.16	0.48	0.50	‡Ab	--	~F.X	$\sim GMP_{ab}$	0.50	0.013
dpGpT	1.83	1.0	0.95	0.61	0.68	‡Ab	~F.X	--	$\simeq TMP_{F.X}$	0.50	0.024

Table 20 (continued)

	Φ_p	Emitting Triplet	Post Relaxation, Energy Transfer								Pre-relaxation Energy Transfer			
			G = Donor		X=Acceptor		X = Donor		G=Acceptor		G = Donor		X = Donor	
			$^1k_{D\to A}$ $\times 10^{12}$	$^1R_0$ Å	$^2k_{D\to A}$ $\times 10^{12}$	$^2R_0$ Å	$^1k_{D\to A}$ $\times 10^{12}$	$^1R_0$ Å	$^2k_{D\to A}$ $\times 10^{12}$	$^2R_0$ Å	$^1k'_{D\to A}$ $\times 10^{12}$	$^2k'_{D\to A}$ $\times 10^{12}$	$^1k'_{D\to A}$ $\times 10^{12}$	$^2k'_{D\to A}$ $\times 10^{12}$
GMP	0.022	G												
AMP	0.001	A												
CMP	0	--												
UMP	0	--												
TMP	0	--												
ApG	0.043	A	0	0	0	0	26	6.3	15	5.7	0.14	0.8	0.5	4
GpA	0.18	A	0	0	0	0	.003	1.4	26	5.0	.14	4	7×10^{-5}	20
CpG	0.009	G	3.2	7.5	0.6	5.7	1.7	6.1	0.3	4.6	1	3	2	5
GpC	--	G	.04	3.6	5.1	8.1	.02	2.9	2.7	6.6	3	10	0.5	2
UpG	--	G	.8	5.9	0.1	4.4	11	5.5	1.7	4.0	2	10	3	20
GpU	0.010	G	.01	2.9	.6	5.6	.14	2.6	8.0	5.2	0.2	3	0.3	6
dpGpT	0.012	T	.9	6.1	1.4	6.6	1.5	7.3	2.5	7.9	4	0	20	0

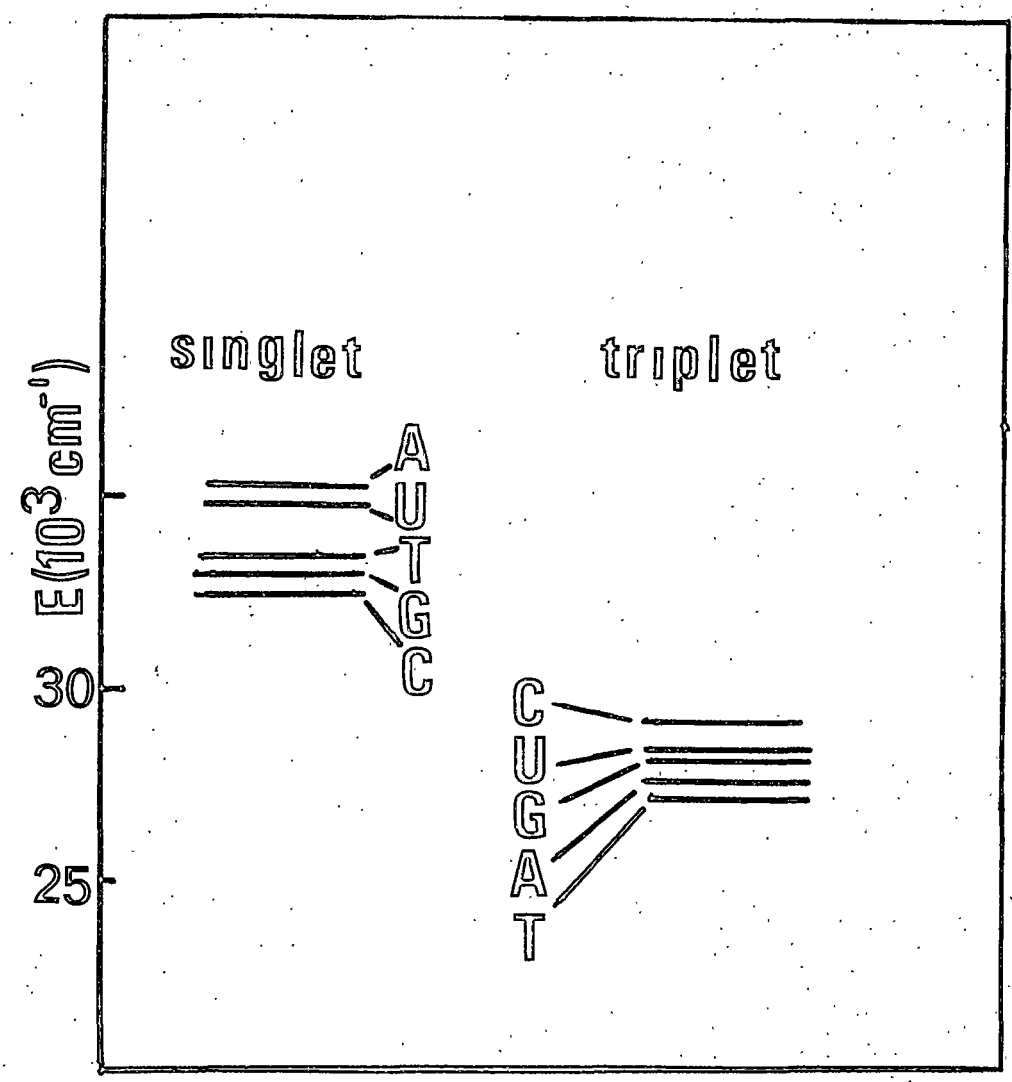

Figure 41. Lowest-lying singlet and triplet energies of the nucleotides (5).

the possible photophysical pathways responsible for the effects seen is given below.

ApG. At the conditions under which data were collected, the shapes of the absorption and fluorescence curves of ApG are what would be expected based on the ε's and Φ_F's of the monomer components. As the AMP is less than 0.1 that of GMP, the shape of the fluorescence curve and the energy of the fluorescence maximum should be near that of GMP, which it is. The shape of the fluorescence curve is independent of λ_{ex} and there is little evidence of an excimer band. These features all indicate that the interaction between the AMP and GMP chromophores is quite small (very weak in the Förster terminology) in both the ground and excited states.

However, the magnitude of the Φ_F and the nature of the emitting triplet definitely give evidence that the two molecules perturb each other to some degree. The Φ_F of ApG (0.033) is near to that of GMP (0.029), λ_{ex} = 265 nm. This is an indication that either there is an efficient transfer of excitation energy at the singlet level from AMP to GMP, or the near presence of AMP somehow causes the Φ_F of GMP to be double what it is in an isolated situation.

The emitting triplet is that of AMP alone.* This indicates energy transfer at the triplet level from GMP to AMP.

The Φ_{PC} due to photoalteration of the GMP present is the same for both GMP and ApG, when monitored either in the fluorescence or absorption modes (λ photolysis = 265 nm in the fluorescence mode). The measured rate of photoproduct formation for ApG is twice that of GMP at -110°C. Of course, if the GMP photochemistry occurs from the triplet state of GMP, then its rate of formation must be near that of the triplet transfer rate to AMP or it could not occur at all in this situation.*

For the situation where excitation is in the region of the absorption maximum of ApG, a case can be made for a scheme which has as its principle feature, efficient energy transfer at the singlet level from AMP to GMP. The calculated rate and efficiency of transfer, by the Förster relation (very weak coupling, post-relaxation) is in agreement with this viewpoint. The estimated rates of

---

*Some investigators have felt they could detect a small amount of GMP triplet emission (52).

*However, the Φ_{PC} of ApG is only $0.25\times\Phi_{PC}$ of GMP at -137°C where only A phosphorescence is seen.

pre-relaxation transfer from AMP to GMP or vice versa (transfer from GMP to AMP now becomes possible due to a nonzero J) are large enough that they might be effective.

The scheme based on the results would be the following: 1) excitation in the absorption maximum region of ApG results in the excitation of either A or G, 2) if G is excited, it undergoes its normal photophysical processes until it reaches ^1T where it undergoes photochemistry at the same rate that it would as a monomer, 3) if A is excited, it efficiently transfers its excitation energy to G at the singlet level causing a proportionate increase in excited state population of G.

As nicely as this scheme fits the results for excitation near the absorption maximum, it does not prove consistent with the results at all λ_{ex}'s within the absorption band. Consider first the shapes of the fluorescence excitation phosphorescence excitation, and photochemical action spectra as compared with the absorption spectrum. All three spectra have the same shape, featuring a shoulder at 280 nm. This in itself is not inconsistent with the previous scheme. In fact, it is a requirement of it. Fluorescence yield and results due to intersystem

crossing should have the qualities of GMP, if it is the chromophore responsible for the effects.

What is inconsistent, is the magnitude of the 280 nm shoulder, and most important, the spectral heights in the entire 270 nm-300 nm region, as compared to the height of the spectral maximum (at ~255 nm). If the yields are equal at 265 nm (where the spectra are normalized) to what is considered to be 100% efficient transfer from AMP to GMP, then the increase in yields for $\lambda_{ex} > 265$ nm should be proportionate to the increased GMP yields at these λ_{ex}'s. At 280 nm, the Φ's of GMP are 15% greater than at 265 nm. The Φ's of ApG at 280 nm would also be 15% larger than at 265 nm if efficient transfer occurred from A to G. However, the Φ's at 280 nm for ApG are more than double the Φ's at 265 nm. At λ_{ex}'s > 280 nm, the disparity between predicted Φ's, based on efficient transfer, and the observed Φ's becomes even larger.

A similar effect is demonstrated from the results obtained when examining the equimolar mixtures of AMP and GMP, and ApG. Excitation at 255 nm shows a two fold increase in both Φ_F and Φ_{PC} when exciting ApG as compared to AMP plus GMP. But the corrected difference spectrum between the two cases is not exactly the absorption (or

fluorescence excitation) spectrum of AMP. Rather, the correlation is fair near the absorption maximum but becomes negative at λ's > 275 nm.

While both the fluorescence excitation spectrum of ApG and the corrected difference spectrum previously described are not in agreement with a singlet energy transfer scheme at all λ_{ex}'s, the two spectra are not in complete agreement with each other. The fluorescence excitation spectrum of ApG is nearly super-imposable with the absorption spectrum of GMP, while the corrected difference spectrum does not have the intensity in the 280 nm region to make the shape equivalent to GMP absorption. Since the two do not agree, a choice must be made on relative reliabilities of the two data sets. The corrected difference spectrum must suffer in the comparison as an additional spectral correction factor, the transmittance factor, was required, because of the higher absorbance used.

Two possibilities are presented, in order of preference, which could account for the experimental results.

1. The increase in yields seen for ApG is the result of a decrease in nonradiative internal conversion of GMP, i.e., singlet energy transfer is not required. Singlet

transfer from A to G might not be effective (as predicted by the Förster relation) because the dinucleotide might not exist in the stacked conformation in solution. Hypochromism and ORD studies give this indication (53).

2. Singlet energy transfer from AMP to GMP is effective in ApG, only in the region of the absorption maximum. The largely increased quantum yields in the low energy region of the absorption band are the result of the same effect that increases the Φ_F of the nucleotides in this region, (relative to that obtained at the absorption maximum), but the effect is even greater for the dinucleotide.

GpA. The absorption spectrum of GpA is similar to an absorption spectrum of an equimolar solution of AMP and GMP, although some evidence of hypochromism is present. The shape of the fluorescence curve presents more evidence for interaction. The curve shape is representative of GMP monomer fluorescence with an added excimer component at λ's > 350 nm. The relative heights of the two bands change with λ_{ex} ; the excimer band is present to the largest

extent (~25% the intensity of the monomer) when exciting near the absorption maximum.

So, unlike ApG, GpA has spectral evidence for interaction in the excited singlet state. The Φ_F, exciting at 265 nm, is slightly less (0.023 vs. 0.029) than that of GMP. This integrated value includes both monomer and excimer contributions. Excitation at 255 nm and a monitoring of the monomer fluorescence at 325 nm indicates that the GMP monomer contribution in GpA is near what would be expected based on the relative absorption of GMP in GpA (see $F^{255}_{GpA}/F^{255}_{A+G}$).

Once again, the emitting triplet is AMP, as it was in ApG. However, the phosphorescence excitation spectrum and photochemical action-spectrum are not coincident with the fluorescence excitation spectrum, as they were in the ApG case. For GpA, the phosphorescence excitation spectrum and photochemical action spectra are more like the absorption spectrum.

The photochemical yields as monitored by the photoproduct formation are, as in the case of ApG, the same as for GMP monomer. The rate of product formation when monitored in the fluorescence mode is, like the ApG case, twice that of GMP monomer.

The photochemical results are much the same in the ApG and GpA cases, indicating that the steady state population of GMP triplet is the same in both cases. The photophysical features are much different in the two cases, however, so that a different explanation must be provided to account for the effects in GpA than was advanced for ApG.

The major feature distinguishing GpA from ApG is the excimer band; this added species could account for the differences seen. The presence of the excimer also gives evidence that the nucleotides are more stacked in GpA than they are in ApG. Charge resonance contribution is required for excimer formation, which means an overlap of space for the two molecules involved. ORD data indicate a stacked conformation for GpA (53).

The following scheme is presented to co-ordinate the results due to photochemistry with the spectral features evidenced.

Excitation at any position in the absorption band produces a combination of excited state GMP monomer and excimer species. The proportion of the species depends on the λ_{ex}. The excimer formed intersystem crosses in a state

such that the triplet excitation resides on the nucleotide which had the lowest energy singlet state (GMP).

The fluorescence excitation spectrum was taken by monitoring 325 nm, the GMP monomer fluorescence maximum. An excitation spectrum taken by monitoring at the fluorescence maximum of the excimer gives a spectrum which more closely resembles the absorption spectrum. It is proposed that excimer Φ_F is independent of λ_{ex} and GMP monomer is λ_{ex} dependent. The corrected difference spectrum of $FX_{A+G} - FX_{GpA}$ (monitoring at 325 nm) qualitatively shows the same manner of λ_{ex} dependence as does the fluorescence excitation spectrum of GpA taken at low absorbance and monitoring at the GMP monomer fluorescence maximum.

In more detail, a photophysical mechanism which could explain the shape of the fluorescence excitation spectrum for GpA is provided in the following paragraph.

Excitation at λ_{ex}'s > 275 nm produces either excimers for those molecules having the proper conformation, or for the remaining fraction of molecules there is efficient energy transfer from AMP to GMP. Excitation at λ_{ex}'s < 275 nm is as effective in promoting excimer formation for those molecules having the proper conformation as it was for λ_{ex}'s > 275 nm. However, singlet transfer

from AMP to GMP is not as efficient as these energies of excitation. This means that k_{IC} for AMP is large at these λ_{ex}. The $_2k_{D\rightarrow A}$ values rather than the $_1k_{D\rightarrow A}$ values must be the correct ones.*

The shapes of the phosphorescence and photochemical action spectra, and the magnitude of the photochemical yields can only be rationalized if the fraction of excimer forming molecules is greater than the fraction of molecules not of a conformation for excimer formation. The Φ_F of the excimer form must also be less than for the monomer.

CpG. The absorption spectrum of CpG is representative of an equimolar sum of CMP + GMP. The shape of the fluorescence is independent of λ_{ex} and there is little evidence of excimer formation. The position of the fluorescence maximum is the same for CMP, GMP, or CpG. Thus, a very weak interaction case applies here.

Unlike the AMP-GMP situations, here the XMP monomer has a significant Φ_F as compared to GMP (0.013 vs. 0.029).

---

*Dr. Leigh Clark has just resolved this ambiguity in favor of the G moment direction used for $_2k_{D\rightarrow A}$ (54).

The Φ_F (λ_{ex} = 265 nm) of CpG is near that of CMP (0.011 vs. 0.013). This is representative of singlet energy transfer from GMP to CMP. The value F^{255}/F^{255} of 0.25 is also consistent with this [i.e., $\Phi_F^{CMP}/(\Phi_F^{CMP} + \Phi_F^{GMP}) = 0.30$].

All of the experimental information points to efficient energy transfer from GMP to CMP at the singlet level, ISC as CMP, followed by triplet energy transfer to GMP. The values of $k_{D\rightarrow A}$ and R_0 as calculated from the Förster relation are consistent with this mechanism.

GpC. Less experimental data were taken for this molecule than were taken for the three previously discussed cases. The data taken exhibit features similar to the GpA situation. Hypochromism is present in the absorption, and a considerable excimer band is present in the fluorescence [I_F(excimer) may equal I_F(monomer) depending on the age of the solution], with the ratio of monomer to excimer intensity being λ_{ex} dependent (note $F^{255}_{CpG}/F^{255}_{C+G}$ vs. $F^{255}_{GpC}/F^{255}_{C+G}$).

The crystal structure of GpC indicates considerably more intramolecular interaction is possible in GpC (3′ → 5′) than in CpG (3′ → 5′), between the G and C portions of the molecules. (The CpG conformation is approximated by

exchanging the C and G positions while retaining the orientation of the sugar-phosphate backbone.)

The photochemical quantum yields are very similar in CpG and GpC, so considering the information available, the scheme for GpC is like that proposed for GpA. A combination of monomer and excimer species are present, and the excimer intersystem crosses with the triplet excitation residing on the base having the lowest singlet state (CMP). CMP does not undergo photochemistry in the triplet state, but transfers its triplet excitation to GMP (the emitting triplet for GpC is GMP). The reduced Φ_{PC} results from ISC by CMP only, rather than by both CMP and GMP.

UpG. The only experimental data for this molecule are the result of experiments conducted with the dinucleotide vs. equimolar monomer mixtures, and the determination of the emitting triplet in the dinucleotide.

Both fluorescence and photochemical yields are reduced in the dinucleotide case, as compared with the equimolar mixture. The reduction in photochemical yield is twice the reduction in the fluorescence yield. No attempt will be made to rationalize these differences. The corrected difference spectrum is roughly equivalent to a GMP

absorption band in shape, which is consistent with a decrease in fluorescence and photochemical yields.

GpU. GpU shows properties similar to the other GpX molecules discussed. There is evidence of an excimer band in the fluorescence, and the monomer fluorescence is less when exciting near the absorbance maximum, as compared to the XpG case (notice $F^{255}_{UpG}/F^{255}_{U+G} = 0.70$, vs. $F^{255}_{GpU}/F^{255}_{U+G} = 0.48$). The Φ_{PC} is greater for GpU than UpG (note the $F^{313}_{GpX}/F^{313}_{X+G}$ values) presumably due to the excimer which intersystem crosses with the triplet excitation on the nucleotide with the lower energy singlet (GMP).

The magnitude of the Φ_{PC} when monitoring in the absorption mode as compared with that in the fluorescence mode is attributed to a much larger Φ_{PC} at $\lambda_{ex} = 280$ nm than at $\lambda_{ex} = 265$ nm. This is clearly evident in the photochemical action spectrum. The intense Hg lines in the region of 270 nm-300 nm were not taken into account when calculating the relative photochemical yields in the absorption monitored mode.

dpGpT. TMP is the only nucleotide having a greater Φ_F ($\lambda_{ex} = 265$ nm) than does GMP (0.036 vs. 0.029). Like

CpG, a very good case can be made for singlet energy transfer, in this situation from TMP to GMP.

The Φ_F (λ_{ex} = 265 nm) GpT is near to that of GMP (0.024 vs. 0.029), and the corrected difference spectrum of $FX_{T+G} - FX_{GpT}$ is very similar to the absorption spectrum of TMP. The fluorescence maximum of GMP + TMP (325 nm) is between the fluorescence maxima of TMP (323 nm) and GMP (327 nm), while the fluorescence maximum of dpGpT (327 nm) is the same as that of GMP.

APPENDIX

APPENDIX

Part A

Room temperature photochemistry of GMP in G-70.

The finding that the low temperature photoproduct of GMP in G-70 could be thermally converted to a room temperature stable product under suitable conditions led to attempts to produce the stable product in quantity at room temperature. While there was some success at producing the product, separation and identification procedures were not successful. A description of the methods used is included here as reference material for future work.

Photolysis for over 100 hours with the high pressure Hg lamp of a preparative scale solution of GMP in G-70 resulted in only minor amounts of product formation as indicated by the intensity of the characteristic 360 nm fluorescence. However, the addition of acetone to the reaction mixture dramatically increased the product yield. That is, the 360 nm fluorescence rose to a maximum within a few hours photolysis time.

The methods used and the results obtained were as follows:

1. The reaction mixture consisted of 2.0 g of GMP, 75 ml of ethylene glycol, and 75 ml of H_2O for the unsensitized reaction. Twenty ml of acetone was added to the mixture for the sensitized reaction.

2. The square quartz dewar contained the reaction mixture. The high pressure Hg lamp was the excitation source. Ethanol contained in a 2.0 cm pathlength quartz cell was used as a chemical filter to exclude ionizing radiation. The solution was stirred with a flow of the N_2 gas emitted from a glass tube extending into the solution and releasing the gas flow just below the point of entry of the excitation beam.

3. Aliquots were removed from the reaction mixture during photolysis and the photoproduct fluorescence intensity determined, to monitor the extent of the reaction.

4. After 4 hours photolysis time, no further photoproduct fluorescence increase was seen (in the acetone sensitized mode).

5. The more volatile solvent components were removed at reduced pressure and temperatures < 50°C. A further reduction in pressure was only effective in producing severe bumping of the solution. A return to atmospheric pressure and the addition of various solvents; ether, DMF,

and methanol resulted in the recovery of < 0.1 g of solutes. Distillation of the solution in an all glass apparatus provided a quantitative separation of solvents and solutes. However, temperatures of up to 190°C were required at the atmospheric pressure prevailing.

6. The residue when redissolved showed a new fluorescence maximum at 385 nm, indicating that the product had undergone a thermal reaction as a result of the separation method.

7. Thin layer chromatography of the residue using concentrated LiCl as the moving phase produced two spots, one fluorescent and one non-fluorescent and both having an R_f value different than GMP.

8. NMR spectra of both parent and product residue produced no resonance peaks when dissolved in D_2O.

The present status of the room temperature stable glycol-GMP product is that while it is possible to produce the product with high yield by means of acetone sensitization, a separation scheme is needed that will not alter the product structurally.

Part B

2-Propanol, guanosine photoadduct.

Other investigators have reported the existence of a photoproduct of guanosine which results when guanosine is dissolved in 2-propanol and irradiated (19). The product is reported to have a structure which is the result of photoaddition of 2-propanol at the 8 position of guanosine. While the photoproduct is reported to have the same optical properties as the parent molecule, unlike the room temperature stable product of glycol-GMP described in Part A, it was felt that an attempt should be made to reproduce their results.

The procedures described below are similar to those reportedly used in the cited work. The results are those experienced by this investigator.

1. The reaction mixture consisted of 0.3 g of guanosine, 200 ml of 2-propanol, 150 ml of acetone, and 300 ml of H_2O.

2. The pyrex immersion cell, previously described, held the reaction mixture. A medium pressure Hg lamp was the excitation source. The solution was stirred during photolysis by means of a flow of N_2 gas released at the bottom of the reaction vessel.

3. Aliquots were removed from the reaction mixture during photolysis and checked for fluorescence properties. A 365 nm fluorescence band was observed to grow in with time of photolysis. Photolysis was conducted for periods of 30, 40, and 50 hours for different samples.

4. Solvents were removed under reduced pressure to the point where precipitation began, and the remaining solution was chromatographed (ascending) on 9-inch strips of Whatman No. 2 paper in a mixture of 1-butanol-water-concentrated ammonia (86:9:5, V/V).

5. The paper chromatography did not resolve the parent material from the product. Mineralight UV excitation of the dried paper showed that the highly fluorescent product had the same R_f value as guanosine, as the fluorescing product zone was situated in the middle of the light absorbing guanosine zone.

6. An NMR spectrum of the parent guanosine gave the characteristic resonance peaks for the compound. The solvent was DMSO and the instrument a Varian HA-100 NMR. The DMSO provided the signal lock.

7. The 2-propanol-guanosine photoresidue gave only a single NMR resonance peak under the same conditions imposed for guanosine. The peak was located in what had

been the region of ribose ring hydrogen resonance. This is contrary to the original report on the photoproduct, which stated that only the C-8 proton resonance of guanosine disappears, along with the introduction of a signal at $\tau = 8.26$ (D_2O) attributed to the two methyls of the $C(CH_3)_2OH$ group.

Guanosine, when irradiated in 2-propanol, then does undergo photochemistry which results in a product which has optical properties different from the parent molecule. The fact that the 2-propanol-guanosine and room temperature stable glycol-GMP products have similar fluorescing properties is suggestive of a similar chemical structure. Whether the products are the result of photoaddition at the C-8 position remains questionable in this author's opinion.

SELECTED REFERENCES

SELECTED REFERENCES

1. Rosenburg, J.M., Seeman, N.C., Kim, J.J.P., Suddeth, F.L., Nicholas, H.B., Rich, A. Nature New Biol. 233, 90-92, (1971).

2. Day, R.O., Seeman, N.C., Rosenburg, J.M., Rich, A. Proc. Nat. Acad. Sci. 70, 849, (1973).

3. Rentzepis, P.M., and Mitchele, C.J. Anal. Chem. 42, 20 A, (1970).

4. Birks, J.B. Photophysics of Aromatic Molecules. Wiley-Interscience, London, (1970).

5. Eisinger, J., and Lamola, A.A. in Excited States of Proteins and Nucleic Acids. Steiner and Weinryb (eds.), Plenum Press, New York, (1971).

6. Daniels, M., and Hauswirth, W. Science. 171, 675, (1971).

7. Eisinger, J., Gueron, M., Shulman, R.G., Yamane, T. Proc. Nat. Acad. Sci. 55, 1015, (1966).

8. Lamola, A.A., Gueron, M., Yamane, T., Eisinger, J., and Shulman, R.G. J. Chem. Phys. 47, 2210, (1967).

9. Eisinger, J., and Shulman, R.G. Science. 161, 1311, (1968).

10. Helene, C., Douzou, P., and Michelson, A.M. Biochim. Biophys. Acta. 109, 261, (1965).

11. Imakubo, K. J. Phys. Soc. (Japan). 24, 1124, (1968).

12. Kleinwächter, V., and Kundelka, J. Chem. Comm. 37, (1972).

13. Gueron, M., Eisinger, J., and Shulman, R.G. J. Chem. Phys. 47, 4077, (1967).

14. Cantor, C.R., and Tao, T. in Procedures in Nucleic Acid Research Vol. 2. Cantoni and Davies (eds.), Harper and Row, New York, (1971).

15. McLaren, A.D., and Shugar, D. Photochemistry of Proteins and Nucleic Acids. Macmillan, New York (1964).

16. Setlow, R.B., and Setlow, J.K. Proc. Nat. Acad. Sci. (U.S.). 48, 1250, (1962).

17. Rahn, R.U., Setlow, J.E., and Hasszu, J.L. J. Biophys. 9, 510, (1969).

18. Merriam, V., and Gordon, M.P. Photochem. Photobiol. 6, 309, (1967).

19. Steinmaus, H., Rosenthal, I., and Elad, D. J. Am. Chem. Soc. 91, 4921, (1969).

20. Ben-Ishai, R., Green, M., Graff, E., Elad, D., Steinmaus, H., and Salomon, J. Photochem. Photobiol. 17, 155, (1973).

21. Steinmaus, H., Elad, D., and Ben-Ishai, R. Biochem. Biophys. Res. Comm. 40, 1021, (1970).

22. Callis, P.R. Private communication.

23. Hatchard, C.G., and Parker, C.A. Proc. Roy. Soc. A235, 518, (1956).

24. Linschitz, H., and Connolly, J.S. J. Am. Chem. Soc. 90, 2979, (1968).

25. Melhuish, W.H. J. Opt. Soc. Amer. 52, 1256, (1962).

26. Parker, C.A. Photoluminescence of Solutions. Parker, C.A. (ed.), Elseivier Publishing Co., New York, (1968).

27. Pabst Circular OR-10, P.L. Biochemical, Milwaukee, Wisconsin, (1969).

28. Izatt, R.M., Christensen, J.J., and Rytting, J.H. Chem. Rev. 71, 439, (1971).

29. Williams, D.R. Chem. Rev. 72, 203, (1972).

30. Drobnik, J., and Augenstein, L. Photochem. Photobiol. 5, 83, (1966).

31. Calvert, J.G., and Pitts, J.N. Photochemistry. p. 557, Wiley & Sons, New York, (1966).

32. Weber, G., and Teal, F.W. Trans. Faraday. Soc. 54, 640, (1958).

33. Brown, I.H., and Johns, H.E. Photochem. Photobiol. 8, 273, (1968).

34. Borresen, H.C. Acta Chem. Scand. 19, 2100, (1965).

35. Melhuish, W.H. New Zealand J. Sci. Technol. B37, 142, (1955).

36. Chen, R.F. Anal. Lett. 1, 35, (1967).

37. Weber, G., and Teal, F.W.J. Trans. Farad. Soc. 53, 646, (1957).

38. Eisinger, J., and Shulman, R.G. J. Mol. Biol. 28, 445, (1967).

39. Lamola, A.A., and Yamane, T. Proc. Nat. Acad. Sci. 58, 443, (1967).

40. Albrecht, A.C., J. Molec., Spect. 6, 84, (1961).

41. Nakanishi, K., Furutachi, N., Funamizu, M., Gunborger, D., and Weinstein, I.B. J. Am. Chem. Soc. 92, 7617, (1970).

42. Secrist, J.A., Barrio, J.R., Leonard, N.J., and Weber, G. Biochem. 11, 3499, (1972).

43. Förster, T. in Modern Quantum Chemistry. O. Sinanoglu (ed.), Vol. 3, Academic Press, New York (1966).

44. Strickler, S.J., and Berg, R.A. J. Chem. Phys. 37, 814, (1961).

45. Callis, P.R. Ph.D. Thesis, U. of Washington, (1963).

46. _____, and Simpson, W.T. J. Amer. Chem. Soc. 92, 3593, (1970).

47. Lewis, T.P., and Eaton, W.A. J. Amer. Chem. Soc. 93, 2054, (1971).

48. Stewart, R.F., and Davidson, N. J. Chem. Phys. 39, 255, (1963).

49. Callis, P.R., Fenconi, B., and Simpson, W.T. J. Amer. Chem. Soc. 93, 6679, (1971).

50. Eaton, W.A., and Lewis, T.P. J. Chem. Phys. 53, 2164, (1970).

51. Stewart, R.F., and Davidson, N. Biopolymers. 1, (1964).

52. Gueron, M., Shulman, R.G., Eisinger, J. Proc. Nat. Acad. Sci. 56, 814, (1966).

53. Warshaw, M.M., and Tinoco, I. J. Mol. Biol. 19, 29, (1966).

54. Clark, L. Private communication. September, 1974.

Morgan, James P
Photochemistry and photophysics of guanines